TR - O -0054

40

High Speed Fiber Optic Link Development for Personal Communication Systems

David Polifko

1992. 12. 17.

ATR光電波通信研究所

Final Report on Activities at ATR Optical and Radio Communications Research Laboratories

- Radio Systems Department -

December 11, 1992

Submitted by

David M. Polifko

Visiting Researcher

- Optical MMIC Group -

Contents

Introduction of Researcher

David Polifko received the BS degree from the University of North Carolina, Charlotte and the MS degree from Drexel University, both in electrical engineering, in 1988 and 1991, respectively. Before attending Drexel, he worked at AT&T Bell Laboratories, in the Electronics and Photonics Materials Research Department. He was with ATR Optical and Radio Communications Research Laboratories in Kyoto, Japan, conducting research in the areas of microwave and millimeter-wave fiber optic links for personal communication systems from April 1991 through December 1992. The greater part of his work at ATR has been documented in over 25 papers which he has authored or co-authored and in three patent applications. He has presented his work at national and international conferences, including two invited talks, and at companies within Japan. He is a member of IEEE, MTT, SPIE, and Tau Beta Pi.

Publication List

H. Ogawa, D. Polifko, and Y. Kamiya, "Fiber optic links for microwave and millimeter-wave transmission," IEICE Optical Communication Systems Group Meeting, Paper CS 91-8 (in Japanese), Hokaido, Japan, May, 1991.

H. Ogawa, D. Polifko, and T. Takenaka, "Fiber optic links for radio communication systems," Proc. 1991 IEICE Fall Conference (in Japanese), Paper B-274, p. 2-274, Tokyo, Japan, September, 1991.

H. Ogawa and D. Polifko, "Balanced laser harmonic generation for fiber optic radio communication links," Proc. 1991 IEICE Fall Conference (in Japanese), Paper B-275, p. 2-275, Tokyo, Japan, September, 1991.

D. Polifko and H. Ogawa, "Effects of laser harmonic generation on fiber optic link performance," Proc. 1991 IEICE Fall Conference, Paper B-276, p. 2-276, Tokyo, Japan, September, 1991.

D. Polifko and H. Ogawa, "Fiber optic link for microwave/millimeter-wave transmission," Dig. 1991 Microwave Workshops and Exhibition (MWE'91), pp. 127-130, Tokyo, Japan, September, 1991.

H. Ogawa, D. Polifko, and H. Kamitsuna, "Millimeter-wave subcarrier multiplexed fiber optic feeder for personal communication systems," IEICE Optical Communication Systems Group Meeting, Paper CS 91-65 (in Japanese), Kyoto, Japan, November, 1991.

D. Polifko and H. Ogawa, "High speed modulation characteristics of millimeter-wave fiber optic links," IEICE Optical Communication Systems Group Meeting, Paper CS 91-66, Kyoto, Japan, November, 1991.

D. Polifko and H. Ogawa, "The merging of photonic and microwave technologies at ATR," Microwave Journal, Horizon House-Microwave, Inc., pp. 75-80, March 1992.

H. Ogawa, D. Polifko, and M. Akaike, "Fiber optic millimeter-wave subcarrier transmission links," Proc. 1992 IEICE Spring Conference (in Japanese), Paper B-426, p. 2-426, Tokyo, Japan, September, 1992.

D. Polifko and H. Ogawa, "Optical modulation method suitable for high carrier frequencies and suppressed carrier transmission," Proc. 1992 IEICE Spring Conference, Paper B-426, p. 2-426, Tokyo, Japan, September, 1992.

D. Polifko and H. Ogawa, "Fiber optic link architectural comparison for millimeter-wave transmission," Proc. SPIE '92, Microwave Optics and Phased Array Processing, Vol. 1703, Orlando, Florida, April, 1992.

H. Ogawa, D. Polifko, and S. Banba, "Fiber optic millimeter-wave subcarrier transmission links," IEICE Radio Communication Systems Group Meeting (in Japanese), Paper CS 92-15, Kyoto, Japan, May, 1992.

H. Ogawa and D. Polifko, "Fiber optic millimeter-wave subcarrier transmission links for personal radio communication systems," IEEE MTT-S Int. Microwave Symposium Digest, pp. 555-558, Albuquerque, New Mexico, June, 1992.

T. Kitazawa, D. Polifko, and H. Ogawa, "Analysis of CPW for $LiNbO_3$ optical modulator by extended spectral domain approach," IEEE Microwave and Guided Wave Letters, pp. 313-315, Vol. 2, No. 8, August, 1992.

D. Polifko, H. Ogawa, and T. Kitazawa, "Millimeter-wave optical transmission with combination narrowband EOM and laser modulation," Proc. Fourth Optoelectronics Conference (OEC '92), Paper 17A2-4, pp. 250-251, Chiba, Japan, July, 1992.

H. Ogawa, S. Banba, H. Kamitsuna, and D. Polifko, "Ka-Band FM video subcarrier transmission using monolithic integrated HEMT photodetector," Proceedings Fourth Optoelectronics Conference (OEC '92), Post Deadline Paper PD-11, Chiba, Japan, July, 1992.

D. Polifko and H. Ogawa, "Millimeter-wave fiber optic technologies for cellular personal communications," Dig. 1992 Microwave Workshops and Exhibition (MWE'92), pp. 299-304, Tokyo, September, 1992.

H. Ogawa, S. Banba, H. Kamitsuna, D. Polifko, and T. Takenaka, "Optical/microwave circuit technologies for microwave and millimeter-wave fiber optic links," Dig. Int. Symposium on Antennas and Propagation, pp. 825-828, Sapporo, Japan, September, 1992.

D. Polifko and H. Ogawa, "Design and characterization of high-speed external optical modulators for millimeter-wave optical communication," Proc. 1992 IEICE Fall Conference, Paper SC-1-6, p. 2-496, Tokyo, Japan, September, 1992.

T. Kitazawa, D. Polifko, and H. Ogawa, "Analysis of coplanar-type waveguide for optical modulator," Proc. 1992 IEICE Fall Conference, Paper C-170, p. 4-196, Tokyo, Japan, September, 1992.

T. Kitazawa, D. Polifko, and H. Ogawa, "Analysis of coplanar-type waveguide for optical modulator by extended spectral domain approach," IEICE Microwave Group Meeting (in Japanese), Kumamoto, Japan, November, 1992.

H. Ogawa, D. Polifko, and S. Banba, "Millimeter-wave fiber optics systems for personal radio communications," IEEE MTT Special Issue, December, 1992

H. Ogawa, H. Kamitsuna, D. Polifko, "Fiber optic microwave subcarrier transmission links using laser diodes as receiving mixer," IEICE Trans. on Electronics - Special Issue on Optical / Microwave Interaction, Devices, Circuits and Systems, February, 1993.

T. Kitazawa and D. Polifko, "Simplified analysis of coplanar waveguide for $LiNbO_3$ optical modulator by variational method," IEICE Trans. on Electronics - Special Issue on Optical / Microwave Interaction, Devices, Circuits and Systems, February, 1993.

D. Polifko and H. Ogawa, "Comparison of traveling wave external modulator microwave mixers," IEICE Trans. on Electronics - Special Issue on Optical / Microwave Interaction, Devices, Circuits and Systems, February, 1993.

D. Polifko and H. Ogawa, "Broadband frequency mixing with traveling wave external modulators," submitted to IEEE Journal of Lightwave Technology, August, 1992.

Patent Applications

D. Polifko and H. Ogawa, "Combination optical receiver and up/down converter using carrier signal re-injection" applied for on July 16, 1991.

H. Ogawa and D. Polifko, "Transmission link systems for high frequency signals", applied for on November 26, 1991.

D. Polifko and H. Ogawa, "Novel frequency mixer using nonlinear external optical modulator" applied for on October 22, 1992.

Research Background

The use of fiber optic (F.O.) systems has flourished with the advent of high quality and reliable low-loss fiber and opto-electronic devices such as semiconductor lasers and photodiodes. Moreover, extension of F.O. communication into the microwave and millimeter wave frequencies has been of particular interest because of system miniaturization and the potential low-loss bandwidth available. At this stage in the evolution of high-speed fiber optics, It is evident that their use is well suited to microwave applications.

Ultra-fast lasers and photodiodes with bandwidths up to Ka-band, which were only available in research laboratories until recently, are now available commercially[1]. New technologies and applications are being realized with these devices. A short list of these subjects might include high-speed communication systems, antenna remoting, radar[2], high speed computer interfaces, sensors, personal communication networks[3], phased array antenna feeds[4] and a more recent topic, optically controlled semiconductor devices[5]. Although the relatively high cost and low availability of high-speed optical devices still prohibit widespread usage, adequate design, test and characterization techniques for these bandwidths must still be developed.

Furthermore, extending F.O. link operating bandwidths to millimeter-wave frequencies requires an different design approach to that of microwave links. At millimeter wave frequencies, electrical circuit behavior and the performance of some optical devices are fundamentally different. Electrical parasitics, transitions and circuit radiation need to be considered in the design of transmitter and receiver modules. Additionally, the device's optical responses must be tailored to the new frequencies.

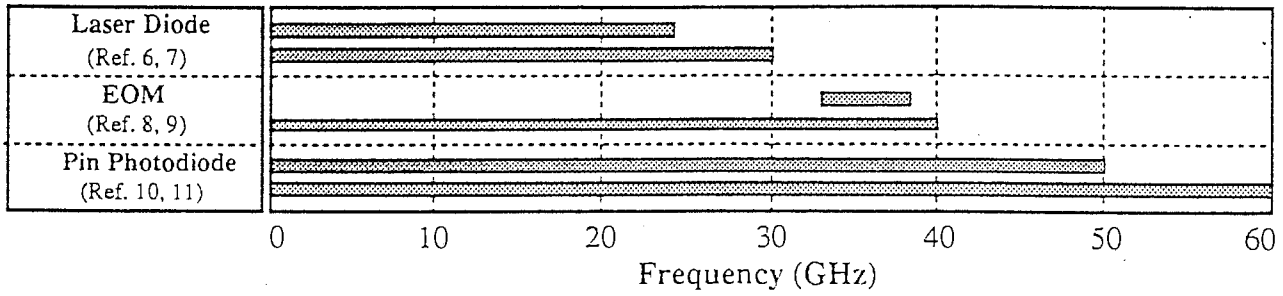

Figure 1. Bandwidths for several laser diodes, photodiodes and EOMs.

Currently, there are two major limitations in achieving millimeter-wave F.O. communication. One is the lack of laser diodes with sufficiently high modulation bandwidths and low noise characteristics. The other is the lack of external modulators with wide bandwidths, low drive voltages and low optical loss (Fig. 1). Direct modulation of laser diodes is in practice, limited to approximately 25 GHz. Laser diodes are also capable of generating harmonic output which in effect doubles or triples the available bandwidth however, this compromises the stability, reliability, and linearity of the device. In the case of external optical modulators (EOM), typically $LiNbO_3$ based Mach-Zehnder interferometers offer the best overall high-speed performance and manufacturing ease. Unfortunately, broadband operation is limited by conductor loss, velocity mismatch between lightwave and electromagnetic waves, and the existence of surface modes restricting the current ceiling of operation to about 50 GHz. Photodiode technology has matured well beyond the modulated sources and presents few obstacles to achieving high-speed F.O. link operation.

To extend F.O. link bandwidths beyond present limitations and to provide optimal performance from available devices, numerous system architectures and lightwave modulation techniques have been proposed and analyzed[12,13,14,15]. Methods of improved light coupling, reactive impedance matching to devices, custom packaging, and use of optical fiber amplifiers have also proven to be effective in improving the performance of F.O. links[16,17,18]. Nearly all of the methods tend to

compromise performance with link simplicity. In most instances, the particular application determines the acceptable trade-offs.

At ATR, the ultimate goal is to develop the technology which would be used in personal communications systems. Such a concept is illustrated with the example of a wristwatch radio telephone which would provide instant access to any other terminal world-wide. Although there are numerous technologies to be developed such as packaging, battery, display etc., the one problem which remains is the delivery of the data signals to each of these terminals.

We envision a network based upon current cellular telephone communication systems. However, the cell diameter would be much smaller, perhaps several hundred meters or less. This small diameter arises from the limited transmission power of such a portable terminals. Thus within an installation of such a system, the number of cells increases quite rapidly. This presents a problem not only in power distribution, but also bandwidth. Future systems will most certainly require bandwidths exceeding the capacity of any copper type of installation. Thus fiber optic (F.O.) links are the only viable solution to providing lossless transmission with wideband capability.

Additionally, the move towards microwave and millimeter-wave frequencies presents many challenges to the F.O. link designer. The work which I have undertaken at ATR hopefully addresses some of the needs for these applications and provides several unique solutions. The following is a summary of the results obtained. For more detailed information on any topic, there is an enclosed publication list for reference.

Specific Research Topics

Extension of Carrier Frequencies in Fiber Optic Links

As was stated in the research background, many novel ways of obtaining high carrier frequencies have been proposed. There are basically three categories of transmission which provide for high carrier frequencies. They are:

1. Direct Modulation
2. External Modulation
3. Indirect Modulation

Direct Modulation is derived from the laser diode being directly modulated through the changing of its bias current. Essentially, the laser diode is forward biased by a DC current/voltage which provides a constant output optical power. If a radio frequency (RF) signal is superimposed on this bias current/voltage, then the optical power will correspondingly change at the same rate. Although this method is extremely efficient, compact and simple to implement, it is severely limited by the laser diode's frequency response which is mostly dominated by the intrinsic parameters as well as the parasitic impedances. Frequencies of up to 30 GHz have been readily demonstrated. To achieve these frequencies, the laser diode must be biased at a large injection current value to extend the relaxation resonance frequency of the diode towards higher frequencies. This higher current limits the device in terms of heating and temperature control. Additionally laser chirp, caused by the heat induced refractive index changes of the diode, and typically low power output have limited direct modulation's usefulness.

External Modulation is an efficient method to apply modulation to a DC (or continuous wave) laser beam. The frequency limitations are typically less prohibitive than direct modulation due to the variety of modulator designs. These designs range from lithium niobate and semi-conductor based Mach-Zehnder devices to multi-quantum well absorption based devices. Overall, these external modulators suffer from high optical losses either due to absorption in the waveguide or due to coupling and mode-mismatch losses. However, by using high power laser diodes which are readily available, these limitations can be overcome. Ideally, these devices are the best performing in terms of frequency response, but their size is extremely prohibitive for integration with other components. Likewise, lithium niobate and nonlinear polymers are not suited towards integration with semiconductor devices, especially the MMIC process.

Indirect Modulation is normally limited to narrow bandwidths and typically poor performance in stability, power output and other detracting factors. Use of external cavities, the inherent electrooptic device's nonlinearity and use of injection locking can all extend the useable frequency range of nominal devices, usually at the expense of output power, bandwidth or complexity in control and stability. Since most of these methods are merely experimental and not practically implemented on a large production scale, these systems were ignored for further applications.

In the most general survey, it was found that to extend the carrier frequencies of the fiber optic links from the current microwave region upwards into the millimeter-wave bands, external modulation techniques provide the most promising cost/performance ratio, as well as lend themselves to currently available technology. The results of this survey are presented in the SPIE paper entitled Fiber optic link architectural comparison for millimeter-wave transmission, published in 1992[19].

Specific Research Topics

External Optical Modulator Test Wafer -General Background

In considering the various F.O. links requirements and performance factors, we identified the need for a millimeter-wave external optical modulator (EOM) in two particularly promising links. The are both shown below in Fig. 2. The first is a conventional link in which the laser is operated in the cw mode. The data is modulated onto the carrier and the composite electrical signal is applied to the EOM. The second link, named dual modulation, requires that the data signal be imposed directly onto the laser diode and the subsequent optical output is upconverted as it passed through the EOM, which is operated at the carrier frequency. In both cases, the bandwidth of the EOM needs to be very narrow, particularly in the second link. Thus, the general requirements for the EOM design included the following:

1. High carrier frequency operation.
2. Negligible (<10%) bandwidth.
3. Low driving voltage, insertion loss (optical and electrical).
4. Use conventional technology for processing.

Of these, the first and second are most important. If we choose a narrowband, high carrier frequency design for the EOM, it could satisfy all of these requirements. Typically in microwave system design, performance can be improved by reducing the bandwidth of the system.

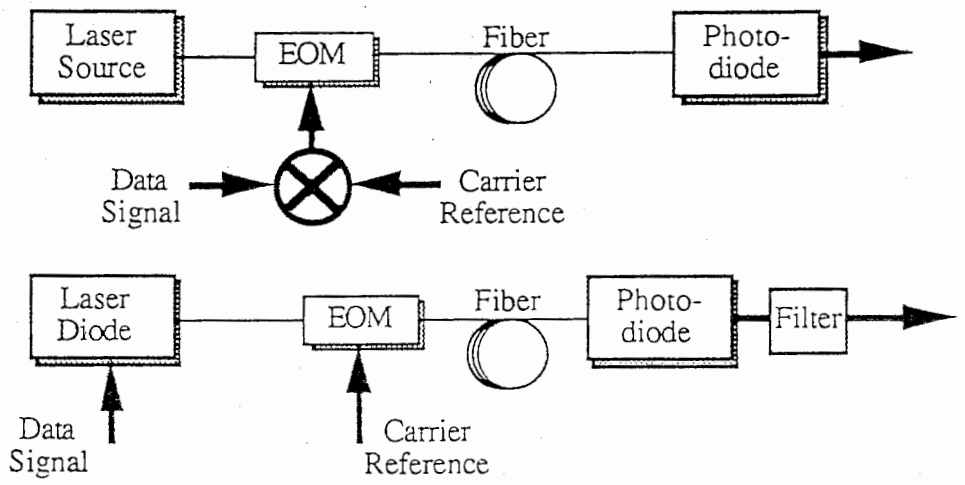

Fig. 2 Conventional EOM FO link and Dual modulation FO link.

Several electrode designs have been developed by others for narrowband modulation schemes using Mach-Zehnder based EOMs. Of these, the resonant line, traveling wave line with index matching and the phase reversal (PR)[20] line are all possible candidates. The resonant line is typically a lumped element approach in which a shorted or open transmission line is used to store energy used for modulation of the crystal's index of refraction. This is not particularly useful for the higher millimeter-wave frequencies since the line length, and hence the interaction between the electrical and optical signals, is very short. Likewise, this does not allow for a very narrow passband since it is difficult to realize a multi-element structure.

The traveling wave transmission line with index matching is a very useful technique to obtain a broadband, yet high carrier frequency response. Since the effective walk-off between the optical and microwave signals is minimized (or eliminated) by lowering the microwave refractive index (typically 3-4) to the index of the optical signal (2.14), high frequency operation is made possible. However, there is an increase in the required power since the useable modulation voltage decreases within the optical waveguide. In index matching, typically, thick buffer layers are used to lower the refractive

index, hence most of the electric field lies in the buffer and not in the optical waveguide. Although, the length of line is no longer limited by the maximum carrier frequency, it is however determined by the electrical insertion loss.

The last type of line is the PR traveling wave line. In this configuration, the differences in the indices of refraction limit the interaction length for a given carrier frequency (typically several mm above 30 GHz). However, if the phase of the electromagnetic wave is shifted by π radians after this interaction length, the next length of line will have an additive effect in the build up of the optical phase delay, as will additional lengths. There are variants on this type of transmission line, such as the intermittent interaction periodic phase reversal line, however they are typically much longer in overall length and thus, insertion loss of these lines becomes a primary concern.

To implement the PR electrode, coplanar waveguides (CPW) are most often used because of the simplicity in shifting the phase by simply displacing the electrode with respect to the optical waveguide. This concept is shown in Fig. 3. Additionally, the electrode structure is inherently in a push-pull configuration, which reduces the required driving voltage by a factor of 2. In the PR electrode, the effective modulation power increases as you add more phase shifted lengths of lines (to be referred to as segments). Thus, your only limitation on the number of segments is the insertion loss of the transmission line and the bandwidth requirements (which in this case is secondary). We chose the PR electrode for our application.

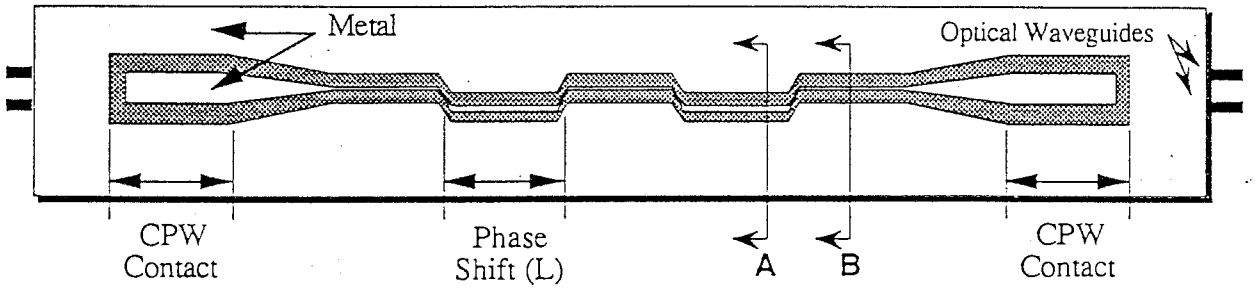

Fig. 3a Phase reversal coplanar waveguide (PR CPW) electrode.

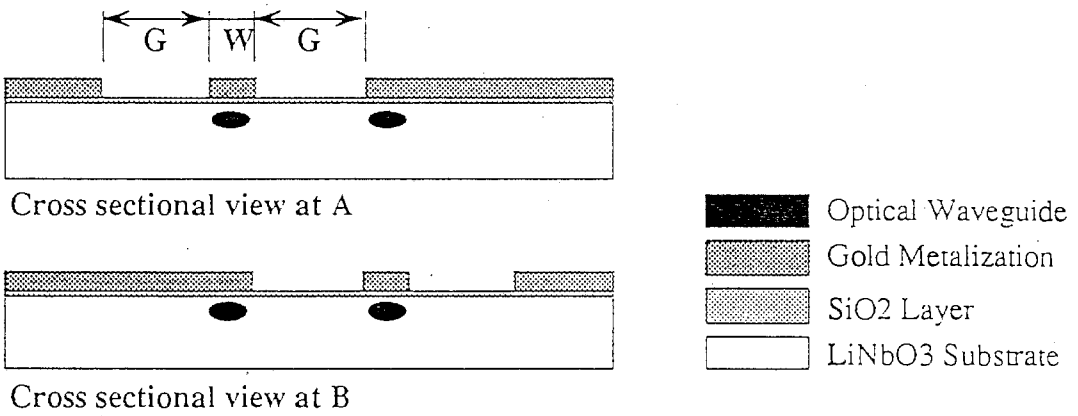

Fig. 3b Phase reversal coplanar waveguide (PR CPW) electrode (sectional view).

Specific Research Topics

External Optical Modulator Test Wafer -Design Fundamentals

In our EOM, we desired a very narrowband response which could be obtained by using many segments. Since the total length of line (several segments) needed to fit within the crystal dimensions (40 mm), we chose to counter-propagate the optical and electrical signals. Under these conditions, for a given frequency, the segment length is much smaller than those for co-propagation. Hence within the same total modulator length, we could incorporate many more segments and thus, have a narrower bandwidth. Also, for a given total length, more segments can be included when higher frequencies are used since the walk-off length decreases for increasing frequency. For higher frequencies, it should be possible to obtain very narrowband responses. It is important to keep in mind however, that the total modulation depth is only a factor of the total line length.

Other design considerations for our EOM included impedance matching to the 50 Ohm system impedance, and minimizing the driving voltage. These quantities, namely impedance and $V\pi$, and the microwave refractive index are very dependent on the electrode and buffer dimensions. Typically, if the buffer layer is thin, the driving voltage can be reduced. Also, if the metalization layer is increased, the microwave losses are reduced. Lastly, if the microwave index of refraction is high, the segment length is further reduced. To summarize, we would like to have the following:

1. Thin buffer layer.
2. Thick metalization layer.
3. High microwave refractive index
4. 50 Ohm impedance of the transmission line.

The following are the effects of changing the various design parameters:

Table 1. Design parameter consequences

Design Parameter	Microwave Impedance	Microwave Refractive Index	Driving Voltage (V-π)
Thin Buffer Layer	Decrease	Increase	Decrease
Thick Metalization	Increase Slightly	Decrease Slightly	Little Effect

Specific Research Topics

External Optical Modulator Test Wafer -Theory and Test Wafers

In considering the different methods by which the previously defined characteristics can be calculated, it is of great importance to include the effects of finite metalization thicknesses, multiple buffer layers with difference indices, as well as the various dimensions of the CPW and crystal thickness. In agreement with Ibaraki University and Dr. Kitazawa, we utilized the extended spectral domain (ESDA) technique to calculate the various waveguide parameters. In the initial phase of this research, calculations were performed on a variety of design permutations with the results being graphically displayed (Such examples are shown in Appendix A). Based on these calculations, a preliminary design of the CPW electrodes was selected. Additionally, several electrical test structures were incorporated into this wafer design which included such devices as:

1. Ring resonators
2. Shorted lines
3. Open lines
4. Various length transmission lines
5. Right angle discontinuities
6. Linear resonators
7. Phase shifted traveling wave lines
8. Line with curved segments

Three sets of transverse dimensions of the CPW lines were selected and are:

1. 7/15 um (center conductor width and gap width [gap on either side on conductor])
2. 10/21 um
3. 15/29 um

Thus, several of the designs were implemented with either one or all of the above lateral dimensions. Linear dimensions (or rather the length of each line) were varied and ranged from 0.25 to 4 cm. All test structures had CPW contact points to allow testing on the wafer probe station. The introduction of these contact points required a taper between the pad and the line. Thus degrading the performance slightly. The composite wafer design (see Appendix B for details drawings of each element) was translated into a photomask with which Sumitomo Corporation fabricated 10 wafers of various metal and buffer heights as shown in the following table (X indicates fabrication):

Table 2. Fabricated wafers.

Metal / SiO_2 (um)	0.5	1	2	3
5	X	X	X	
10	X	X	X	
15	X	X	X	X

The general structure of the completed wafers is shown in Figure 4 below.

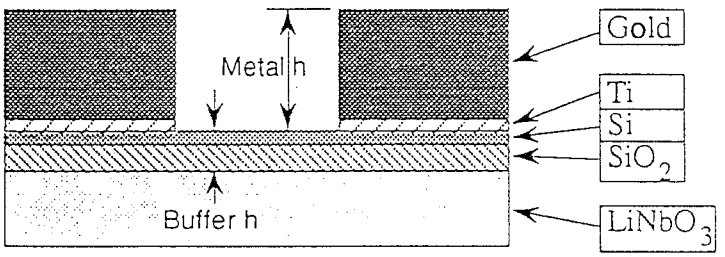

Fig. 4. Physical structure of EOM.

In this structure, the material dielectric constants and/or processing variances are:

1. Silicon = 11.9 to 12 - 1000 Å± 10% (0.09 to 0.11 um typically)
2. Silicondioxide = 4 to 4.4 - (shrinkage is approximately 7.5%)
3. Lithium niobate = 43 Perpendicular, 28 Parallel (usually 500 um thickness)

. . . . . .

4. Titanium layer = 0.015 to 0.02 um
5. Gold metalization = As shown in table

Accuracies in the measurement of the individual wafer layers is approximately ±20 Å. Additionally, there are errors associated with under/over etching of the titanium layer which affects the final V-π (10% variation).

Specific Research Topics

External Optical Modulator Test Wafer -Measurement Set-up

After the wafers were received at ATR and visually inspected, the wafers were loaded into an Cascade Microtech microwave probe station vacuum chuck. Since there were no optical waveguides infused into the crystal, all measurements were purely electrical. The following measurements were performed on the wafer:

1. Insertion loss of all straight, curved, right-angle, phase shifted lines, open and shorted lines.
2. Return loss of all straight, curved, right-angle, phase shifted lines, open and shorted lines.
3. Resonance frequency of the straight and ring resonators.
4. DC resistance between the two probe's center conductor.
5. Time Domain Reflectrometry or open and short lines.

The measurements were made on a calibrated HP8510B automated network analyzer which was swept from 0.45 to 40 GHz (800 point resolution/ramp/0 dBm power). The calibration was accomplished using a short - open - line CPW standard. The DC resistance measurements used a Fluke digital multi-meter which was connected to the HP8510B's bias ports. Calibration of the system resistance was accomplished by shorting the probes together on a CPW line. Typical DC system resistance was approximately 4 Ohms.

Time domain (TD) measurements were made using the built-in TD capabilities of the HP8510B in time bandpass mode with minimum window, and a lowpass step. Smoothing was used on occasion in all measurements to remove spurious responses caused by the microwave probes.

The results of the measurements are summarized as:

1. Refractive index were calculated from TDR and from the return loss resonance peaks.
2. DC resistance was measured directly.
3. RF Insertion loss per cm was calculated from 4, 3, and 2 cm length lines.
4. Return loss was measured yet did not lead to any conclusive results due to the return loss of probe becoming large for extended frequency. Thus, impedance was difficult to measure quantitatively measure. Most results showed return loss of traveling wave lines to be less than 10 dB.

Specific Research Topics

External Optical Modulator Test Wafer -Measurement Results

The following results are the calculations from the extended spectral domain analysis and measurements of the microwave refractive index and the impedance (calculation only). Measurements of the dielectric and metalization thicknesses were performed by Sumitomo Cement. The measured microwave refractive index was calculated from the two methods previously described (time domain and return loss). The two measurements were weighted and averaged together to form the number in the table.

Table 3. Measured and calculated values for the test wafer.

Design Heights Met/SiO2 (um)	Metal Height (um)	SiO2 Measured (um)	SiO2 with Shrinkage (um)	Microwave Refractive Index	Impedance (Ohms)	Measured Micr. Refr. Index
15/1	15.20	0.99	0.921	2.269	39.05	2.34
5/2	5.26	1.99	1.851	2.323	55.77	2.33
15/0.5	18.10	0.52	0.484	2.401	33.82	2.61
10/1	9.94	0.99	0.921	2.443	43.48	2.43
5/1	4.95	1.02	0.949	2.656	49.51	2.71
10/2	10.05	2.06	1.916	2.132	49.62	2.17
15/2	14.30	2.06	1.916	2.015	45.26	1.99
15/3	15.30	3.10	2.883	1.844	47.90	1.84
10/0.5	10.10	0.52	0.484	2.681	39.37	2.80
5/0.5	5.00	0.52	0.484	2.946	44.54	2.97

Sample electrical measurements for the straight through line insertion and return loss, shorted line return loss, and the right angle bend's insertion and return loss are presented in Appendix B (Sample measurements of the test wafer).

Specific Research Topics
External Optical Modulator Test Wafer -Discussion

From the comparison between the measurements and the predicted results from the ESDA approach, it is clear that although the results are quite good, several sources of measurement, processing and computational error exist. They are summarized as follows:

1.Computational (ESDA)
The ESDA technique is very accurate and can be used to calculated complex structures (especially in this case of multiple dielectric, anisotropy, thick metalization and different dimensions). However, since there are imperfections within the processing, leading to variations in dimensions, effective dielectric constants, etc., it would be difficult for any program to incorporate all of the variables to accommodate the minor variations. Thus, within the limitations of the ESDA technique, the results are accurate, however, since these precise specifications can not be fabricated, there will always remain differences between what is designed and what is built.

2. Processing
As outlined previously, the processing techniques used by Sumitomo cement are subject to dimensional variances which in turn produce variations in the wafer characteristics. These results are also dependent on environmental conditions at the time of processing. Additionally, Sumitomo has not fully characterized all of the material elements within their processing. Therefore, if we use only published values (of dielectric constant for example) then these could possibly differ from actual manufactured results.

The measured DC resistivity of the gold electrodes is substantially higher than calculations of the same dimension structure. This phenomenon arises from the fact that when the gold is evaporated or sputtered onto the surface of the substrate, the surface is pitted and uneven. Thus, since at microwave frequencies, the current is confined primarily to the surface (fraction of a micron), the effective resistivity increases because of the added surface area. This is easily accountable by increasing the resistivity constant.

3. Measurements
For our measurement system, it has been roughly estimated that the TDR method results in an variance within the refractive index of $\eta \pm 0.047$ and is due to the limited resolution of the network analyzer (40 GHz bandwidth). Also, placement of the cursor (to read the peak of the reflected line) is a source of error also.

The average measured variation in refractive index between the TDR and shorted line method is about 0.045. The average variation in refractive index between the 4, 3, 2 and 1 cm line are 0.045 for the TDR method and 0.052 for the shorted line method. The shorted line method shows less precision since it is primarily a graphical method of determining the refractive index.

4. Calculations (from measured data)
There is negligible error in the calculation of the refractive index from the TDR method since it is the limited resolution of the network analyzer which is the dominating factor. In the calculations based on the shorted line measurements (reflection coefficient), the precision is determined by the ability to distinguish between the peaks and troughs of the reflection coefficient response.

Within the measurement and calculational accuracy and precision, the measurement exhibit good agreement with the predicted values of the microwave refractive index.

Specific Research Topics

External Optical Modulator Final Design

-General Background

At this point in the design stage, we believed that the ESDA was able to accurately predict the microwave refractive index of the CPW structure. This value is essential to determining the length of phase shifted line to use for a given center carrier frequency. At this point we decided that the final wafer should include a variety of modulator designs (various center frequencies and bandwidths) each using the same CPW dimensions, buffer and metalization heights, as well as several electrical characterization structures. Design center frequencies were originally chosen to be:

20, 26, 32, 38 and 45 GHz.

Our goal at this point was to be able to use this refractive index information to accurately design for a given center frequency with little or no error. However, a 1.3% difference in desired and measured refractive index would cause a center frequency shift of 0.75% of the carrier (e.g. 0.3 GHz at 40 GHz). This was considered acceptable in most applications especially since the best percentage 3 dB bandwidth obtainable is 10% of the carrier (e.g. 4 GHz at 40 GHz) and in most instances, 15-20% is more common.

Specific Research Topics
External Optical Modulator Test Wafer
-Design Fundamentals

Although the desired design frequencies were 20, 26, 32, 38, and 45 GHz, due to a calculational oversight, the actual center frequencies (measured) were roughly:

18.7 (9seg), 23.76 (11seg), 29.37 (11seg), 34.3 (13seg), 39.43 (15seg) GHz

These values are shown with the number of segments included, since for a relatively small amount of segments the actual center frequency shifts to lower than desired frequency. However, when many segments are used, the measured center approximates the desired frequency. The particulars will be shown in the theory section.

Additional constraints on the dimensions were imposed by Sumitomo and by our desire to incorporate many designs within one chip. Also, DC pads were needed to test the voltage response and balance the arms of the Mach-Zehnder interferometer.

From the ESDA calculations, it was determined that a Si02 buffer layer or 0.5 um and a metalization of 8 um yielded a 50 Ohm impedance, microwave refractive index of approximately 3 (for 25/7/25 = GWG), and still provided for minimal insertion loss, minimal return loss, and low driving voltage.

The Mach-Zehnder interferometer arms were approximately 40 mm in length. Within each MZ, several individual electrode patterns were placed allowing for several different responses. With this particular length of optical waveguide, the two arms needed to be separated by 25 um to reduce the effects of coupling. DC pads incorporated into small length lines provided for a method of DC testing the modulators, since the phase reversal modulators do not give sufficient response (especially for an even number of segments) at or near 0 frequency.

At this point in the design stage it was also under consideration as to the method of testing these modulators without the need to package each on. Since there were essentially 25 Mach-Zehnders with a total of 130 electrodes, it would be quite cost-prohibitive to package and test each one individually. Of course there was redundancy within the design to allow for damages and processing errors. This still left 25 MZ and 26 unique electrodes. So, it was at this point decided to split the wafer into two parts, each with identical modulator designs except that on one half the modulators would have CPW contacts and on the other half, their would be pads for K-connector attachment and mounting. Also on the CPW probe contact half, there would be the electrical property characterization structures.

Specific Research Topics

External Optical Modulator Final Design -Theory

The theory of operation for the phase shifted coplanar electrode EOM is given in the following source and associated papers which can be found in its reference section:

Alferness et al.,"Velocity-Matching Techniques for Integrated Optic Traveling Wave Switch/Modulators", IEEE Jour. Quantum Electron., Vol., QE-20, No.3, March, 1984.

Other basic calculations are given in Appendix H for frequency response, percentage bandwidth, location of response nulls, and approximate center frequency.

Specific Research Topics

External Optical Modulator Final Design -Measurement Set-up

To accommodate the testing of the external optical modulators we designed. It was decided to divide the wafer into two halves, both with identical designs except for the electrode contact pads. One half would be designed to accommodate a coaxial transition, such as a Wiltron K-connector. The other half of the wafer was to have coplanar waveguide contacts on each of the electrodes for testing with the microwave probes as had been done in the test wafer testing.

However, two horizontal optical fiber probes were added to the measurement test set-up to facilitate bringing an optical signal in and out of the crystal as shown below in Figure 5.

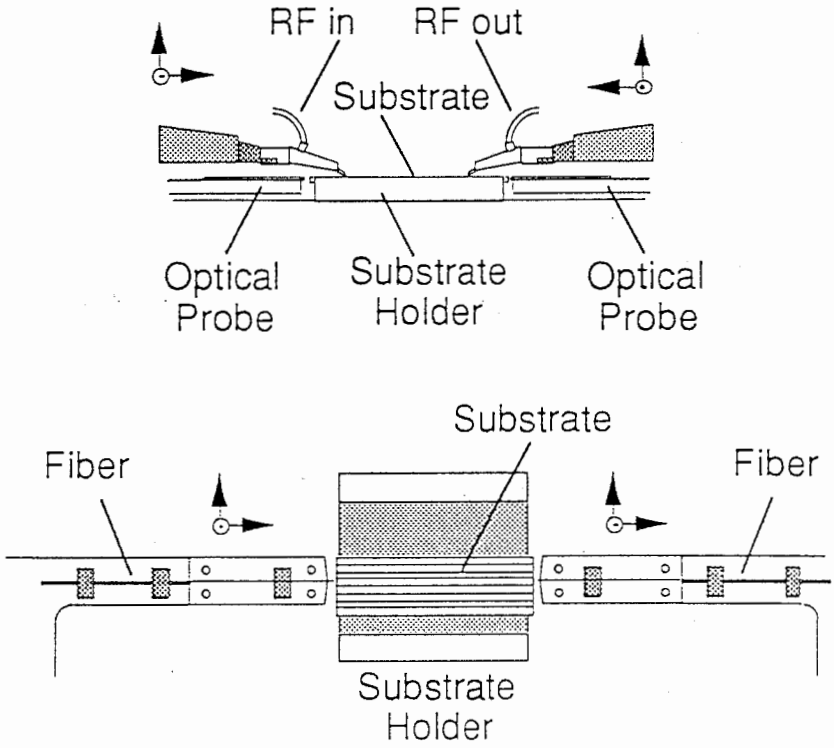

Fig. 5. Schematic of the optical probe station modifications.

The design of these probes if given in Appendix F. The optical fiber was laid in the probe and taped into place. The input fiber was polarization maintaining fiber with a built-in polarizer. The output fiber was standard single mode fiber. Polarization of the input fiber was matched to the input of the optical waveguide of the EOM.

Additional components to this measurement set-up included an amplifiers on the output of the photodetector which was included in the calibration, thus not affecting the measurement results. This amplifier was required due to the low dynamic range of the HP 8510 network analyzer and the relatively high insertion loss of the total link.

The laser sources in these experiments ranged from a Nd:YAG with 30mW output power to an external cavity source with 12mW output power to laser diodes from Ortel with output powers up to 4mW. All had polarization control and built in isolators.

Specific Research Topics

External Optical Modulator Final Design -Measurement Results

Sample measurements are presented in Appendices D and E for unpackaged and packaged modulators.

Specific Research Topics

External Optical Modulator Final Design -Discussion

It is quite evident from the sample measurements in the appendices D and E that the on wafer probe station measurements are quite effective in measuring the true response of the external optical modulators. In effect, all of the packaging parasitics have been removed. One problem remains however: the effects of the un-calibrated probe and photodetector responses. Since the probes and photodetector cannot be included within the ANA calibrations, their cumulative affect is present in the final on-wafer measurements. But, the photodetector response, in general is considered flat or at least a constant slope with respect to frequency. Likewise, the insertion loss of the microwave probes can be viewed as a frequency dependent attenuation.

Thus, in the final calibration, a length of lossy coaxial transmission line (which had a constant slope) was included within the calibration standard set. The effects of the photodetector loss and microwave probes can be effectively subtracted during calibration if the proper length of lossy transmission line is selected.

Unfortunately, the only remaining problem is the resonances of the microwave probes. Since these cannot be effectively calibrated out of the measurement, the effects can only be subtracted after the measurement is made. This is why the smoothed drawings of the final measurements were made. In order to locate any probe resonances, the two probes were shorted together on a coplanar waveguide and the insertion loss was measured. The insertion loss, however low, would show any major insertion losses of the probe resonances. After this plot was made, the resonances were subtracted from the final measurements by hand.

In the future, a method for calibrating the total system should be implemented. This would require accurate characterization of the photodetector frequency response as well as the entire probe characteristics. Although feasible, it is not an easy task to accomplish.

In the measurements of the packaged modulators, it is clearly seen that the frequency response is limited by the packaging of the lithium niobate crystal. This should indicate the need for more advanced packaging techniques which limit the insertion and return losses.

Overall, a method of characterization in the optical and electrical domain, or external optical modulators in lithium niobate has been designed, fabricated and tested. Results are very good and can be further optimized to provide true responses of any future modulator designs.

General Discussion and Recommendations for Future Work

The next logical phase for this work, is redesign for higher frequency modulation of the EOM and for narrower bandwidth. With these two features improved, the original goal of realizing narrowband modulation from 40 to 60 GHz is feasible. However, the microwave packaging must be altered to accommodate a 40 to 60 GHz coaxial connector. Likewise, a measurement facility must be designed to accommodate frequencies over 40 GHz, which is the current limitation of the HP 8510 Network Analyzer. Crystal thickness must also be reduced to minimize the effects of surface mode generation. The current thickness of 500 um is limited to approximately 30-40 GHz operation depending on the lateral and longitudinal dimensions.

Other problems which must be addressed are the insertion loss of the EOM (electrode and fiber to fiber losses). Particularly the electrode thickness. With the current 8dB/cm (at 40 GHz) loss, we anticipate substantial losses at 60 GHz operation. Thus reducing the length of the electrode as well as increasing its thickness are two possible methods of reducing the loss. Perhaps with this particular design, however, there are limitations on just how much you can actually reduce the insertion loss before other factors start to dominate.

If these new designs are fabricated and tested, packaging of the best modulators should begin as well as a comparison to the predicted performance. Actual use in a transmission system under operating conditions would also prove to be beneficial as well as useful to locate any potential design flaws. Other designs methodologies, such as MMIC compatible processing technology, for the EOMs is another factor to consider for future work. Since the lithium niobate technology is reaching its maturity as well as the fact that it is bulky and consumes large quantities of power, it is important to consider alternatives in design and processing techniques.

Conclusions

Overall, this research project displayed useful results pertaining to the development of high speed fiber optic links and their associated technology. Practical results, including the high speed fiber optic link survey, dual modulation links, and the external optical modulator designs provide a solid base from which further work in this area can be accomplished.

Acknowledgements

The author would like to thank Drs. K. Habara, Y. Furuhama, E. Ogawa, and M. Akaike for their generous support and encouragement of this work. He would also like to thank Dr. Hiroyo Ogawa for his interest, patience, support and assistance during the author's stay at ATR. Thanks are also given to the administrative staff of ATR Opt. & Rad. Comm. Research Labs for their continual help. Lastly, he would like to thank Dr. Kitazawa from Ibaraki University for his assistance in theoretical calculations and the engineers at Sumitomo Cement for their support and fabrication of our modulators, particularly, Mr. Sugamata. Without the contributions of all of these people, my research would not have progressed.

References

(1) R. Marsland,"Who Needs High-Speed Photodetectors?", Lasers & Optronics, pp.43-45, April, 1991.

(2) I. Newberg et al.,"DFB laser: external modulator fiber optic delay line for radar applications", Proc. SPIE, Vol. 1102, Opt. Tech. for Micr. Appl. IV, pp. 93-96, 1989.

(3) H. Ogawa et al., " Fiber Optic Millimeter-wave Subcarrier Transmission Links for Personal Radio Communication Systems", to be published in IEEE MTT Int. Micr.Symp. Dig., 1992.

(4) A. Seeds et al.,"Optical Control of Phased Array Antennas: A European Perspective", IEEE MTT-S Int. Micr.Symp. Dig., pp. 1343-1346, 1990.

(5) A. Paolella et al.,"Optical Response of the GaAs MESFET at Microwave Frequencies and Applications", IEEE MTT-S Int. Micr. Symp. Dig., pp. 487-490, 1991.

(6) E. Meland et al.,"Extremely High-Frequency (24GHz) InGaAsP Diode Lasers with Excellent Modulation Efficiency", Electronics Letters, Vol. 26, No. 21, pp. 1827-1829, October, 1990.

(7) R.S. Tucker and I.P. Kaminow,"High Frequency Characteristics of Directly Modulated InGaAsP ridge waveguide and Buried Heterostructure Lasers", J. Lightwave Tech., LT 2, pp. 385-393, 1984.

(8) M. Izutsu et al.,"Millimeter-wave Light Modulator Using $LiNbO_3$ Waveguide with Resonant Electrode", in *Tech. Dig. CLEO'88*, 1988, pp. 485-486, 1988.

(9) D. Dolfi et al.,"40GHz Electro-optic Modulator with 7.5V Drive Voltage", Electronics Letters, Vol. 24, No. 9, pp. 528-529, April 1988.

(10) D. Wake et al.,"50GHz InGaAa Edge-coupled PIN Photodetector", Electronics Letters, Vol. 27, No. 12, pp. 1073-1075, June 1991.

(11) R. Marsland,"Who Needs High-Speed Photodetectors?", Lasers & Optronics, pp.43-45, April, 1991.

(12) D. Polifko et al.,"Comparison of Two Architectures for Fiber Optic Distribution Inside Ka-Band Communication Satellites," IEEE MTT-S Int. Micr. Symp. Dig., pp. 317-320 , 1991.

(13) A. Kellner et al.,"Externally Modulated Modelocked Laser diodes for Microwave Transmission Links", Electronics Letters, Vol. 25, No. 19, pp. 1291-1292, September, 1989.

(14) G. Simonis and K. Purchase,"Optical Generation, Distribution, and Control of Microwaves Using Laser Heterodyne", IEEE Trans. MTT, Vol. 38, No. 5, pp. 667-669, May, 1990.

(15) S. Thaniyavarn et al.,"Millimeter-wave signal generation and control using optical heterodyne techniques and electro-optic devices", Proc. SPIE, Vol. 1371, High-Frequency Analog Fiber Optic Systems, pp. 250-251, 1990.

(16) S. Wanuga et al.,"A low loss L-Band Microwave Fiber-Optic Link for Control of a T/R Module", Proc. SPIE, Vol. 1374, Integrated Optics and Optoelectronics II, pp. 97-106, 1990.

(17) J. Schlafer et al.,"Microwave Packaging of Optoelectronic Components", IEEE Trans. MTT, Vol. 38, No. 5, pp. 518-522, May, 1990.

(18) K. Hagimoto et al.,"A 17Gb/s Long-Span Fiber Transmission Experiment Using a Low-Noise Broadband Receiver with Optical Amplification and Equalization", Tech. Dig. Conf. on Optical Amplifiers and Their Applications, Vol. 13, pp. 100-103, Monterey, California, August, 1990.

(19) D. Polifko and H. Ogawa, "Fiber optic link architectural comparison for millimeter-wave transmission," Proc. SPIE '92, Microwave Optics and Phased Array Processing, Vol. 1703, Orlando, Florida, April, 1992.

(20) Alferness et al.,"Velocity-Matching Techniques for Integrated Optic Traveling Wave Switch/Modulators", IEEE Jour. Quantum Electron., Vol., QE-20, No.3, March, 1984.

Appendix A - Test Wafer Layout

The following pages (A1-A12) include the rough layout of the test wafer and the image taken from the computerized CAD layout.

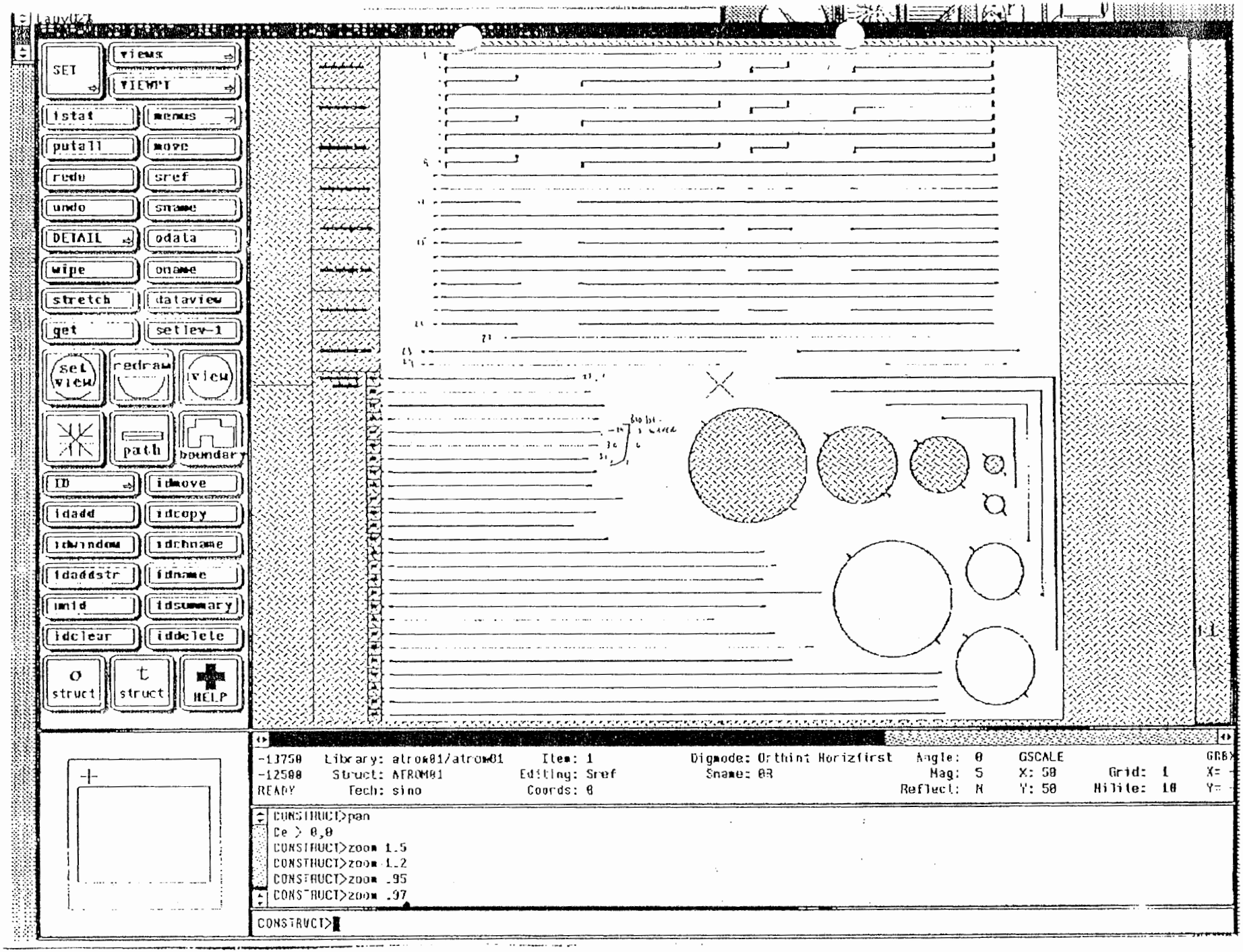
SET
views
VIEWPT
istat
menus
putall
move
redo
sref
undo
sname
DETAIL
odata
wipe
oname
stretch
dataview
get
setlev-1
set view
redraw
view
path
boundary
ID
idmove
idadd
idcopy
idwindow
idchname
idaddstr
idname
idmid
idsummary
idclear
iddelete
o struct
t struct
HELP
-13750 Library: atrom01/atrom01 Item: 1 Digmode: Orthint Horizfirst Angle: 0 GSCALE GRBX
-12500 Struct: ATROM01 Editing: Sref Sname: 03 Mag: 5 X: 50 Grid: 1 X=
READY Tech: sino Coords: 0 Reflect: N Y: 50 Hilite: 10 Y=
CONSTRUCT>pan
Ce > 0,0
CONSTRUCT>zoom 1.5
CONSTRUCT>zoom 1.2
CONSTRUCT>zoom .95
CONSTRUCT>zoom .97
CONSTRUCT>

5cmX5cm circuit area (divided into 1mm rectangles, each colored block is 3mm wide)

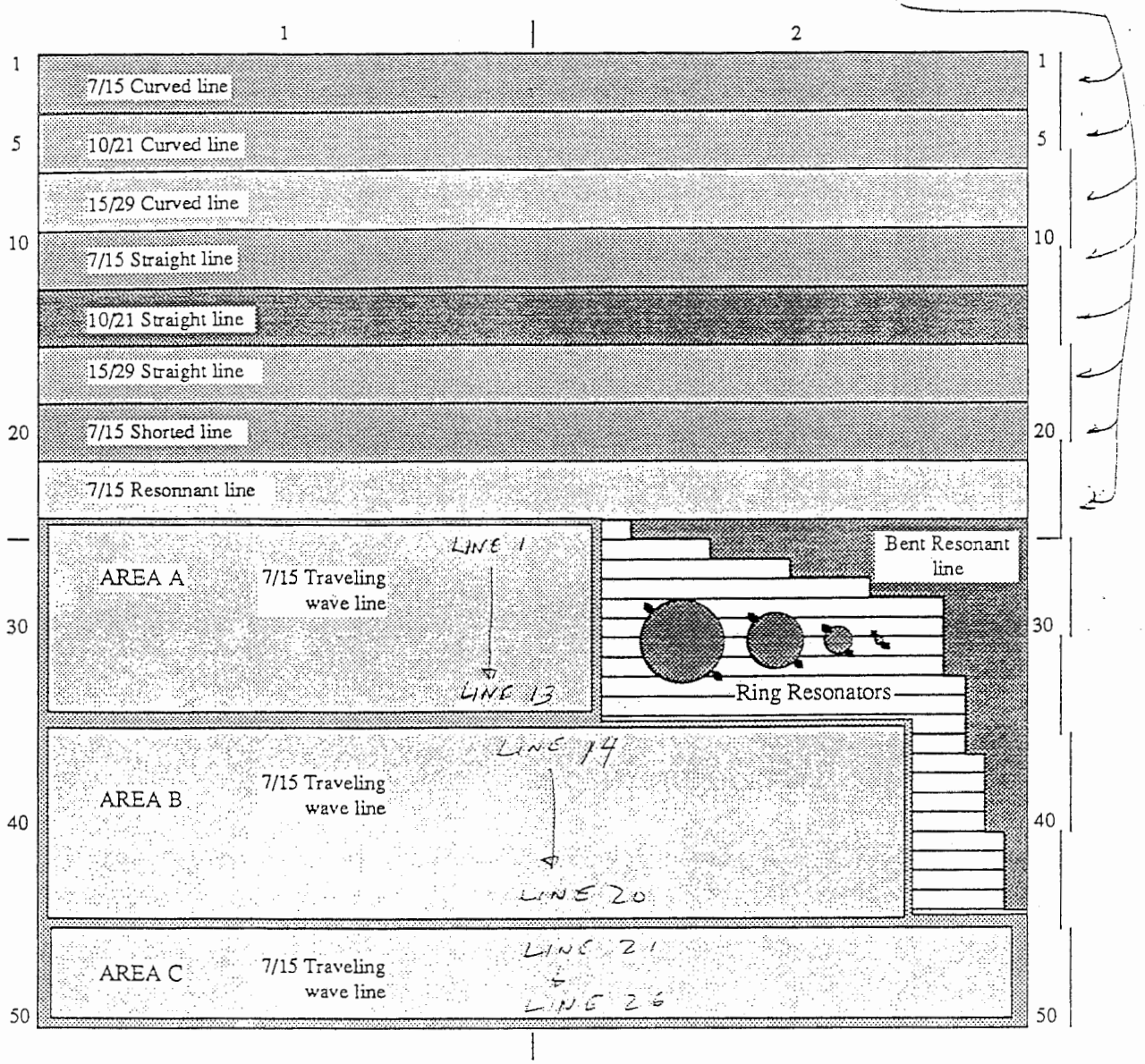

1SHIFT = 2×(X) + 2×(Y) A3

EX. LINE 1 : 2 × 550 + 2 × 75 = 1250 μm

Alternating segment

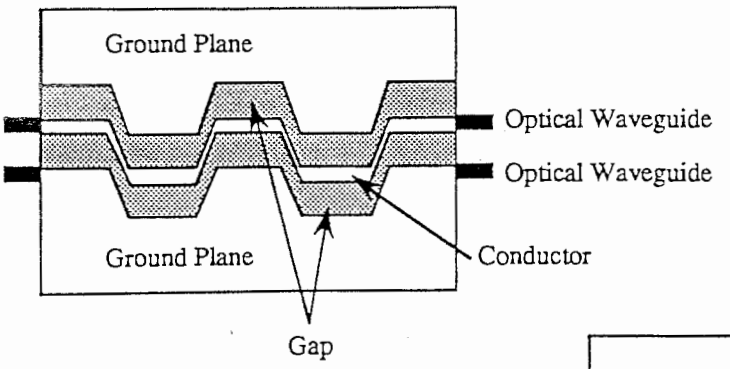

ex.: 2 SHIFTS

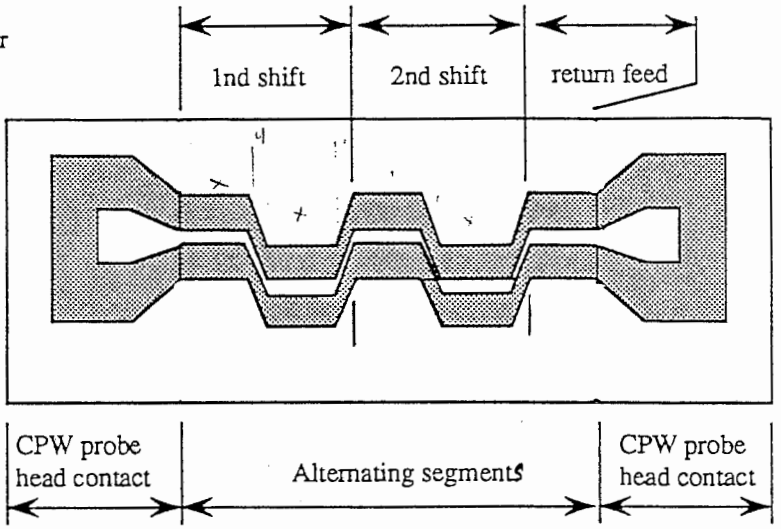

SEE WAFER LAYOUT DRAWING

Line Number	# of shifts	dimension X	dimension Y	dimension Z	dimension W	dimension G
1	10	550 μm	75 μm	22 μm	7 μm	15 μm
2	10	600				
3	10	650				
4	9	700				
5	8	800				
6	7	900				
7	6	1000				
8	5	1250				
9	4	1500				
10	4	1750				
11	3	2000				
12	2	2500				
13	2	3000				
14	12	1000				
15	10	1250				
16	8	1500				
17	8	1750				
18	6	2000				
19	4	2500				
20	4	3000				
21	22	600				
22	16	800				
23	18	1000				
24	12	1500				
25	9	2000				
26	6	3000				

AREA A

AREA B

AREA C

ALL HAVE 1 RETURN FEED LINE

ALL DIMENSIONS IN μm

A4

TRAVELING WAVE LINE

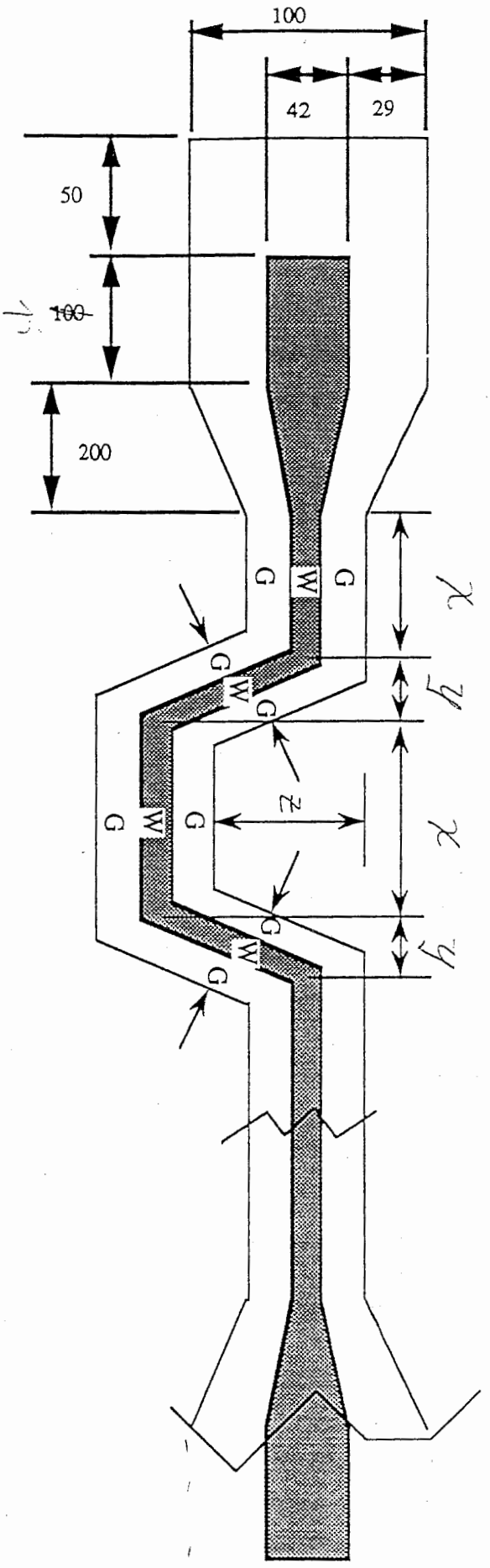

SAME AS OPPOSITE SIDE

Layout for Curved, Straight, and Shorted lines

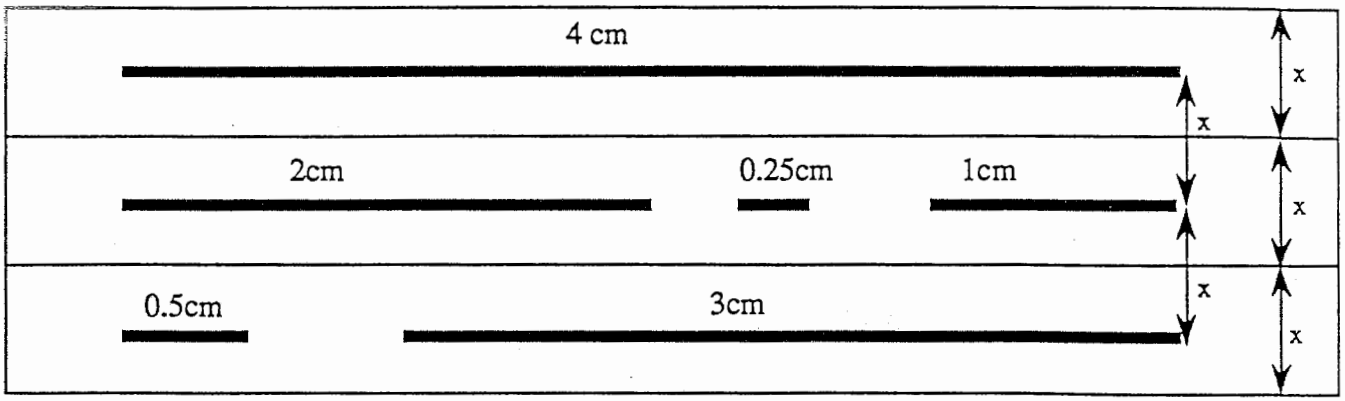

Layout for Resonnant Lines

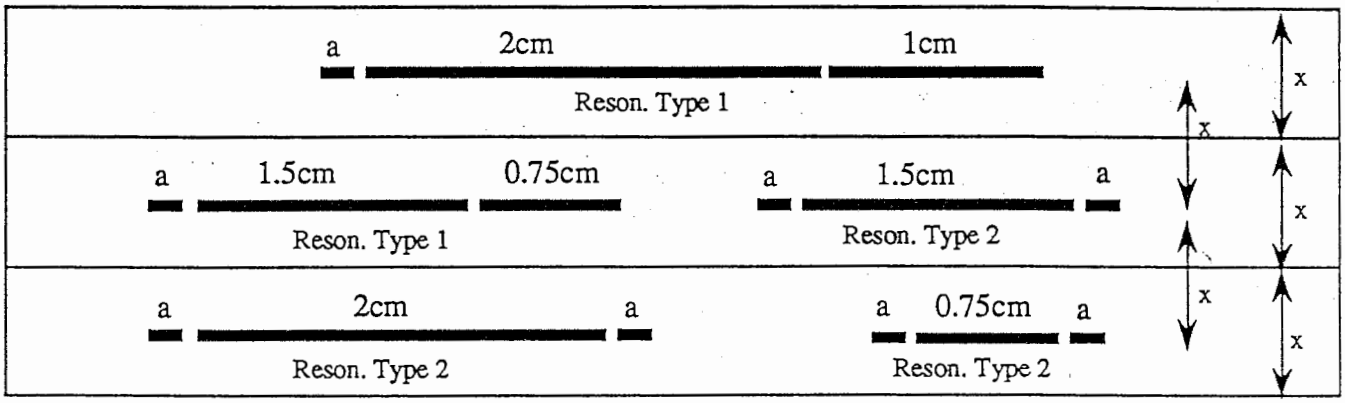

x = 1mm a = 300 μm

Layout for Bent Resonnant Lines

a - Total length 2 + 2 = 4 cm
b - 1.5 + 1.5 = 3 cm
c - 1 + 1 = 2 cm
d - 0.5 + 0.5 = 1 cm

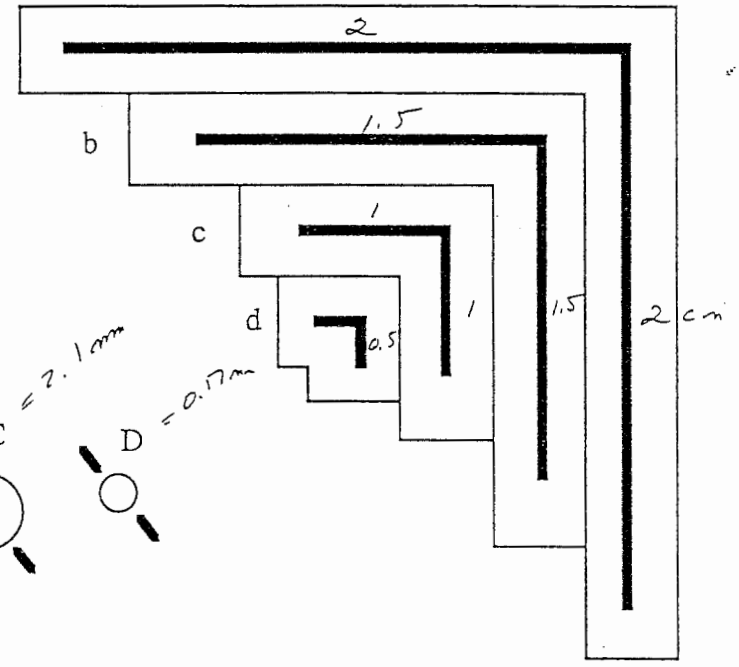

Circular Resonators

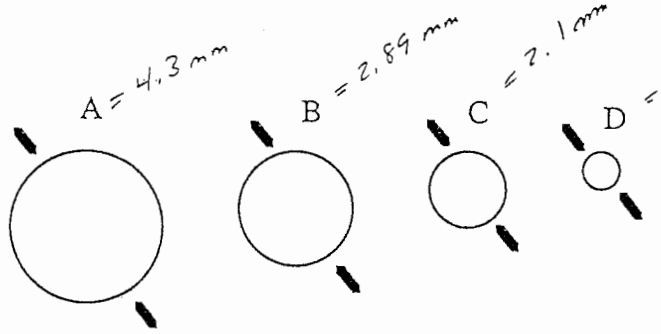

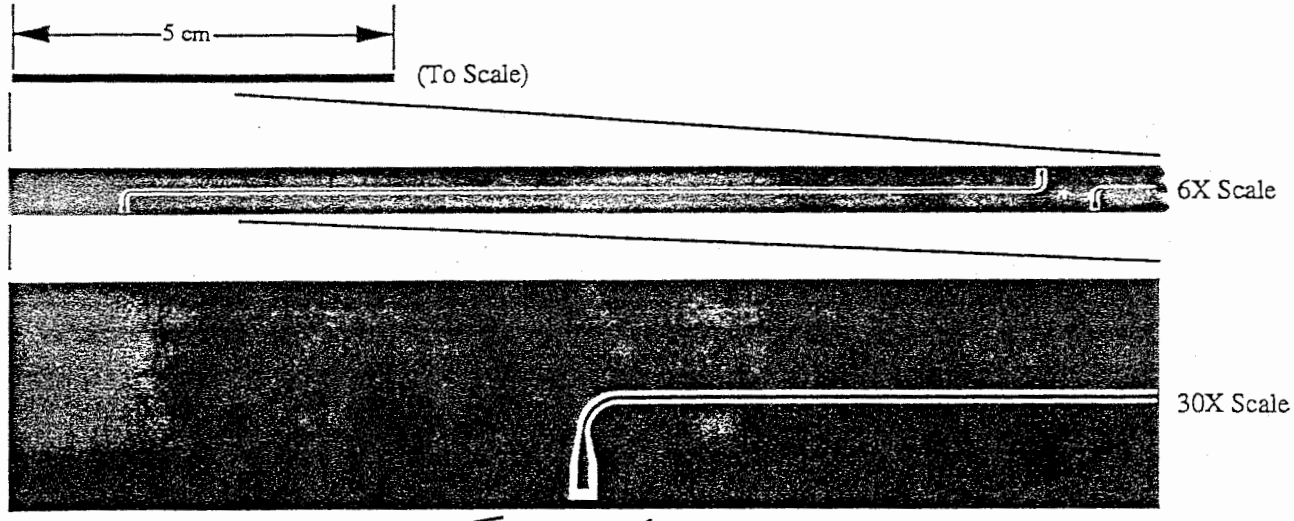
5 cm
(To Scale)
6X Scale
30X Scale

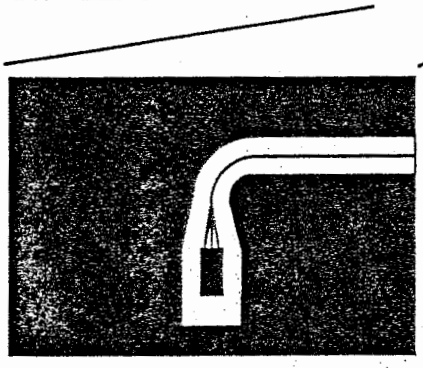
60X Scale

Not to scale
G
W
G
100 μm
lengths given on pg. 4
Uniform/
Symetrical
Taper
100 - ~~200~~ (7)
100
150
50
29
42
29
100
DIMENSIONS IN MICRONS

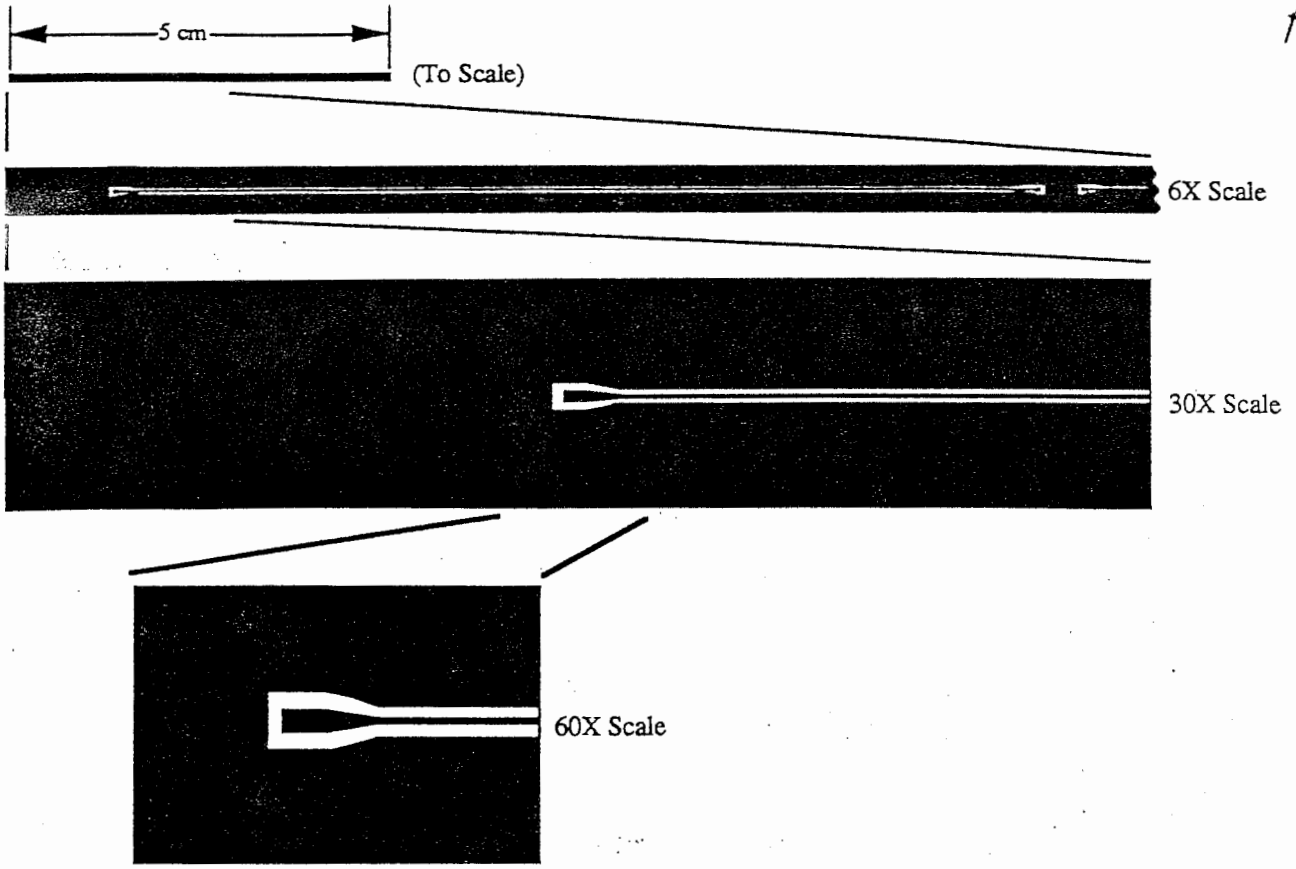

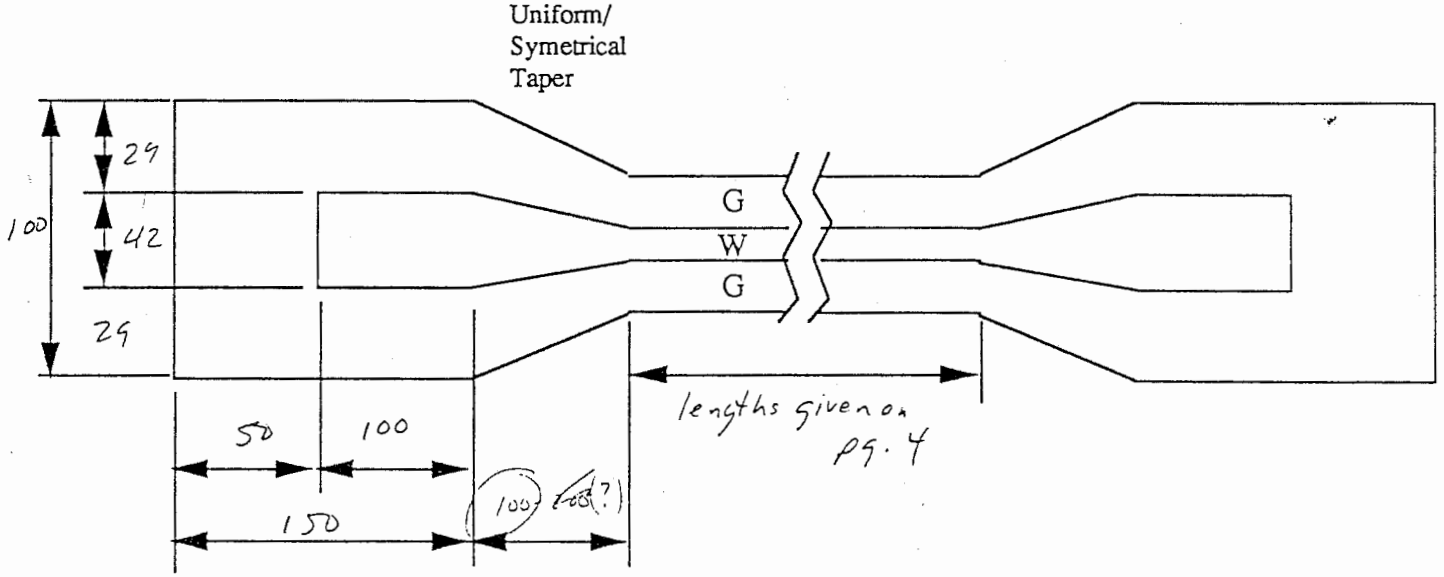

DIMENSIONS IN mm

Line is symetrical with respect to the center (half-way point)

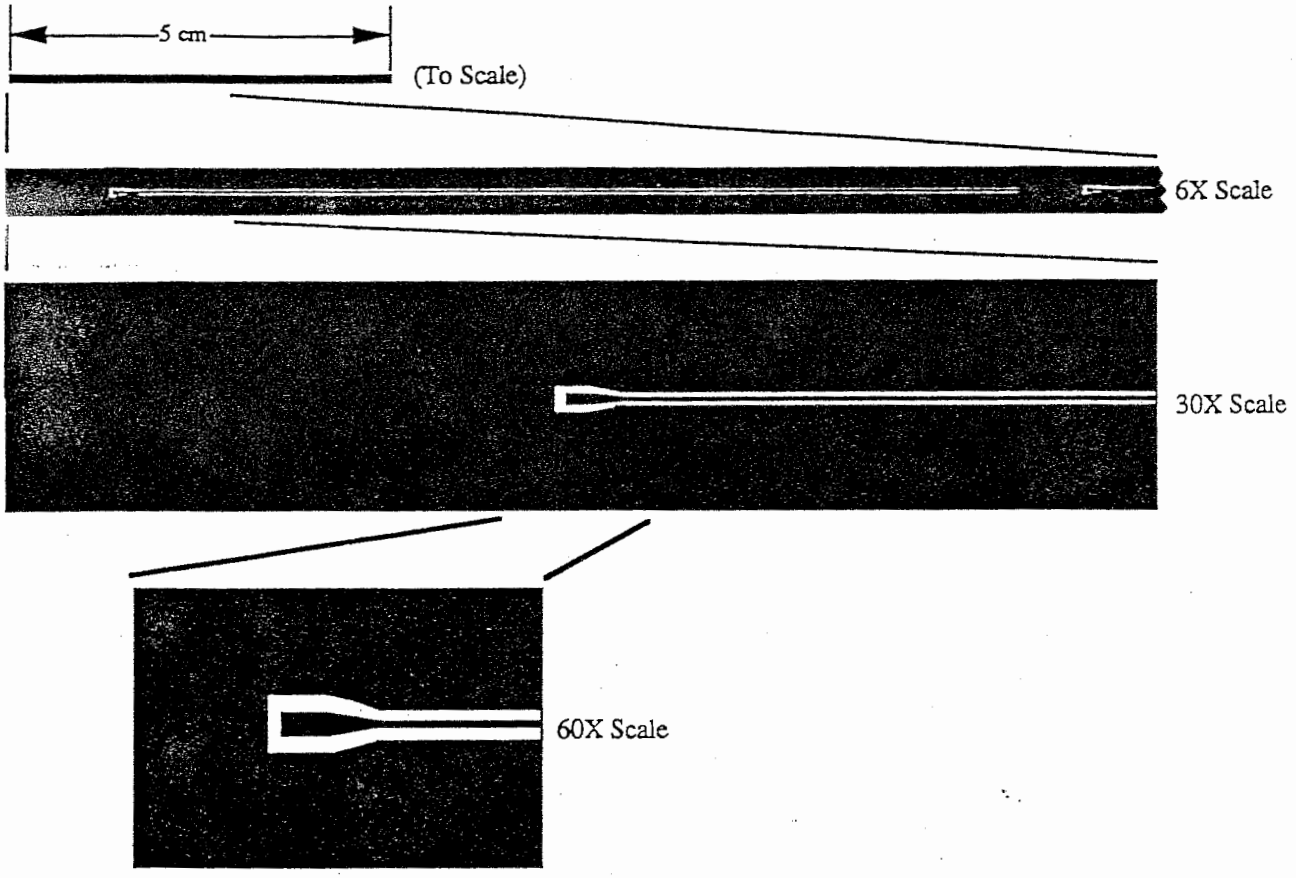

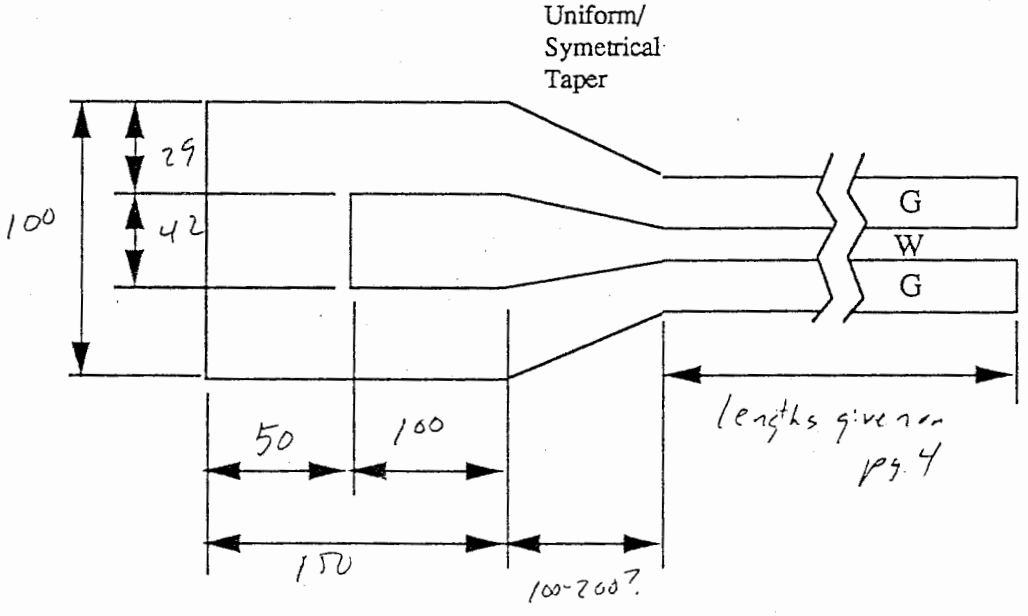

At end of transmission line there is a short to ground

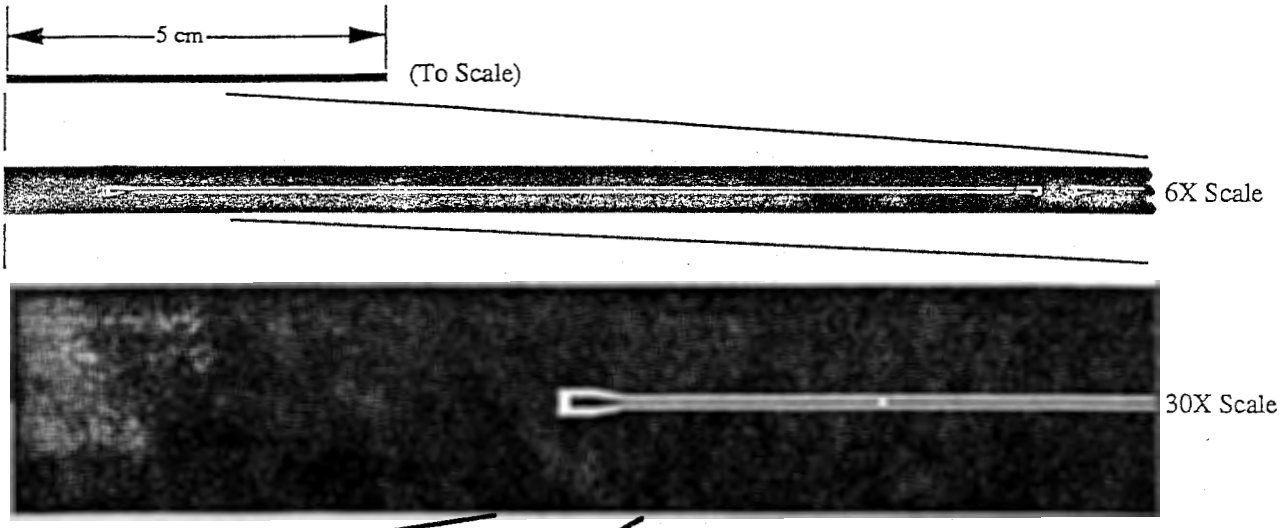
5 cm
(To Scale)
6X Scale
30X Scale

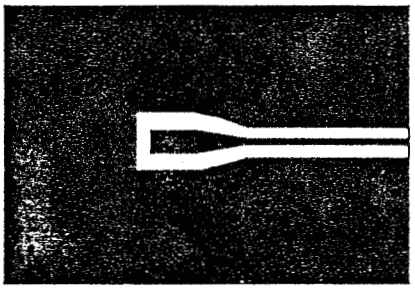
60X Scale

gap is ≤5μm
≈ 100μm
Reson. Type1
300μm
G
W
G
lengths given on pg. 4

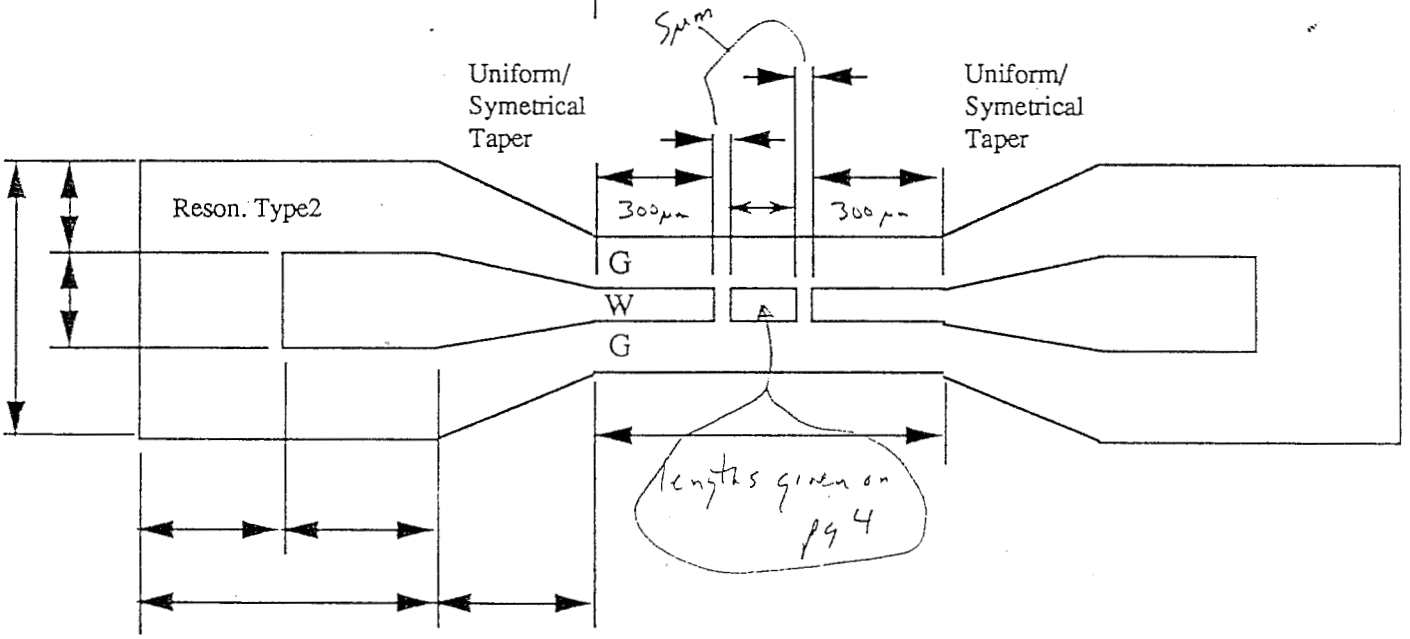
5μm
Uniform/
Symetrical
Taper
Uniform/
Symetrical
Taper
Reson. Type2
300μm
300μm
G
W
G
lengths given on
pg 4

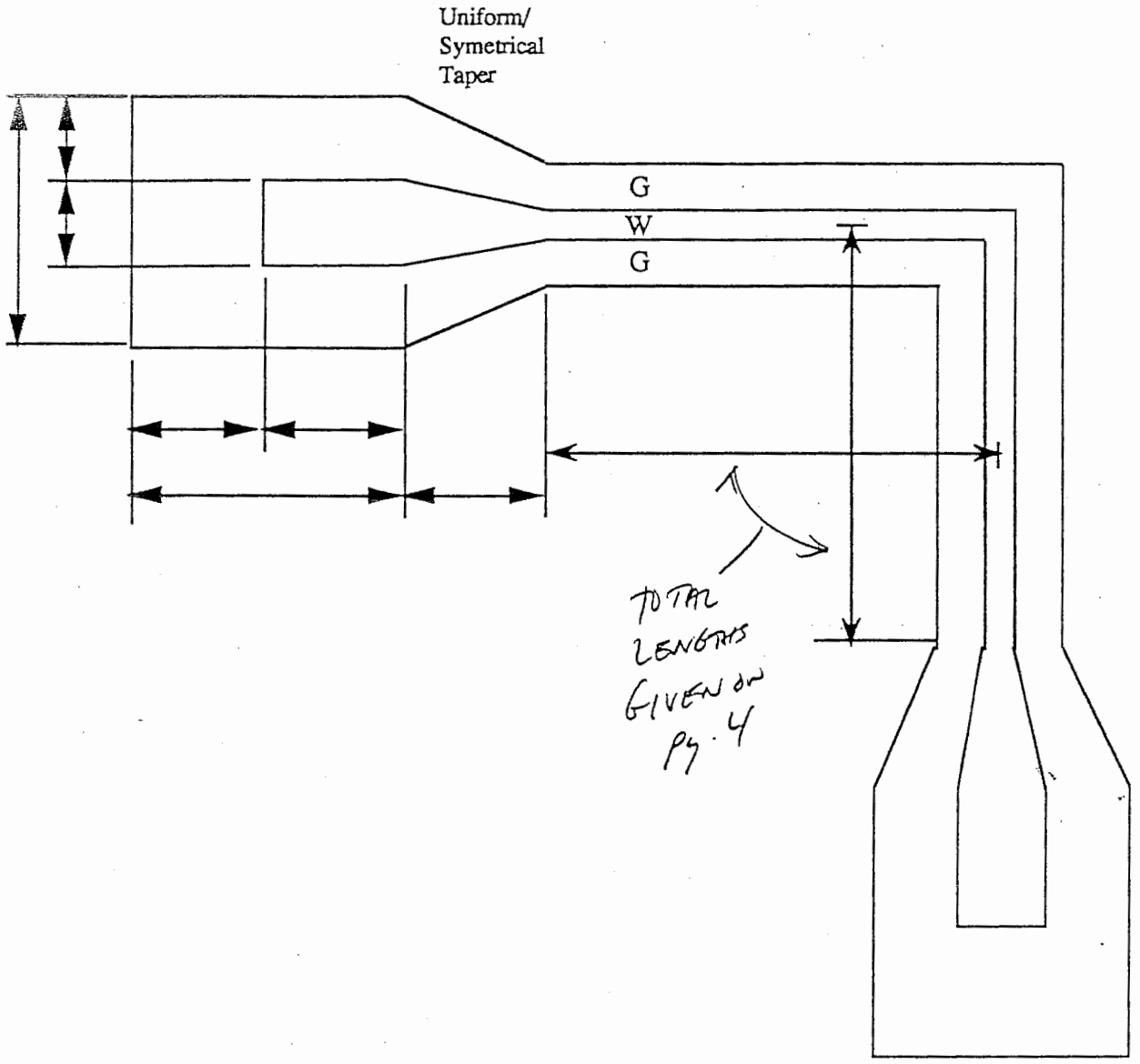
Uniform/
Symetrical
Taper
G
W
G
TOTAL
LENGTHS
GIVEN ON
Pg. 4

A4

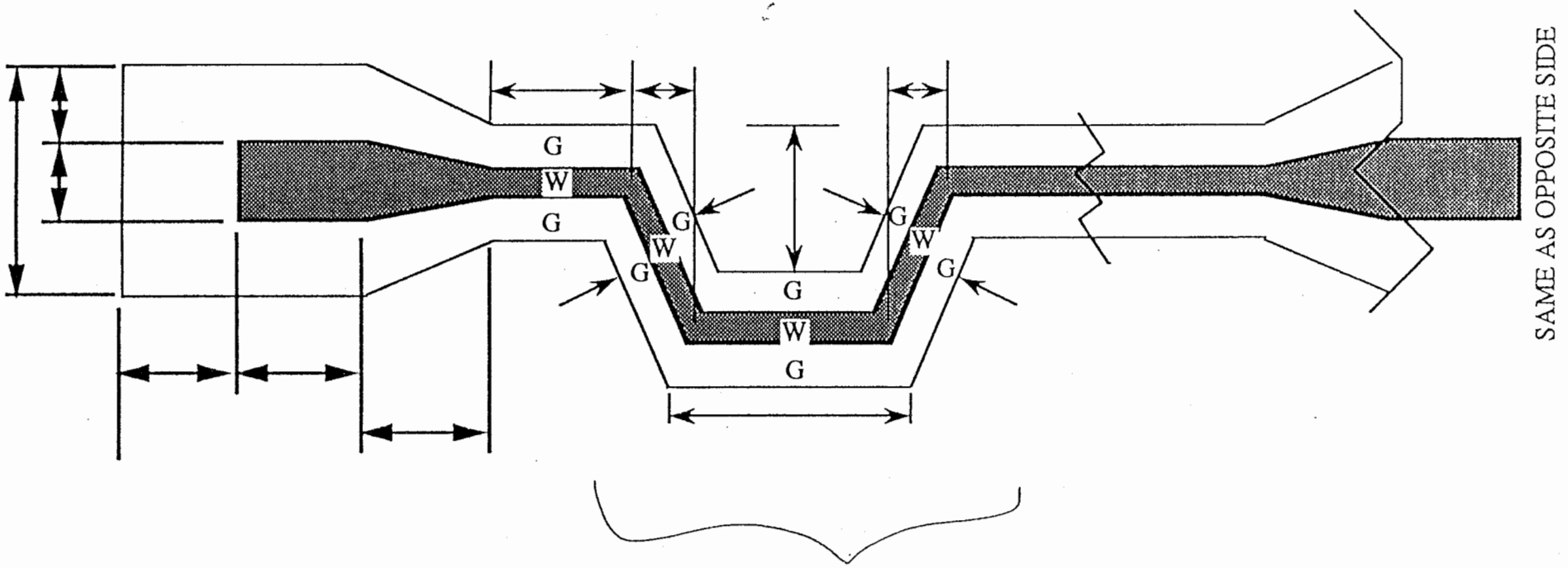

Several
Sections
of this
Structure

Will send more
info when I finish
the design.

12

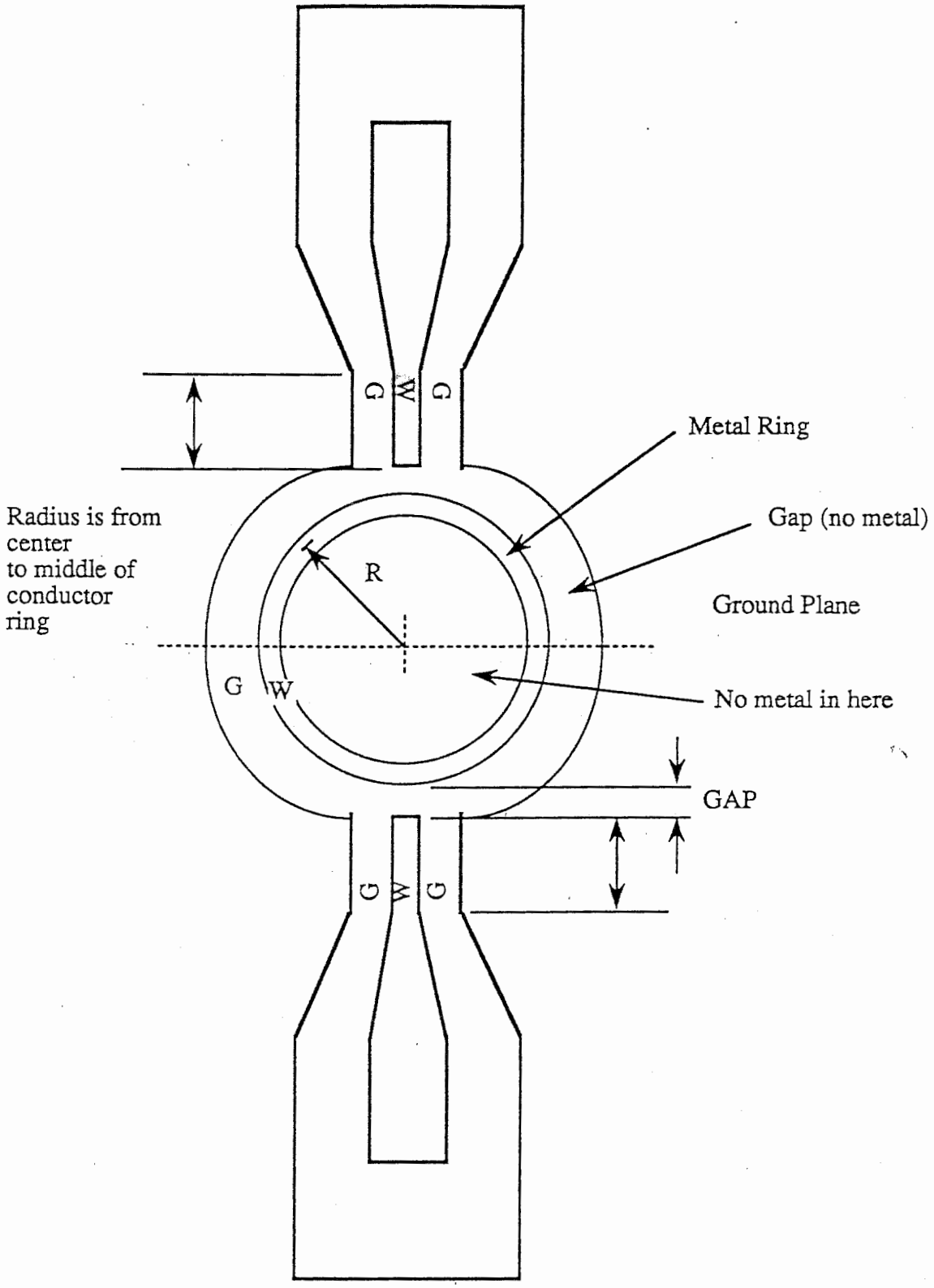
G
W
G
Metal Ring
Gap (no metal)
Radius is from center to middle of conductor ring
R
Ground Plane
G
W
No metal in here
GAP
G
W
G

Appendix B - Sample measurements of the test wafer

The following pages (B1-B14) include the following measurements of the wafer:

SiO_2 = 0.5 um
Electrode = 10 um

1. -Return loss of shorted lines (1, 2, 3, and 4 cm in length)
2. -Return and Insertion loss of straight through lines (1, 2, 3, and 4 cm in length)
3. -Return and Insertion loss of through - right angle bend - lines (1, 2, 3, and 4 cm in length)

   The dimensions are printed in the title block of each graph.
   All are taken with the HP 8510B ANA under calibration , 0.045 to 40 GHz.
   Date of measurements: 6-9-1992

4. Measurement of resistance vs. metalization height.

0.5/div

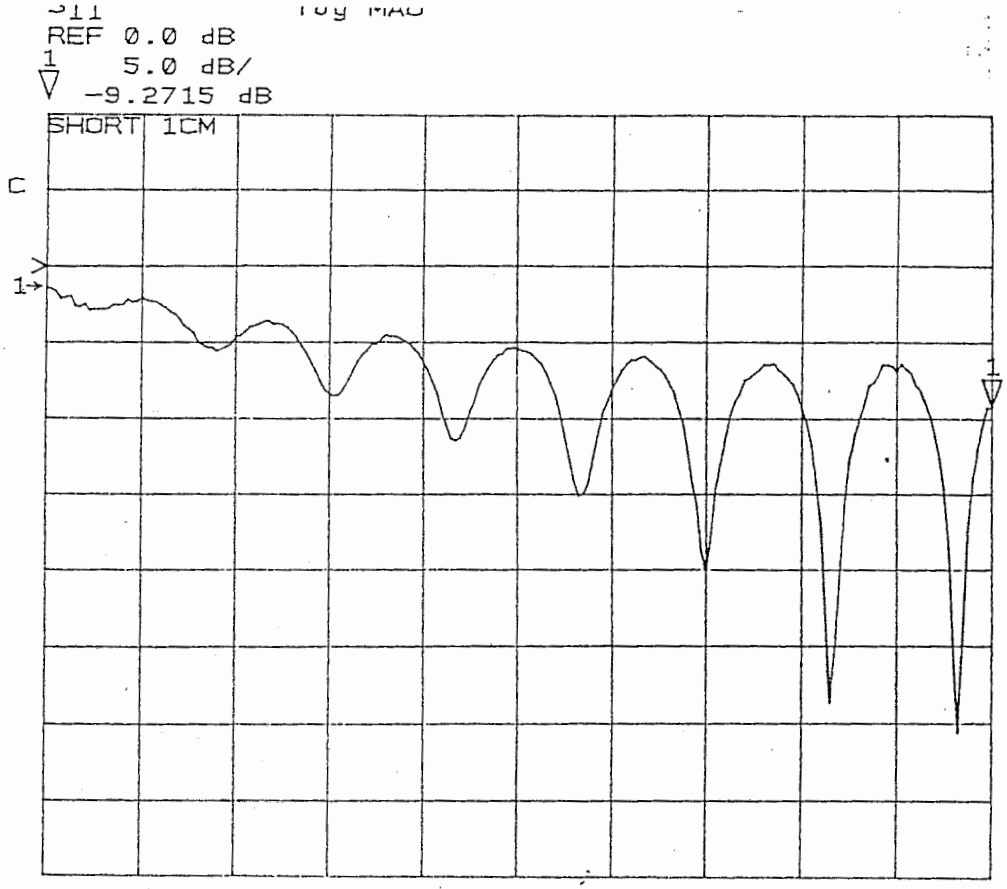

18

0.5/div

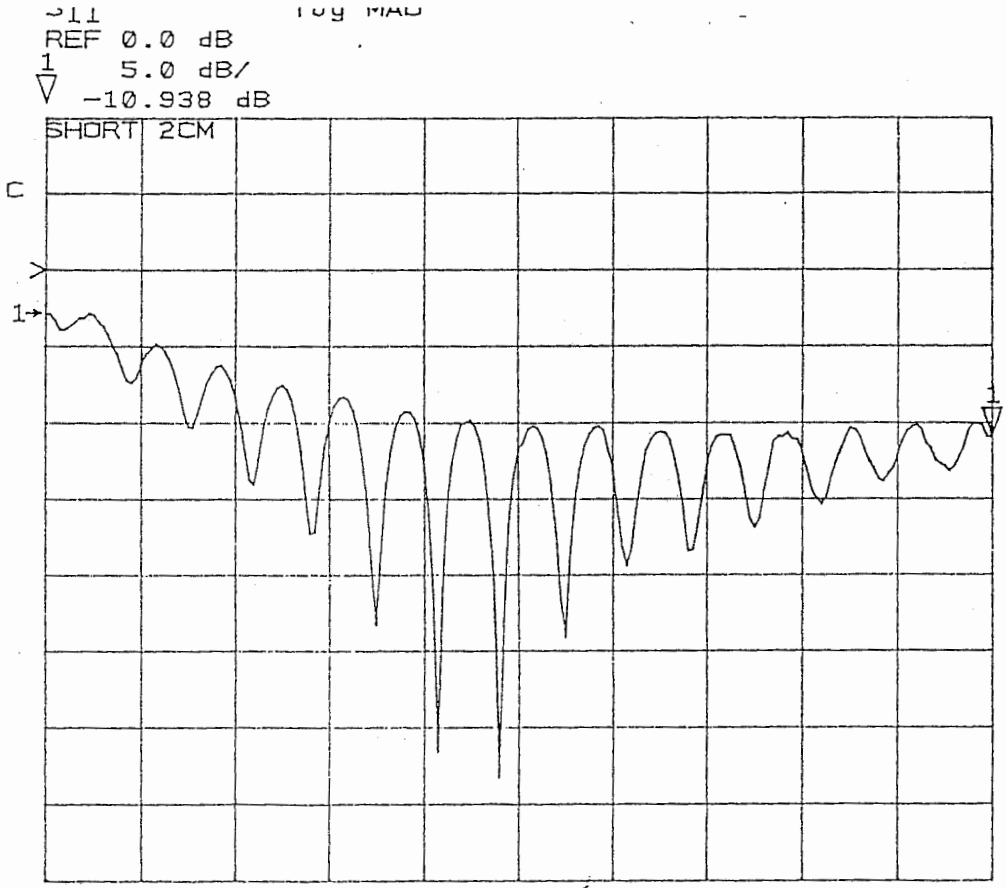

28

0.5/10

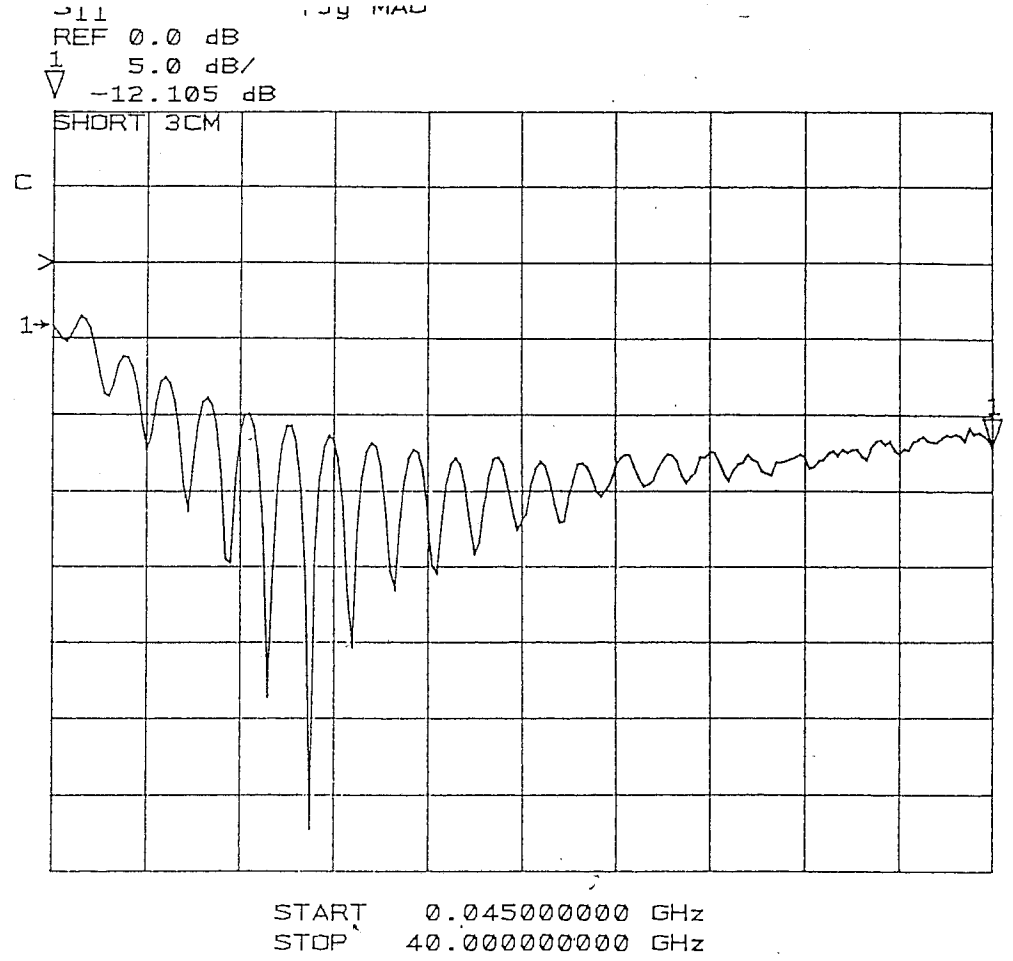

6/3/92
0.5/10

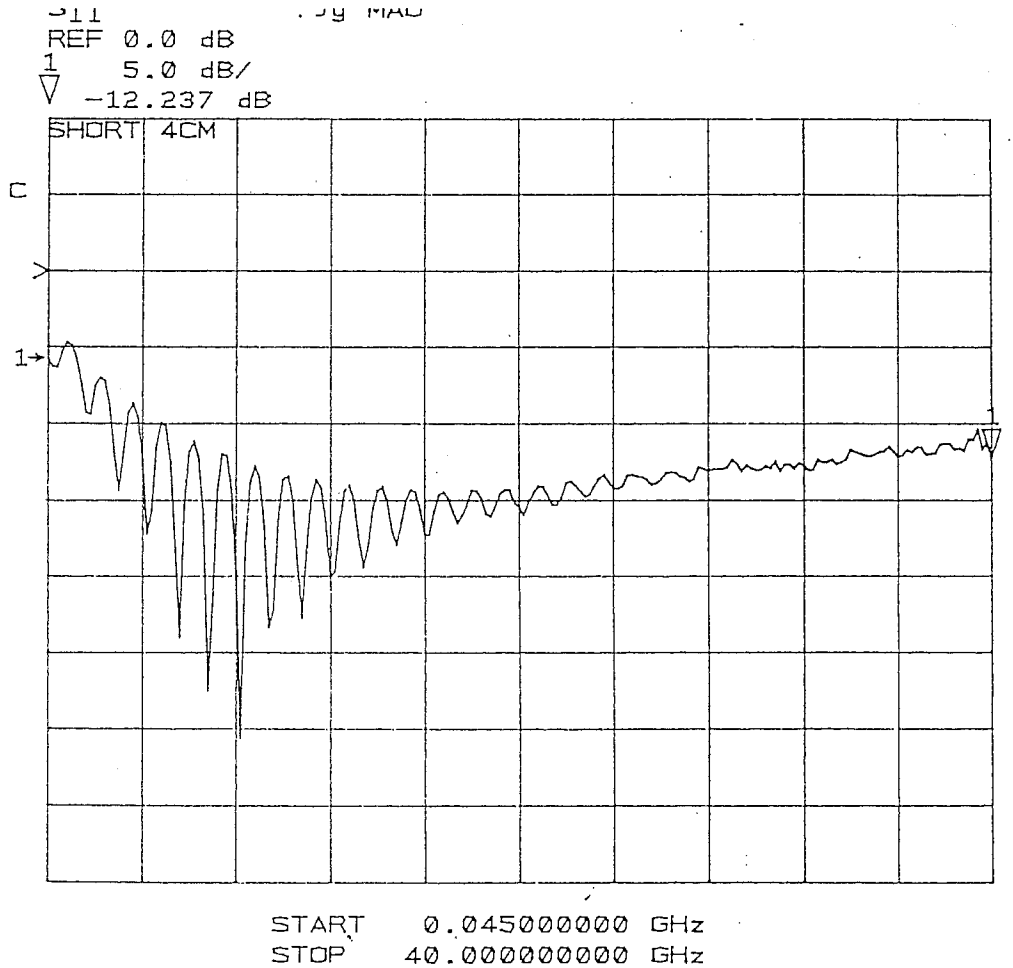

6/9/92
0.5/10
1cm
11.5 (VC)
(3.8c)

S21 log MAG
REF 0.0 dB
Δ 10.0 dB/
1 -9.0117 dB

S11 log MAG
REF 0.0 dB
1 10.0 dB/
▽ -10.755 dB

LS 7/15 1CM

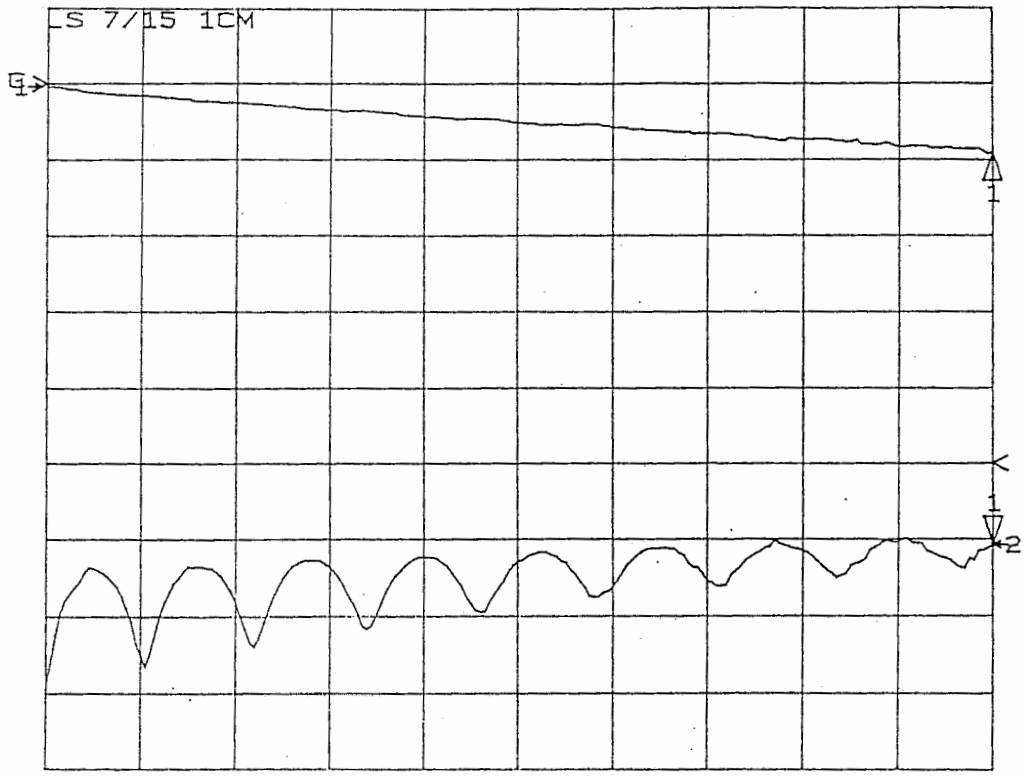

START 0.045000000 GHz
STOP 40.000000000 GHz

6/9/92
0.5/10
φ2cm LS
11.5 (VC)
(3.8c)

S21 log MAG
REF 0.0 dB
Δ 10.0 dB/
1 -16.068 dB

S11 log MAG
REF 0.0 dB
1 10.0 dB/
▽ -11.496 dB

LS 7/15 2CM

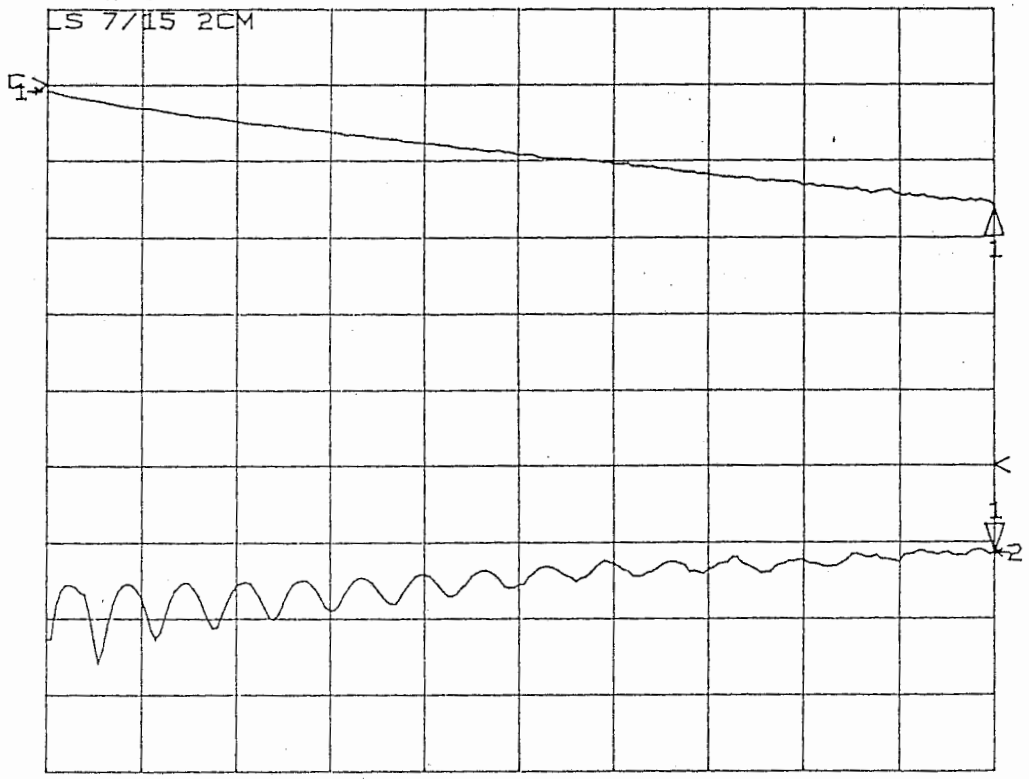

START 0.045000000 GHz
STOP 40.000000000 GHz

0.5/10

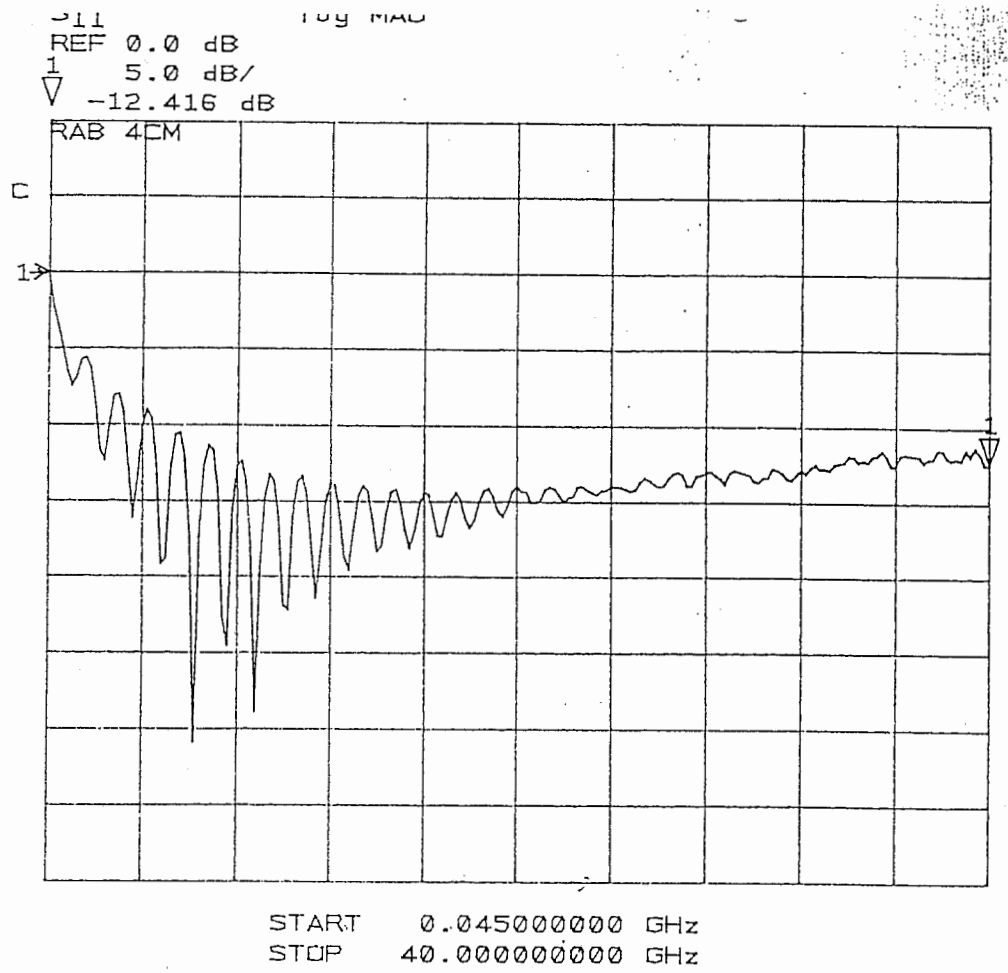

4/7/16
0.5/10

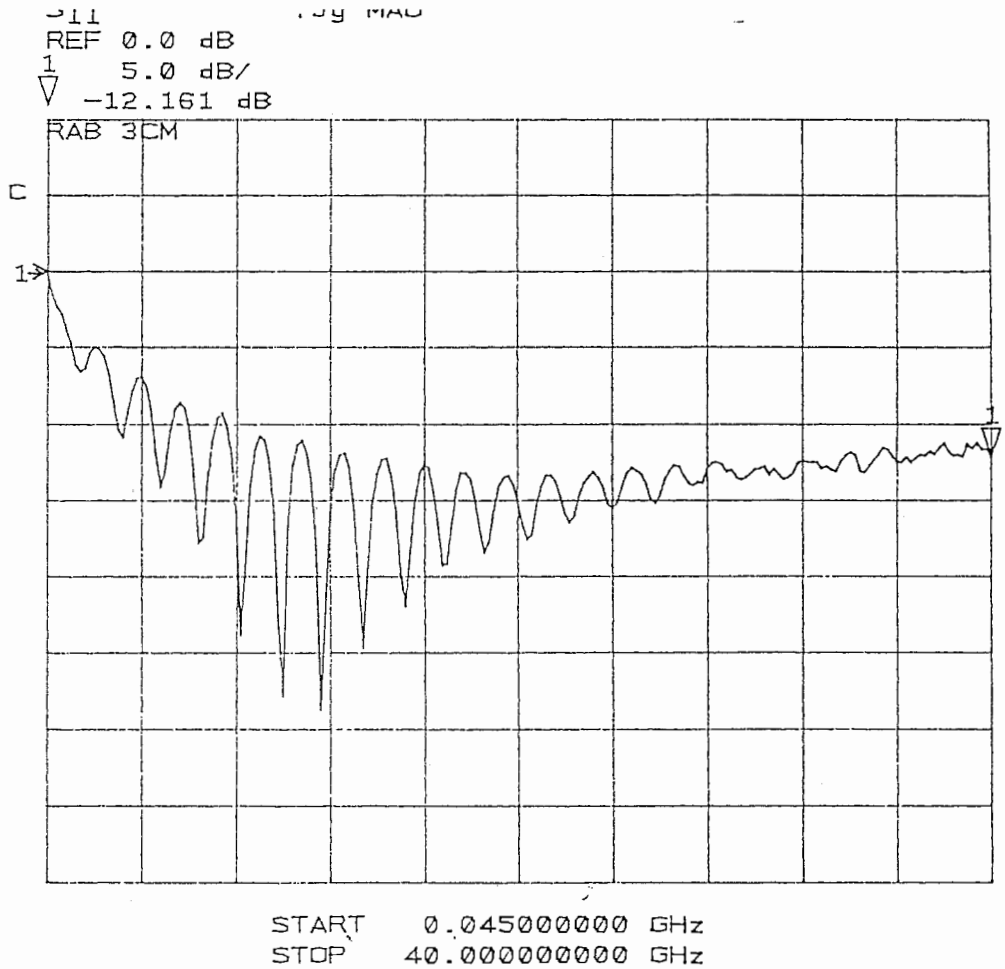

Appendix C - External Optical Modulator Wafer Layout

The following pages (C1-C15) include the rough layout of the modulator wafer and the image taken from the computerized CAD layout.

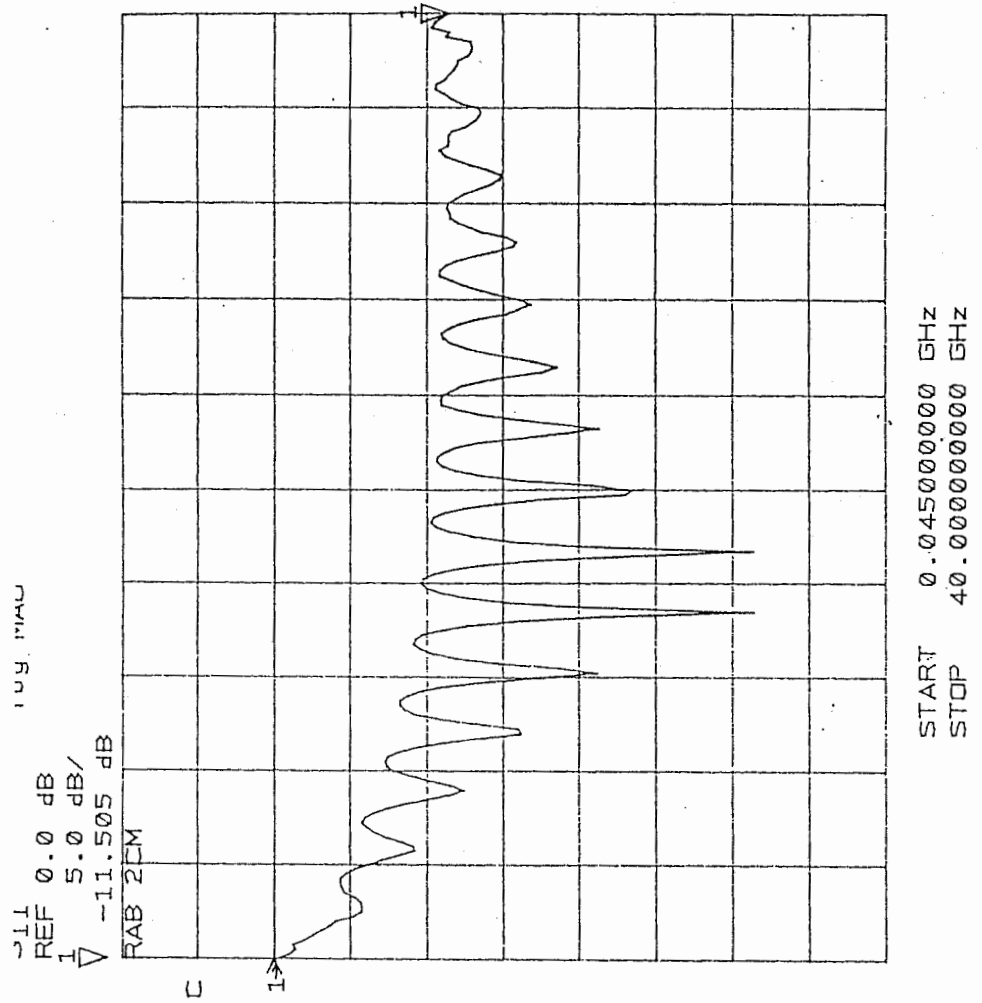

Appendix C - External Optical Modulator Wafer Layout

The following pages (C1-C15) include the rough layout of the modulator wafer and the image taken from the computerized CAD layout.

Appendix C - External Optical Modulator Wafer Layout

The following pages (C1-C15) include the rough layout of the modulator wafer and the image taken from the computerized CAD layout.

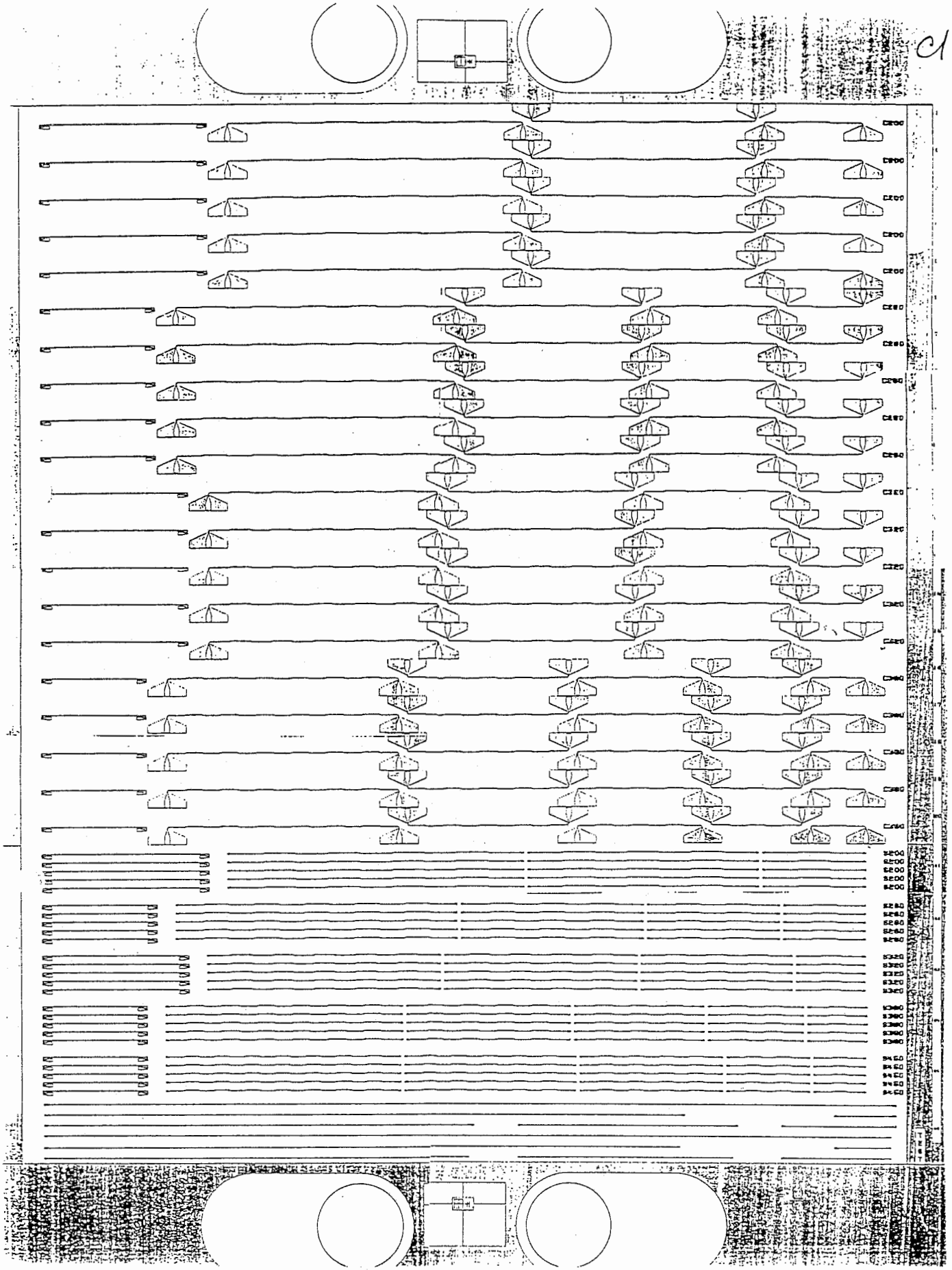

New Photomask Layout (General)

~~5~~ 4cmX5cm circuit area ~~(divided into 1mm rectangles (except the test structures which are 0.75mm width rectangles, each colored block is 5mm wide)~~

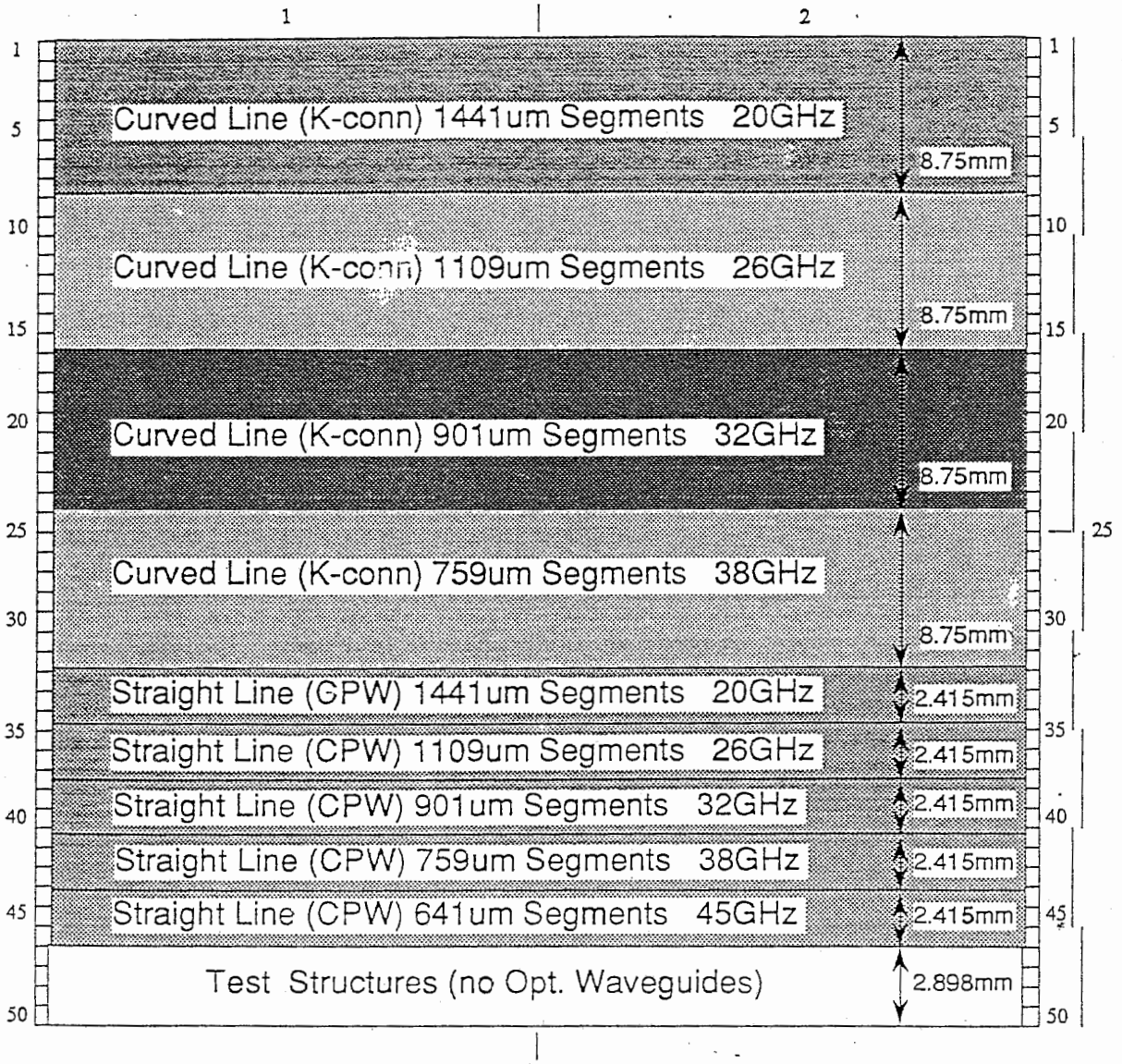

Example of above straight and curved lines, coax feeds alternate as shown for better spacing

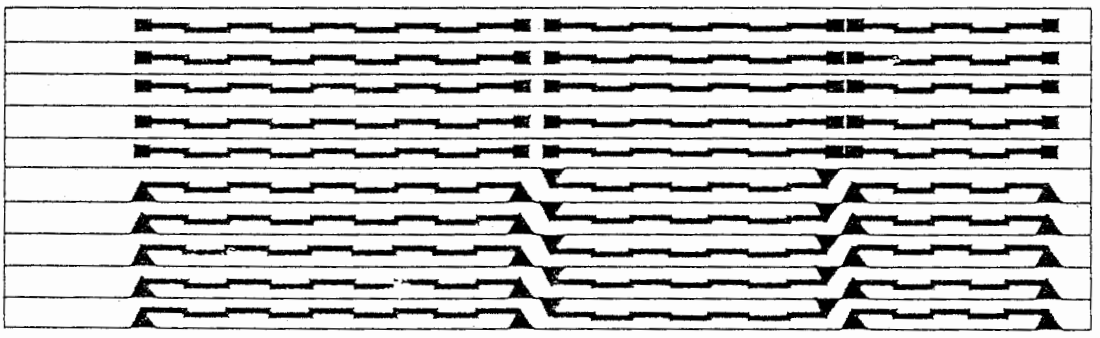

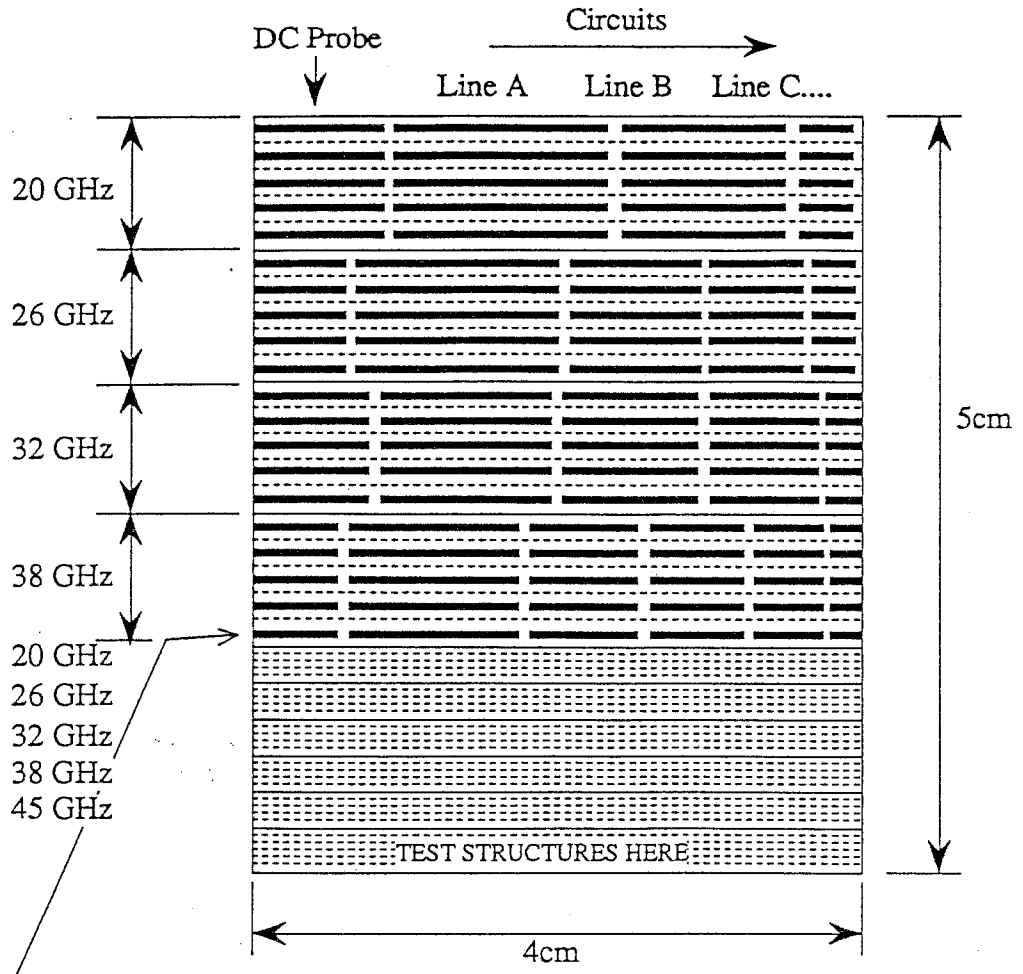

Metalization Circuit Area 4cm x 5cm

Dotted lines are divisions betweem similar designs ----------
Solid thin lines are divisions between different design frequencies ————
Solid thick lines are actual metal circuits which correspond to the table of dimensions. ————

The first circuit on each line is the DC Probe line

This page is approximately to scale: ———— 2cm
———— 1cm

NEW WAFER LAYOUT

Traveling wave - phase shifted lines - DIMENSIONS

All Dimensions in um (microns)
St. refers to a straight line with CPW contacts on both ends of the line
Crv. refers to a line with curved feeds to allow for coax to CPW transition (for packaging)
Spacing refers to the distance between each TW line on the same optical waveguide

#	Dim X	Dim Y	DC Prb test line	# shifts line A	# shifts line B	# shifts line C	# shifts line D	# shifts Line E	Dim K	Total Length	St or Crv	Freq GHz
1	1441	75	8000	4	3	1	-	-	40	39889	C	20
2	1441	75	8000	4	3	1	-	-	40	39889	C	20
3	1441	75	8000	4	3	1	-	-	40	39889	C	20
4	1441	75	8000	4	3	1	-	-	40	39889	C	20
5	1441	75	8000	4	3	1	-	-	40	39889	C	20
6	1109	75	5500	5	3	2	1	-	40	39894	C	26
7	1109	75	5500	5	3	2	1	-	40	39894	C	26
8	1109	75	5500	5	3	2	1	-	40	39894	C	26
9	1109	75	5500	5	3	2	1	-	40	39894	C	26
10	1109	75	5500	5	3	2	1	-	40	39894	C	26
11	901	75	7000	5	4	3	1	-	40	39890	C	32
12	901	75	7000	5	4	3	1	-	40	39890	C	32
13	901	75	7000	5	4	3	1	-	40	39890	C	32
14	901	75	7000	5	4	3	1	-	40	39890	C	32
15	901	75	7000	5	4	3	1	-	40	39890	C	32
16	759	75	5000	6	4	3	2	1	40	39993	C	38
17	759	75	5000	6	4	3	2	1	40	39993	C	38
18	759	75	5000	6	4	3	2	1	40	39993	C	38
19	759	75	5000	6	4	3	2	1	40	39993	C	38
20	759	75	5000	6	4	3	2	1	40	39993	C	38
21	1441	75	8000	4	3	1	-	-	40	39889	S	20
22	1441	75	8000	4	3	1	-	-	40	39889	S	20
23	1441	75	8000	4	3	1	-	-	40	39889	S	20
24	1441	75	8000	4	3	1	-	-	40	39889	S	20
25	1441	75	8000	4	3	1	-	-	40	39889	S	20
26	1109	75	5500	5	3	2	1	-	40	39894	S	26
27	1109	75	5500	5	3	2	1	-	40	39894	S	26
28	1109	75	5500	5	3	2	1	-	40	39894	S	26
29	1109	75	5500	5	3	2	1	-	40	39894	S	26
30	1109	75	5500	5	3	2	1	-	40	39894	S	26
31	901	75	7000	5	4	3	1	-	40	39890	S	32
32	901	75	7000	5	4	3	1	-	40	39890	S	32
33	901	75	7000	5	4	3	1	-	40	39890	S	32
34	901	75	7000	5	4	3	1	-	40	39890	S	32
35	901	75	7000	5	4	3	1	-	40	39890	S	32
36	759	75	5000	6	4	3	2	1	40	39993	S	38
37	759	75	5000	6	4	3	2	1	40	39993	S	38
38	759	75	5000	6	4	3	2	1	40	39993	S	38
39	759	75	5000	6	4	3	2	1	40	39993	S	38
40	759	75	5000	6	4	3	2	1	40	39993	S	38
41	641	75	5000	7	5	4	2	1	40	39923	S	45
42	641	75	5000	7	5	4	2	1	40	39923	S	45
43	641	75	5000	7	5	4	2	1	40	39923	S	45
44	641	75	5000	7	5	4	2	1	40	39923	S	45
45	641	75	5000	7	5	4	2	1	40	39923	S	45

Test Pattern Structures

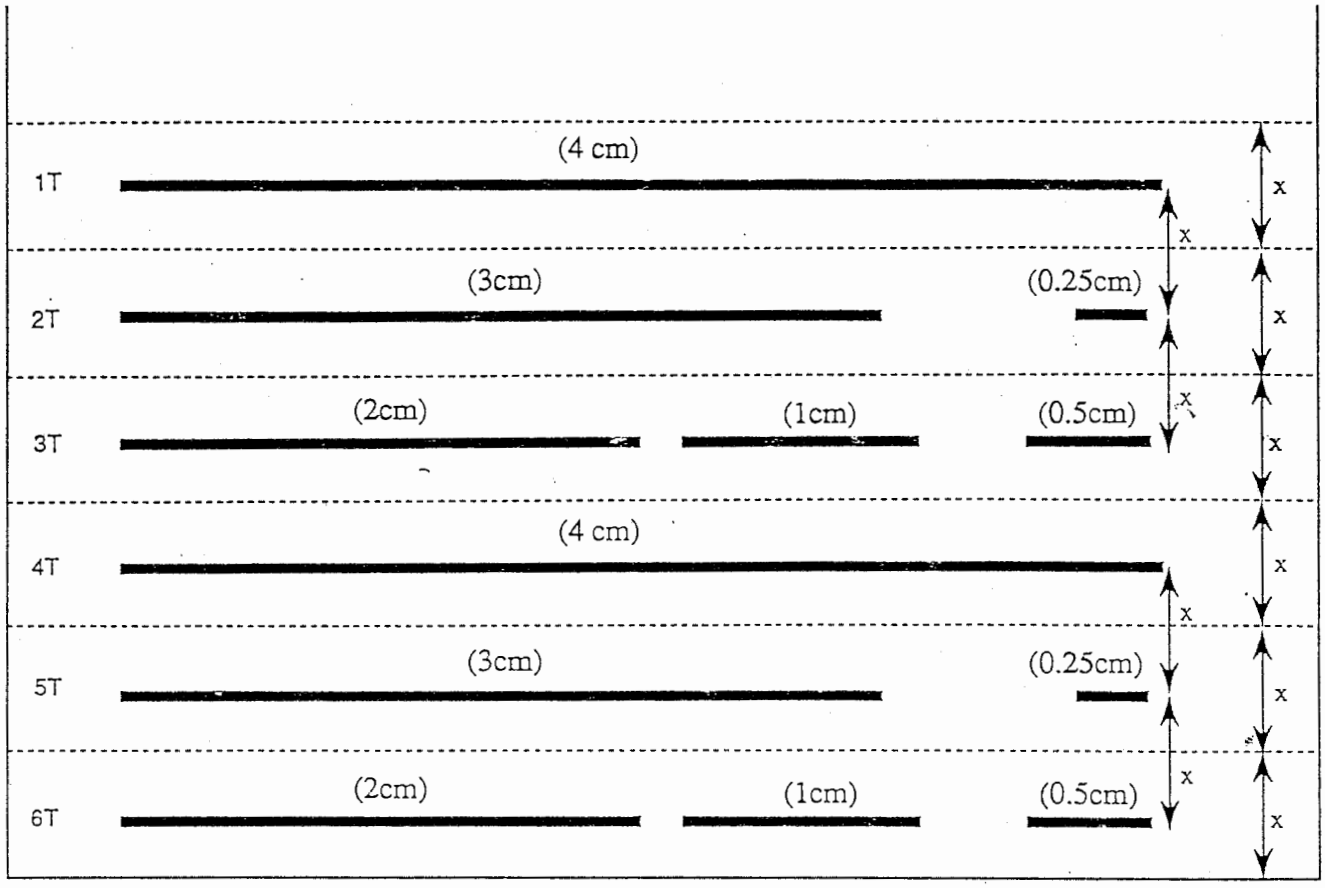

Notes:

1. All lettering above in parenthesis are will not be on the mask, they are there only for reference.
2. The numbers on the left side of the drawing should be made on the mask for use when measuring the wafer. They should be at least 2mm to the left of the line.
3. Lines 1T-3T are straight two port lines and lines 4T-6T are shorted lines.
4. The distance x = **0.483mm**
5. The dotted lines above are only for reference,they will not be on the final wafer
6. These test structures should be on the **bottom** of the wafer and do not need optical waveguides below them.

DC Probe test line - (CPW Probe type contacts)

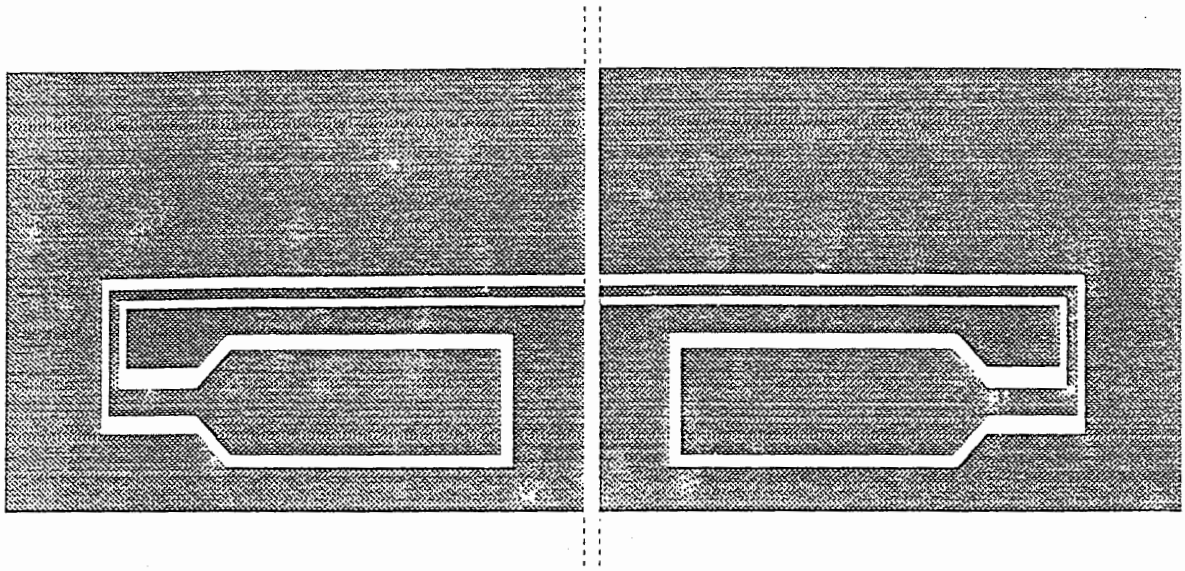

Metalization (top view)

Opt. waveguide position under metal

G = 25
W = 7
G = 25

See additional page for dimensions (DC Prb test line)

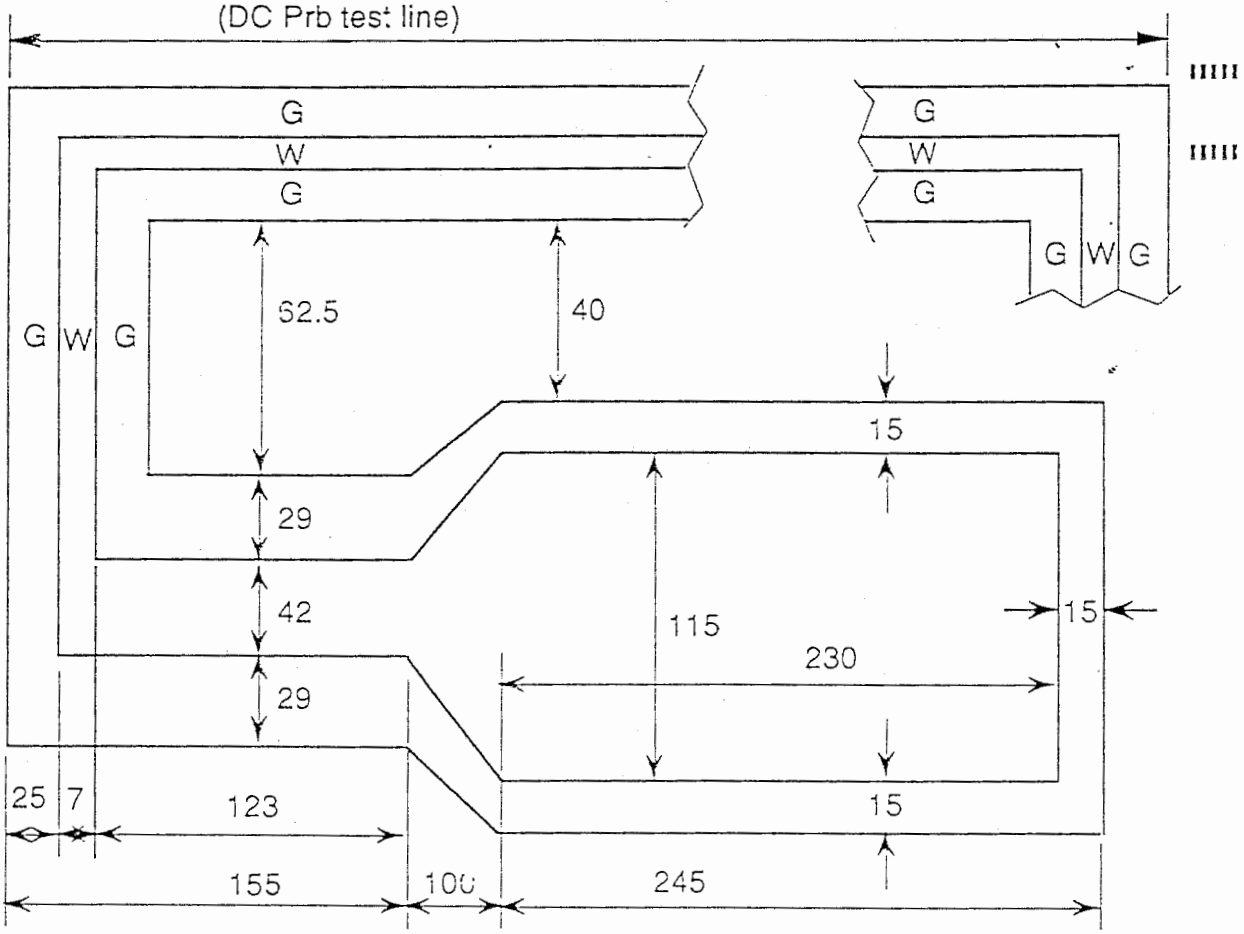

Straight Line (2 port through) - CPW Probe contacts (lines 1T-3T)

(Also contact dimensions are for TW lines)

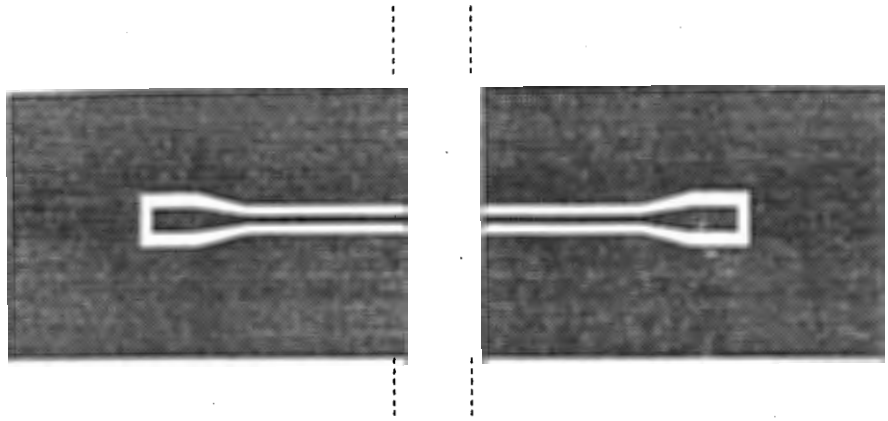

Metalization (top view)

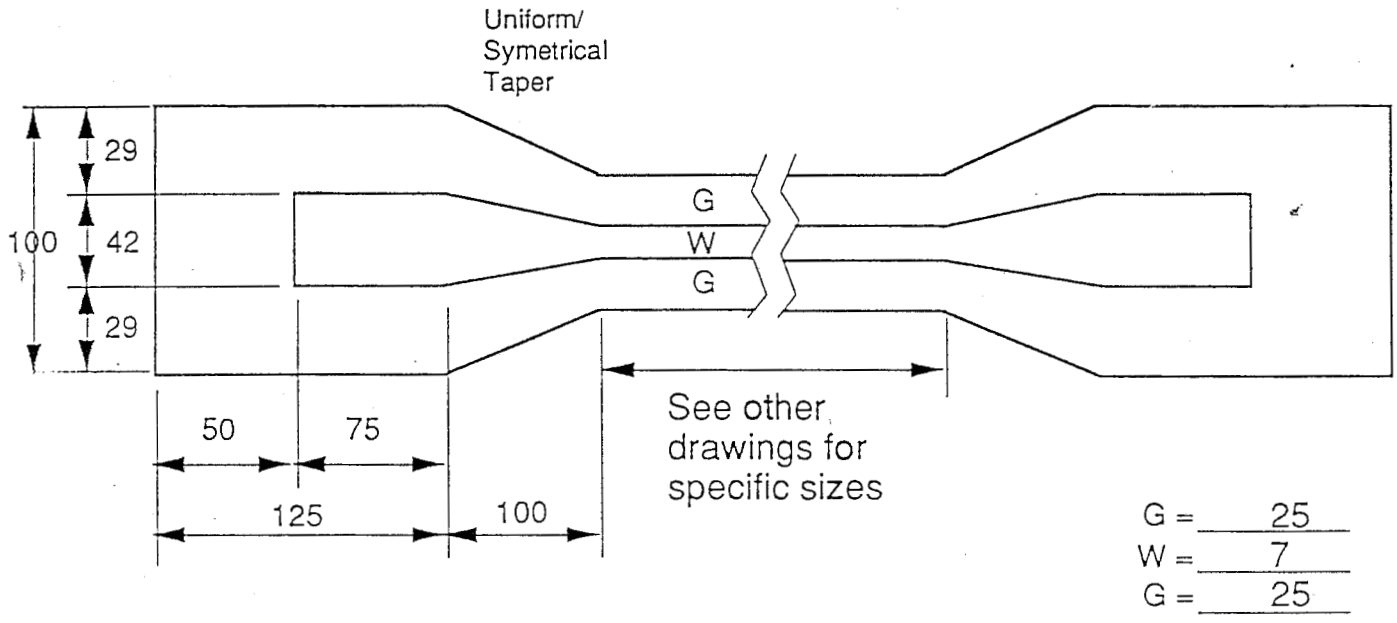

CPW line is symetrical with respect to the center (half-way point)

Shorted Line (1 port) - CPW Probe contact (lines 4T-6T)

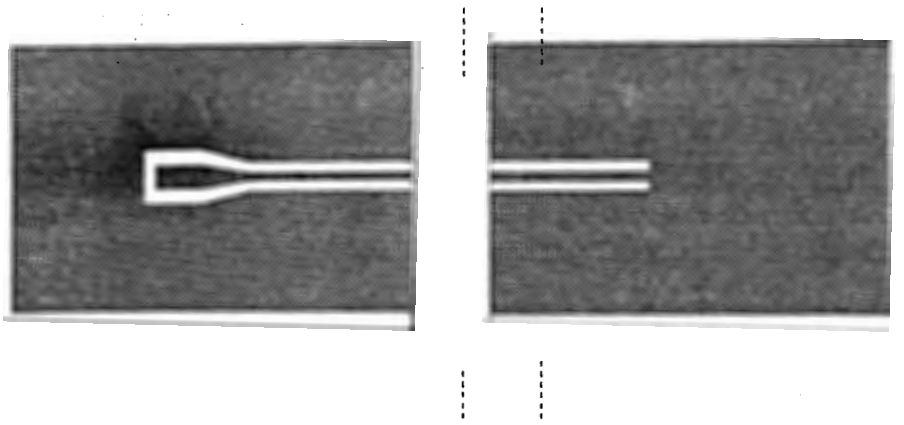

Metalization (top view)

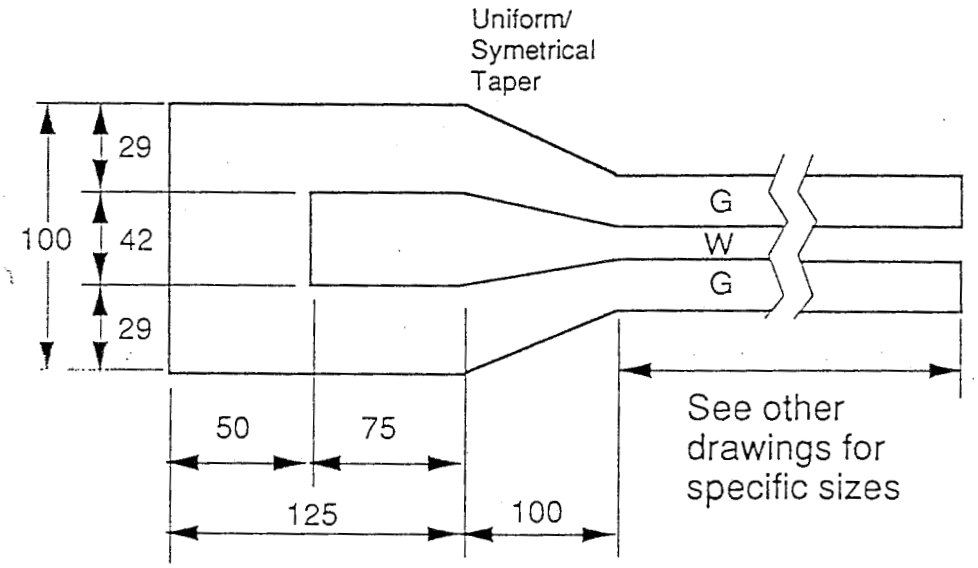

G = 25
W = 7
G = 25

Phase Shifted Travelling Wave Modulator Concept

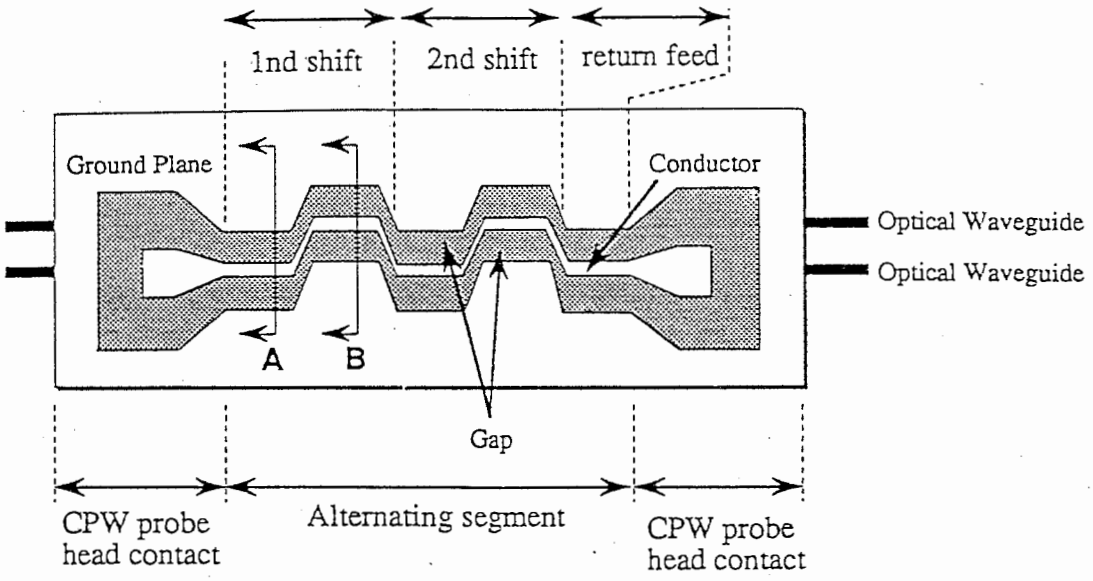

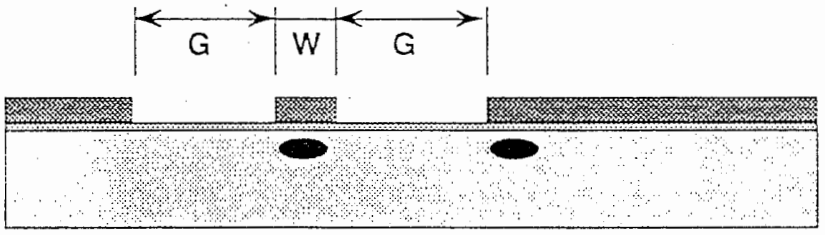

Cross sectional view at A

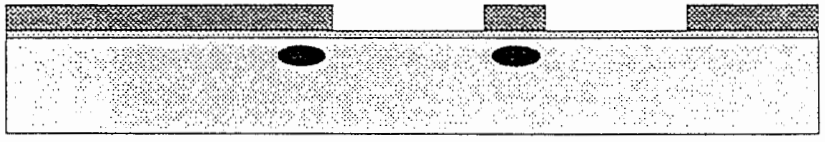

Cross sectional view at B

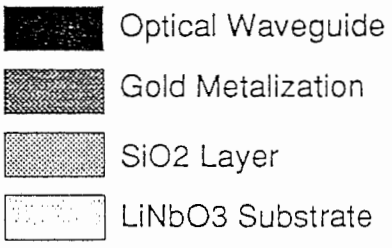

CD

Dimensions in um (microns)

G = 25
W = 7
G = 25

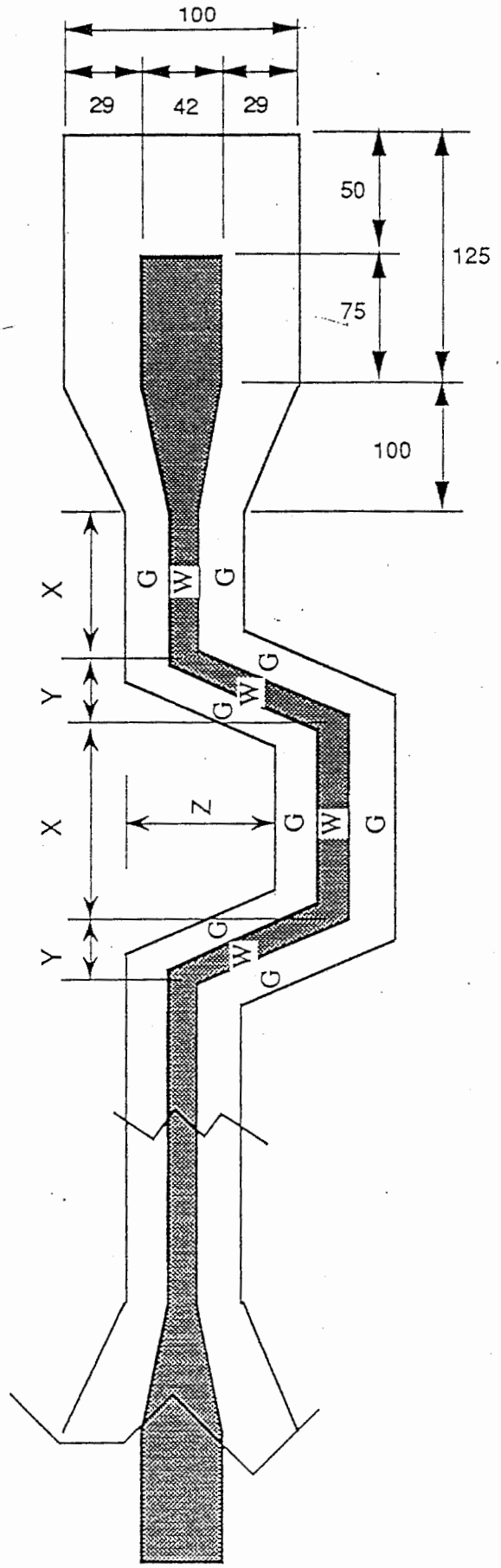

SAME AS OPPOSITE SIDE

Curved Line (2 port through) - K-connector launch

(TW-Phase Shifted Lines)

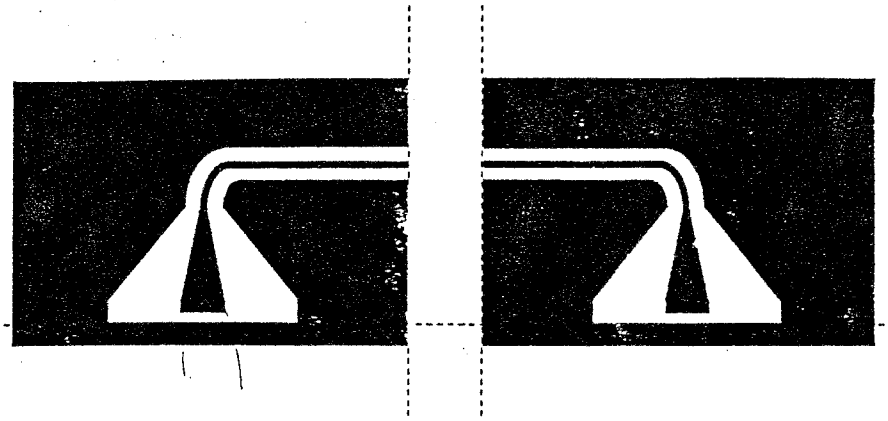

Wafer should be cut on this line

Metalization (top view)

Between the vertical dotted lines are the phase shift travelling wave lines - for dimensions, see other pages

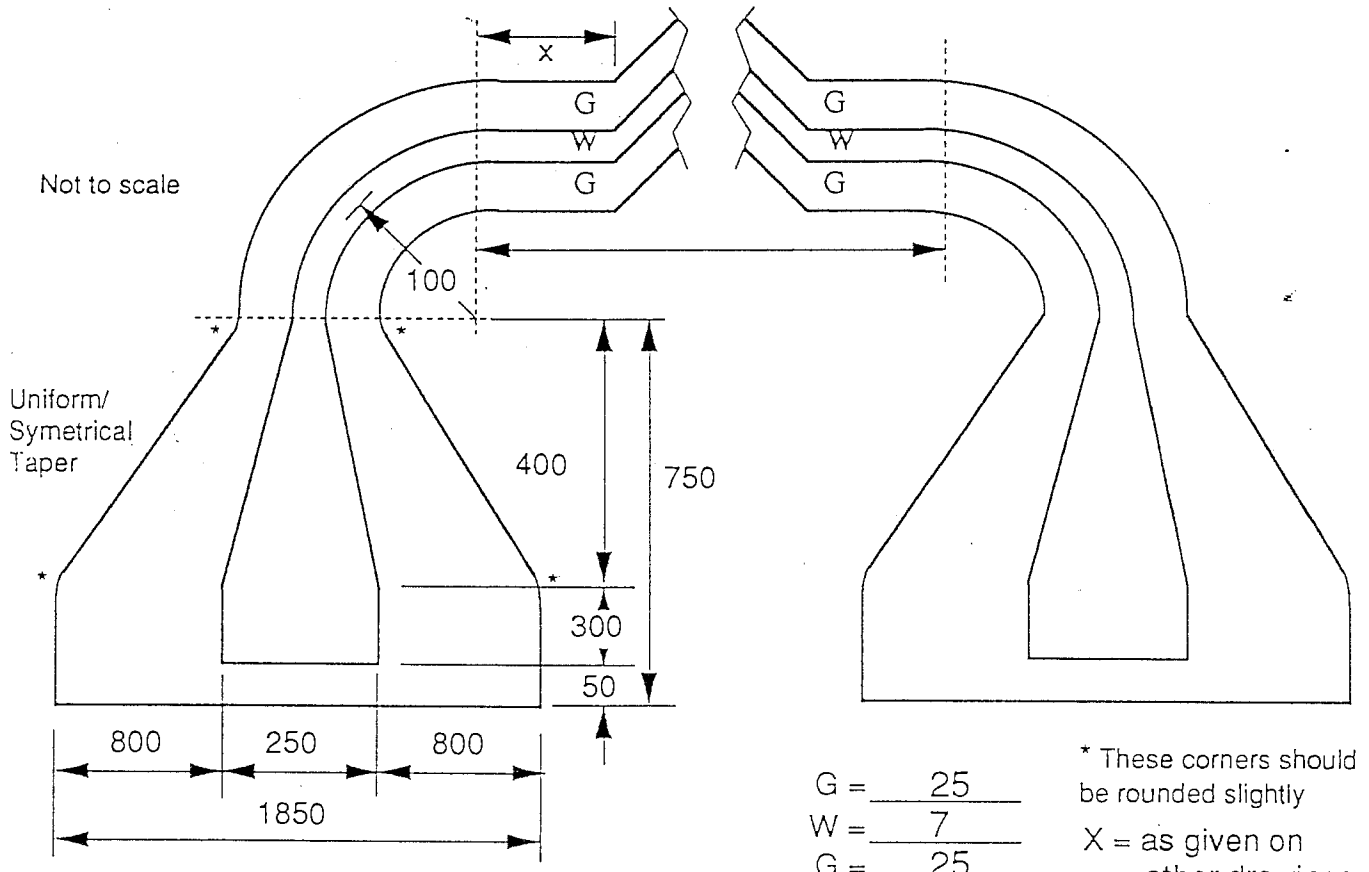

G = 25
W = 7
G = 25

* These corners should be rounded slightly

X = as given on other drawings

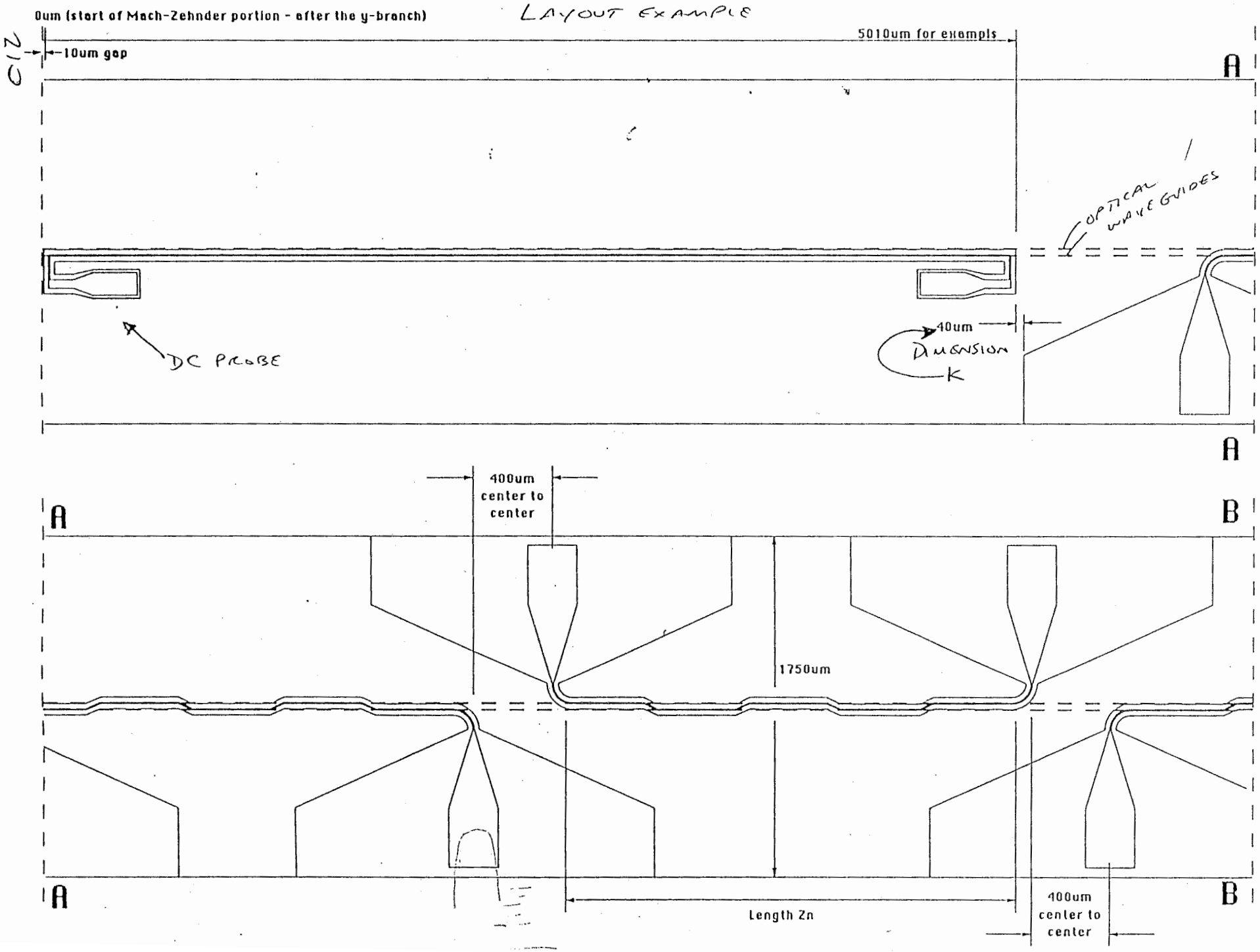
LAYOUT EXAMPLE
0um (start of Mach-Zehnder portion - after the y-branch)
5010um for exampls
10um gap
A
A
OPTICAL WAVEGUIDES
DC PROBE
40um
DIMENSION
K
400um
center to
center
A
B
1750um
A
B
Length Zn
400um
center to
center

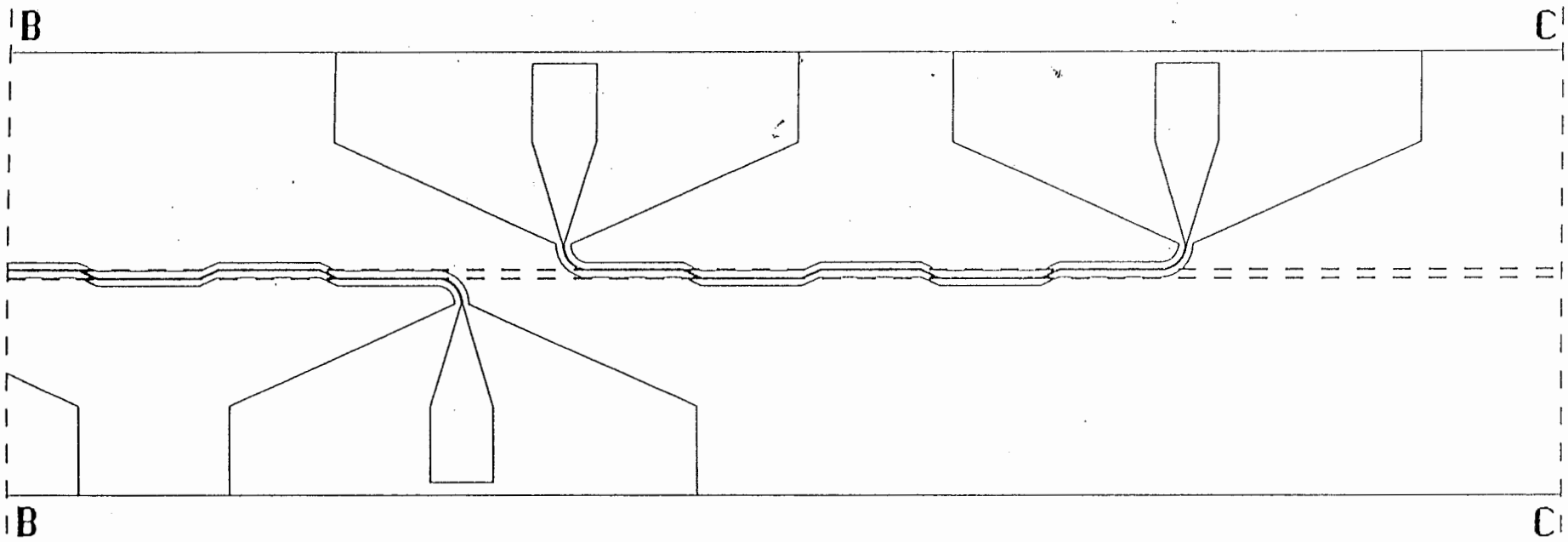
B
C
B
C

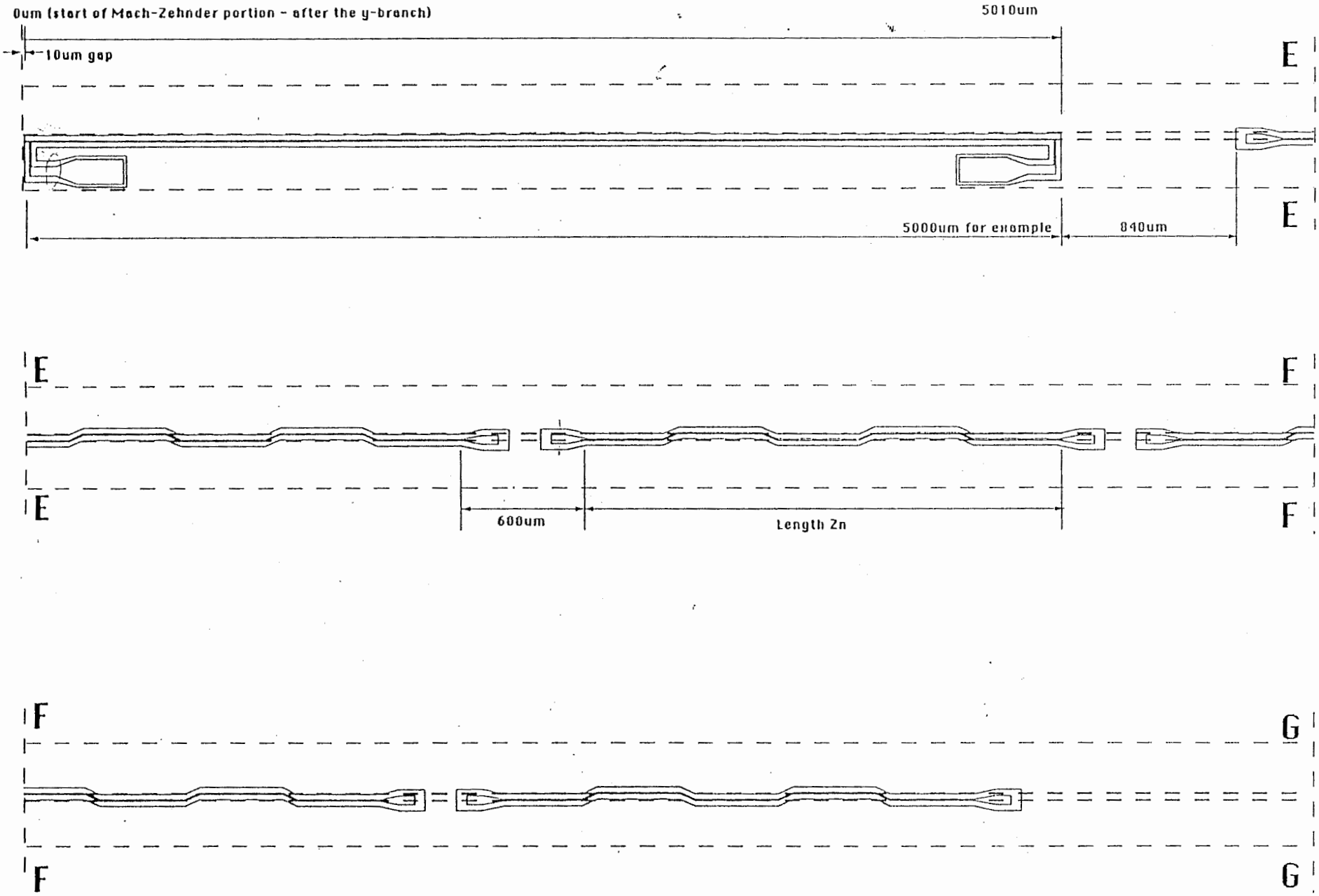
0um (start of Mach-Zehnder portion - after the y-branch)
5010um
10um gap
E
E
5000um for example
840um
E
F
E
F
600um
Length Zn
F
G
F
G

(1)

$$\lambda = \frac{c}{2f(n_o - n_m)}$$

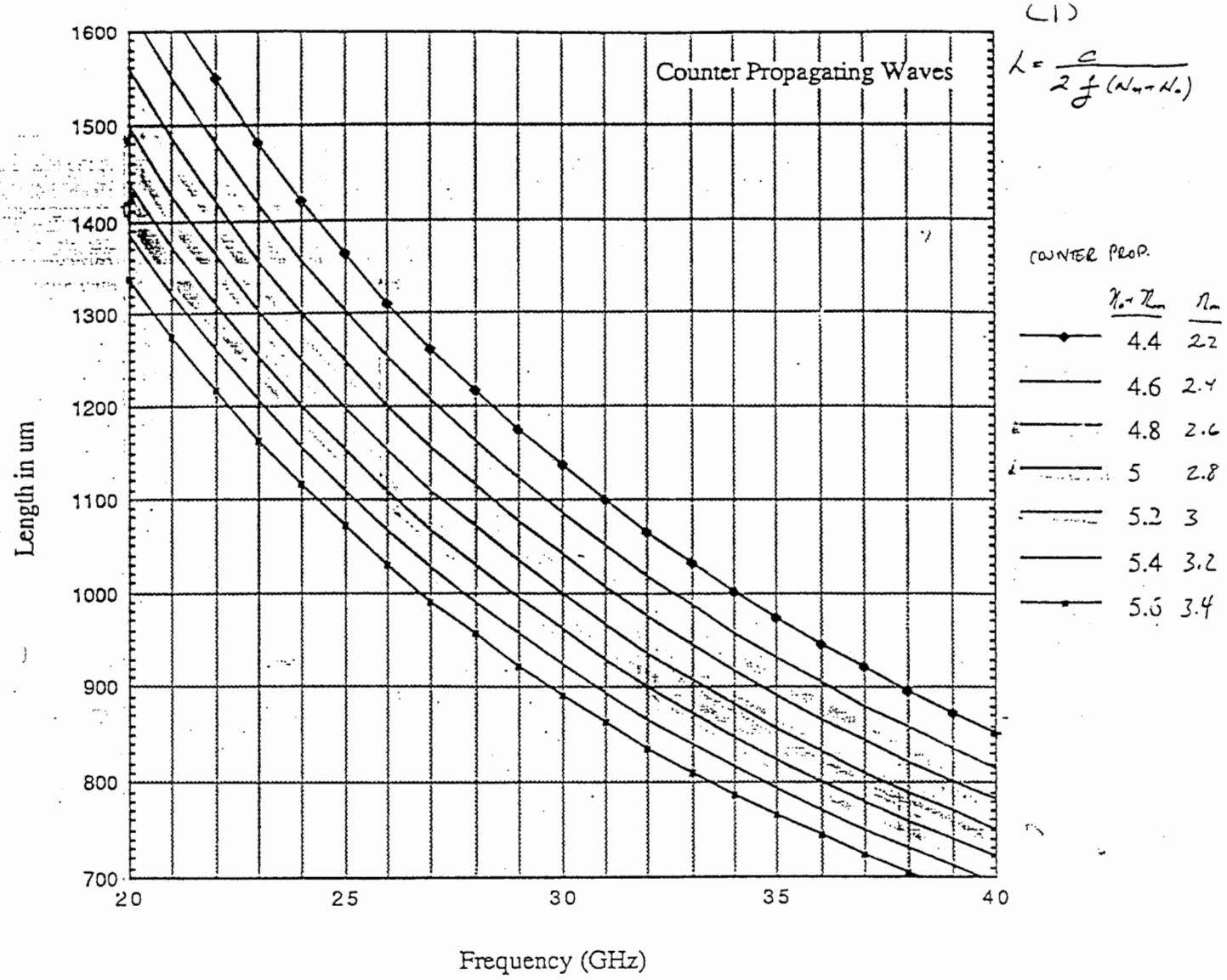

	GHz	4.4	4.6	4.8	5	5.2	5.4	5.6
1	20	1703	1629	1561	1499	1441	1388	1338
2	21	1622	1552	1487	1428	1373	1322	1275
3	22	1549	1481	1419	1363	1310	1262	1217
4	23	1481	1417	1358	1303	1253	1207	1164
5	24	1419	1358	1301	1249	1201	1157	1115
6	25	1363	1303	1249	1199	1153	1110	1071
7	26	1310	1253	1201	1153	1109	1068	1029
8	27	1262	1207	1157	1110	1068	1028	991
9	28	1217	1164	1115	1071	1029	991	956
10	29	1175	1124	1077	1034	994	957	923
11	30	1136	1086	1041	999	961	925	892
12	31	1099	1051	1007	967	930	895	863
13	32	1065	1018	976	937	901	867	836
14	33	1032	987	946	908	874	841	811
15	34	1002	958	918	882	848	816	787
16	35	973	931	892	857	824	793	765
17	36	946	905	867	833	801	771	744
18	37	921	881	844	810	779	750	723
19	38	897	858	822	789	759	730	704
20	39	874	836	801	769	739	712	686

	GHz	4.4	4.6	4.8	5	5.2	5.4	5.6
21	40	852	815	781	749	721	694	669
22	41	831	795	762	731	703	677	653
23	42	811	776	744	714	686	661	637
24	43	792	758	726	697	670	646	622
25	44	774	741	710	681	655	631	608
26	45	757	724	694	666	641	617	595
27	46	741	708	679	652	627	603	582
28	47	725	693	664	638	613	591	570
29	48	710	679	651	625	601	578	558
30	49	695	665	637	612	588	566	546
31	50	681	652	625	600	577	555	535
32	51	668	639	612	588	565	544	525
33	52	655	627	601	577	554	534	515
34	53	643	615	589	566	544	524	505
35	54	631	603	578	555	534	514	496
36	55	619	592	568	545	524	505	487
37	56	608	582	558	535	515	496	478
38	57	598	572	548	526	506	487	470
39	58	587	562	538	517	497	479	461
40	59	577	552	529	508	489	470	454
41	60	568	543	520	500	480	463	446

Ex. $n_o - n_m = 5.2$

$$\lambda = \frac{c}{2(20\,GHz)5.2} = 0.1441\,cm$$

@ 38 $L = 759\,\mu m$

IF $n_o - n_m = 5.145$

$$\lambda = \frac{c}{2(20\,GHz)(5.145)} = 0.14567\,cm$$

@ 38 $L = 767\,\mu m$

σ 218 MHz

$\Delta = 15.7\,\mu m$ @ 20 GHz

Δ 8 mm @ 38

Appendix D - Sample measurements of the external optical modulator wafer

The following pages (D1-D19) include the following measurements of the wafer:

SiO2 = 0.5 um
Electrode = 8 um

Electrical (wafer Z-26) Pages D1-D11

1. -Return and Insertion loss of straight through lines (1, 2, 3, and 4 cm in length)
2. -Return loss of shorted lines (1, 2, 3, and 4 cm in length)
3. -DC pad for 20 GHz EOM (8mm)
4. -DC pad for 45 GHz EOM (5mm)
5. -Return and Insertion loss of traveling wave line (20GHz EOM)

The dimensions are printed in the title block of each graph.
All are taken with the HP 8510B ANA under cal. , 0.199004975 to 39.99999975 GHz.
Date of measurements: 10-12-1992

Optical (wafer Z-26) pages D12-D19

1. -Optical link response 7 segment, 32 GHz EOM, (optical waveguide No. 11)-measurement
2. -Optical link response 7 segment, 32 GHz EOM, (optical waveguide No. 11)-smoothing
3. -Optical link response 9 segment, 32 GHz EOM, (optical waveguide No. 11)-measurement
4. -Optical link response 9 segment, 32 GHz EOM, (optical waveguide No. 11)-smoothing
5. -Optical link response 11 segment, 32 GHz EOM, (optical waveguide No. 11)-measurement
6. -Optical link response 11 segment, 32 GHz EOM, (optical waveguide No. 11)-smoothing
7. -Optical link response 11 segment, 32 GHz EOM, (optical waveguide No. 11)-measurement
8. -Optical link response 11 segment, 32 GHz EOM, (optical waveguide No. 11)-smoothing

Measurements 7,8 are taken with different frequency sweeps (20-40 GHz)
The dimensions are printed in the title block of each graph.
All are taken with the HP 8510B ANA under cal. , 0.199004975 to 39.99999975 GHz.
with New Focus 0-40 GHz photodetector (included in the response curves)
Date of measurements: 10-16-1992

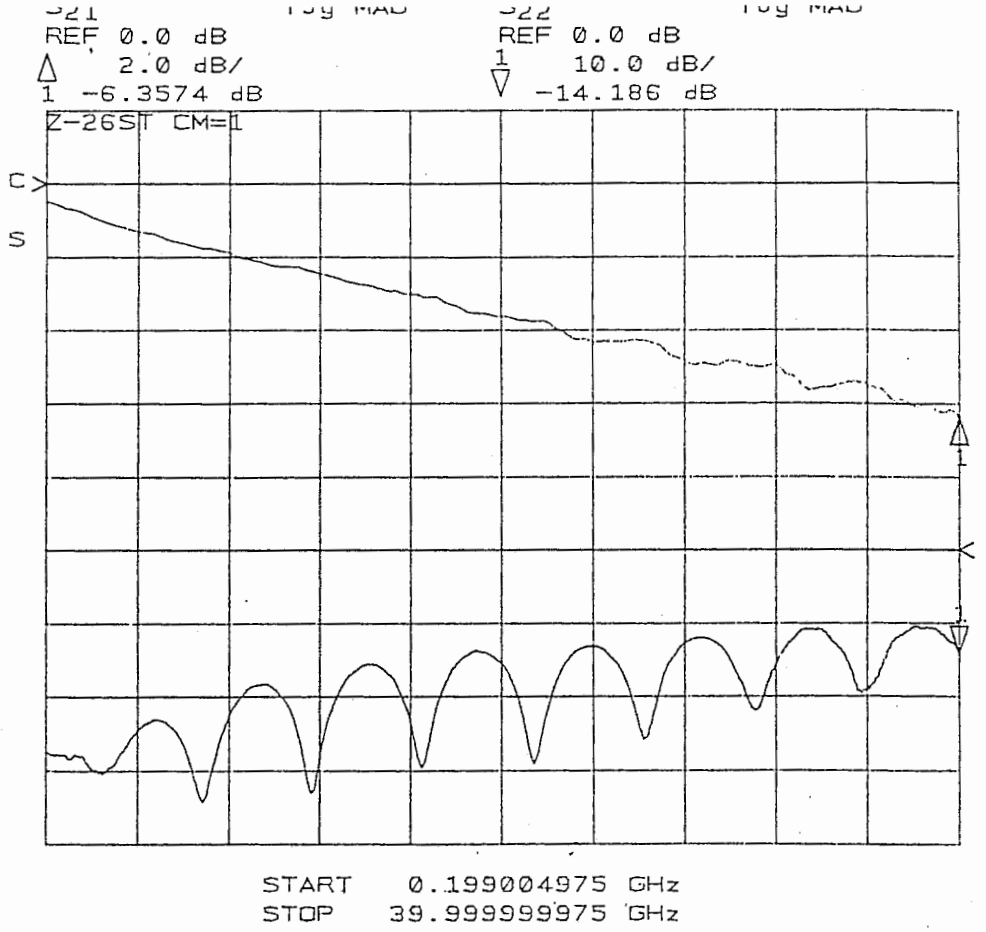
S21
Log MAG
REF 0.0 dB
2.0 dB/
1 -6.3574 dB
S22
Log MAG
REF 0.0 dB
10.0 dB/
1 -14.186 dB
Z-26ST CM=1
C
S
START 0.199004975 GHz
STOP 39.999999975 GHz

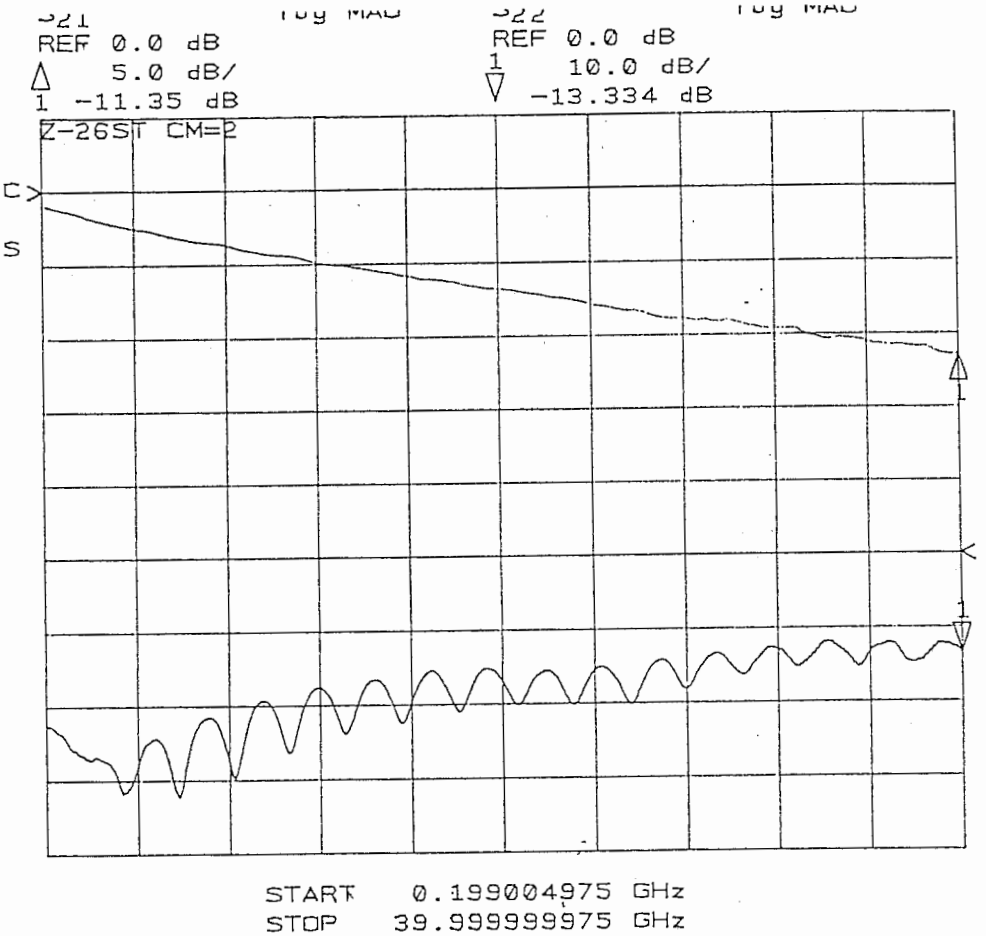
S21
Log MAG
REF 0.0 dB
5.0 dB/
1 -11.35 dB
S22
Log MAG
REF 0.0 dB
10.0 dB/
1 -13.334 dB
Z-26ST CM=2
C
S
START 0.199004975 GHz
STOP 39.999999975 GHz

S21 Log MAG
REF 0.0 dB
Δ 5.0 dB/
1 -16.431 dB

S22 Log MAG
REF 0.0 dB
1 10.0 dB/
▽ -13.684 dB

Z-26ST CM=3

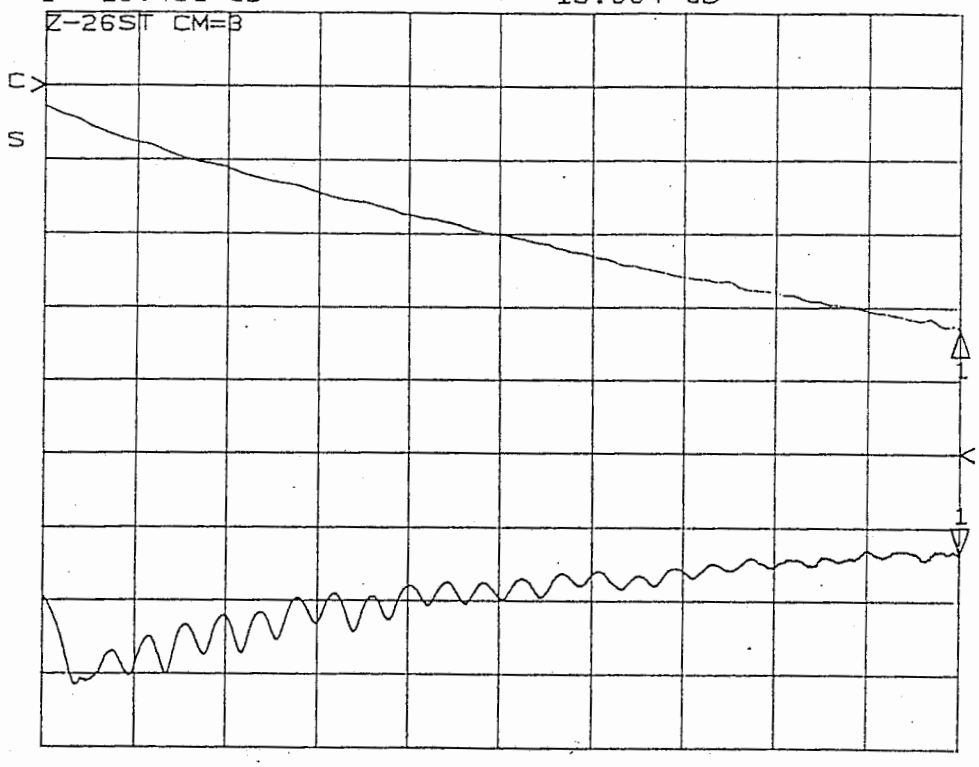

START 0.199004975 GHz
STOP 39.999999975 GHz

03

S21 Log MAG
REF 0.0 dB
Δ 5.0 dB/
1 -22.316 dB

S22 Log MAG
REF 0.0 dB
1 10.0 dB/
▽ -13.001 dB

Z-26ST CM=4

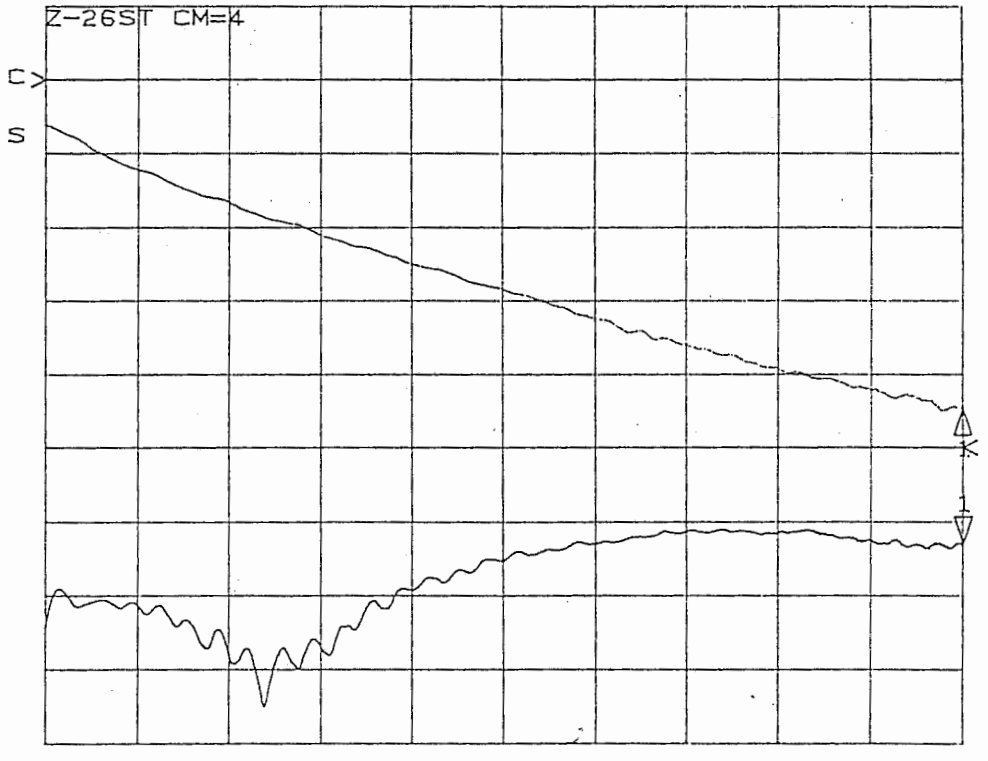

START 0.199004975 GHz
STOP 39.999999975 GHz

04

S11 y MAG
REF 0.0 dB
1 5.0 dB/
-12.078 dB
Z-26ST CM=1
C>
S

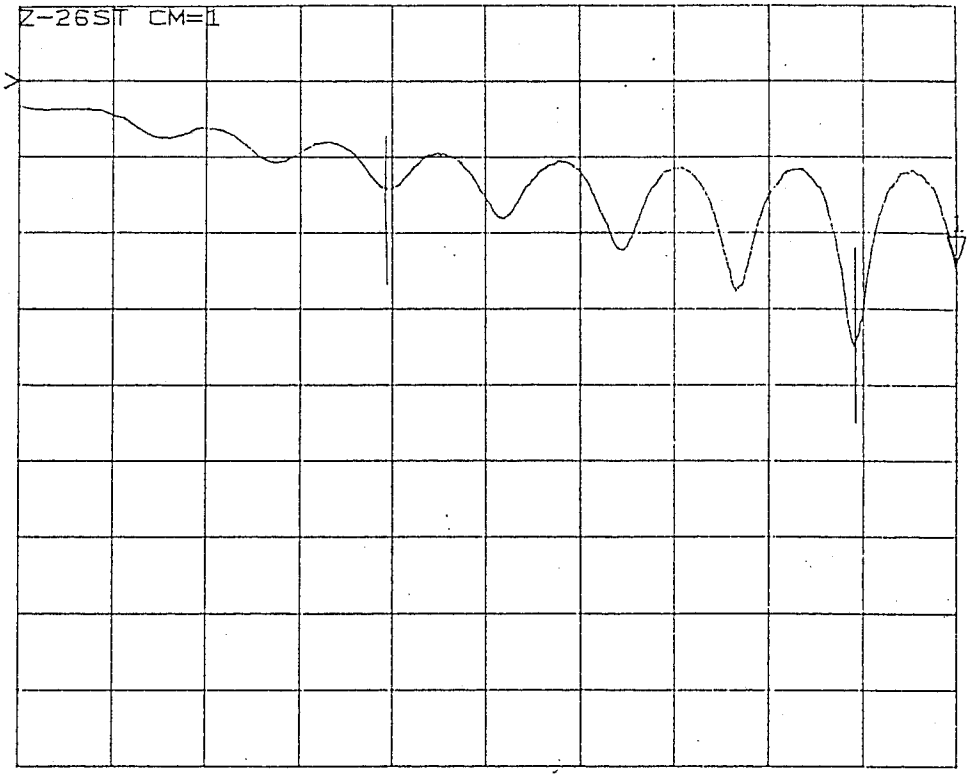

START 0.199004975 GHz
STOP 39.999999975 GHz

S11 y MAG
REF 0.0 dB
1 5.0 dB/
-12.17 dB
Z-26ST CM=2
C>
S

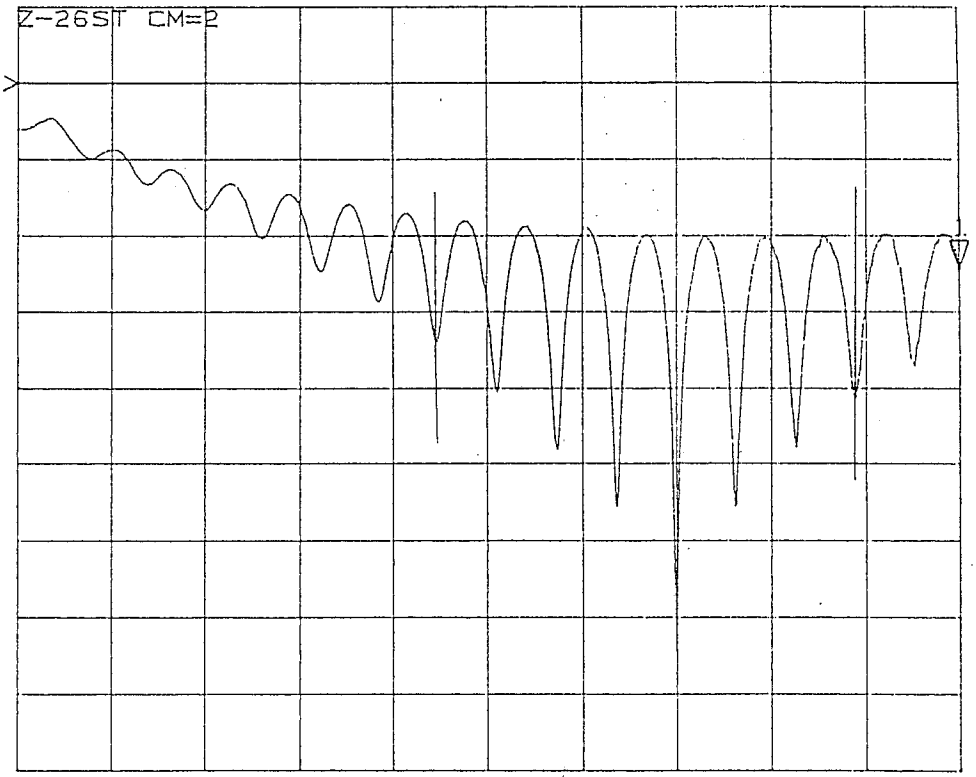

START 0.199004975 GHz
STOP 39.999999975 GHz

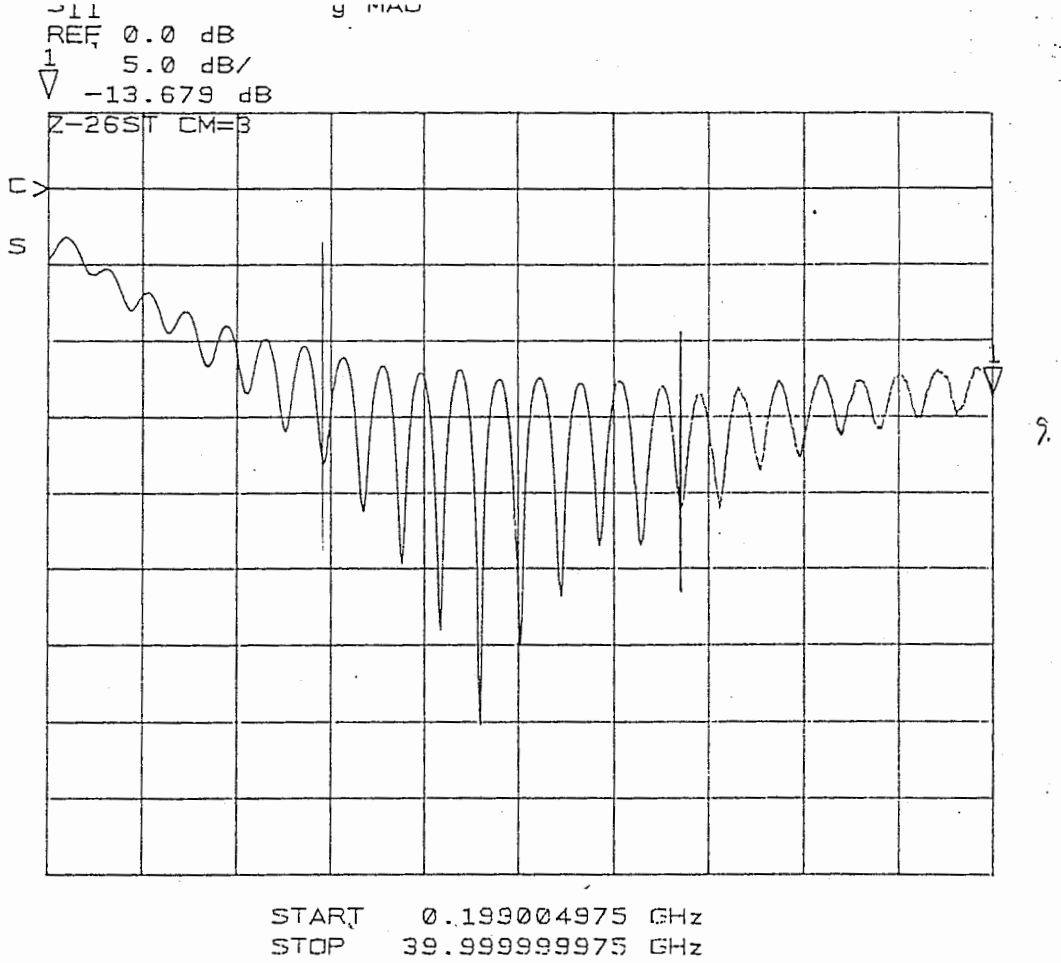
S11
REF 0.0 dB
1 5.0 dB/
-13.679 dB
Z-26ST CM=3
C>
S
START 0.199004975 GHz
STOP 39.999999975 GHz

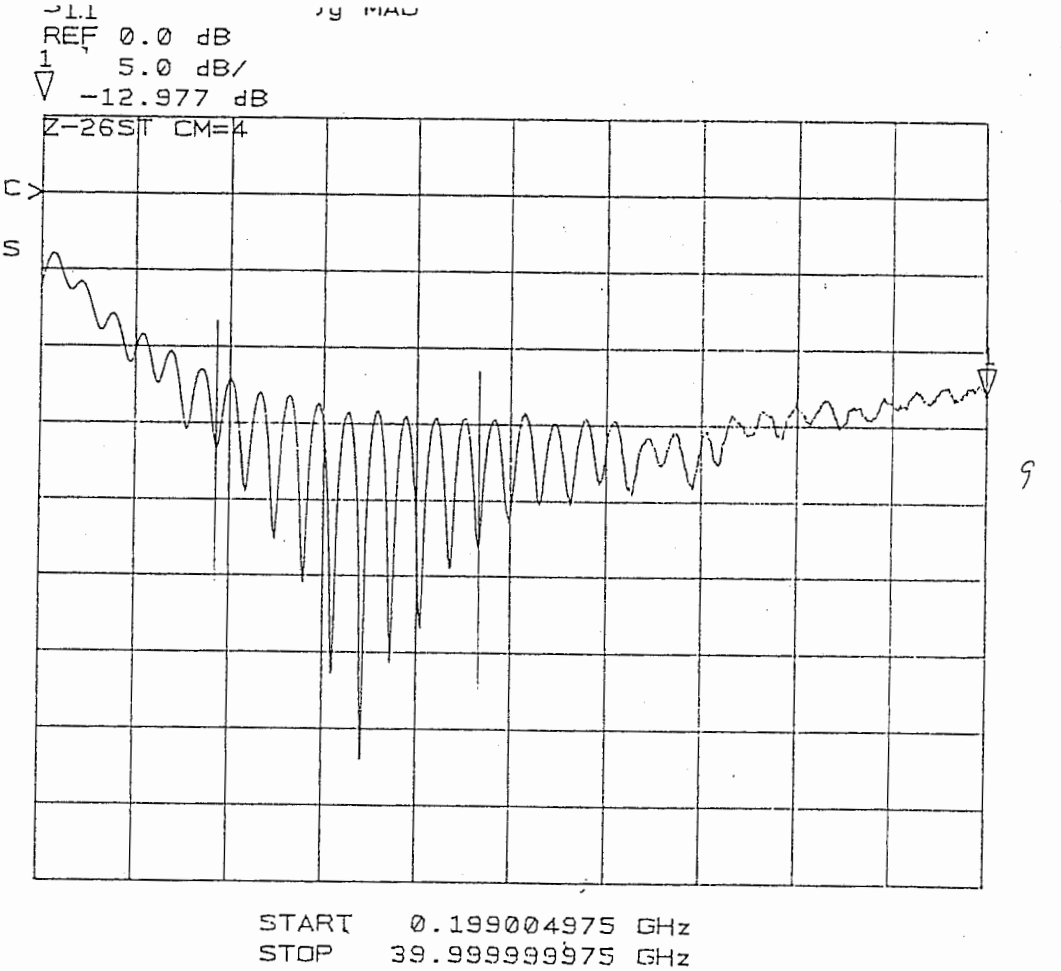
S11
REF 0.0 dB
1 5.0 dB/
-12.977 dB
Z-26ST CM=4
C>
S
START 0.199004975 GHz
STOP 39.999999975 GHz

S21 REF 0.0 dB
10.0 dB/
1 -31.619 dB

S22 REF 0.0 dB
1 10.0 dB/
0.0233 dB

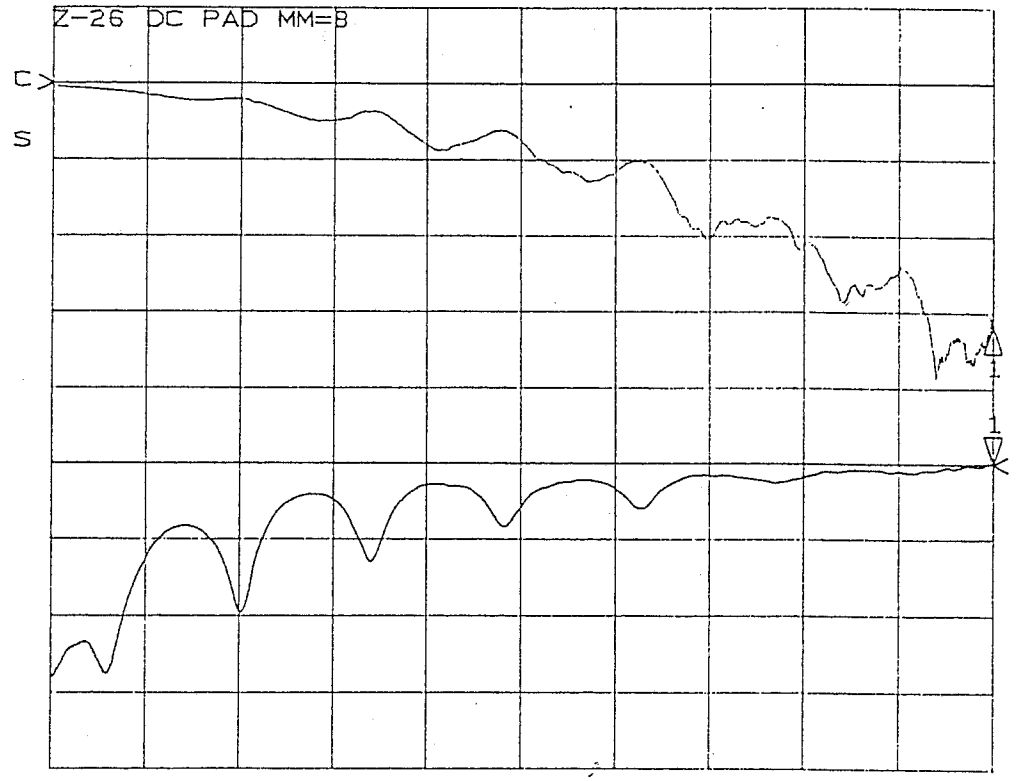

START 0.199004975 GHz
STOP 39.999999975 GHz

S21 REF 0.0 dB
10.0 dB/
1 -29.998 dB

S22 REF 0.0 dB
1 10.0 dB/
0.2820 dB

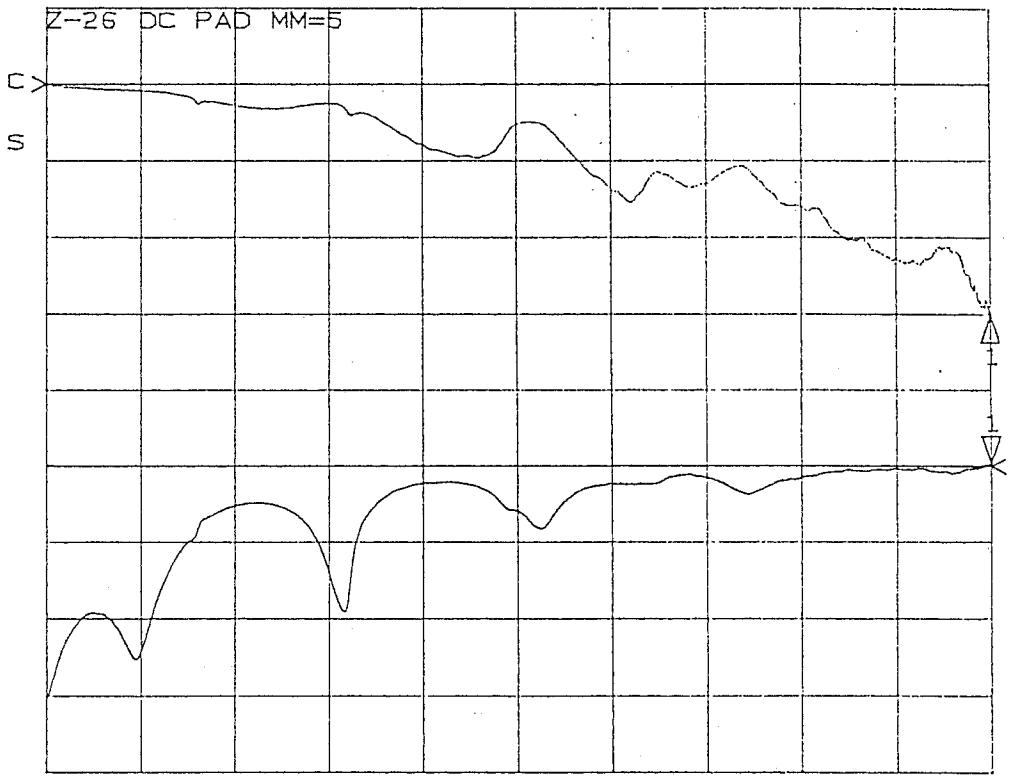

START 0.199004975 GHz
STOP 39.999999975 GHz

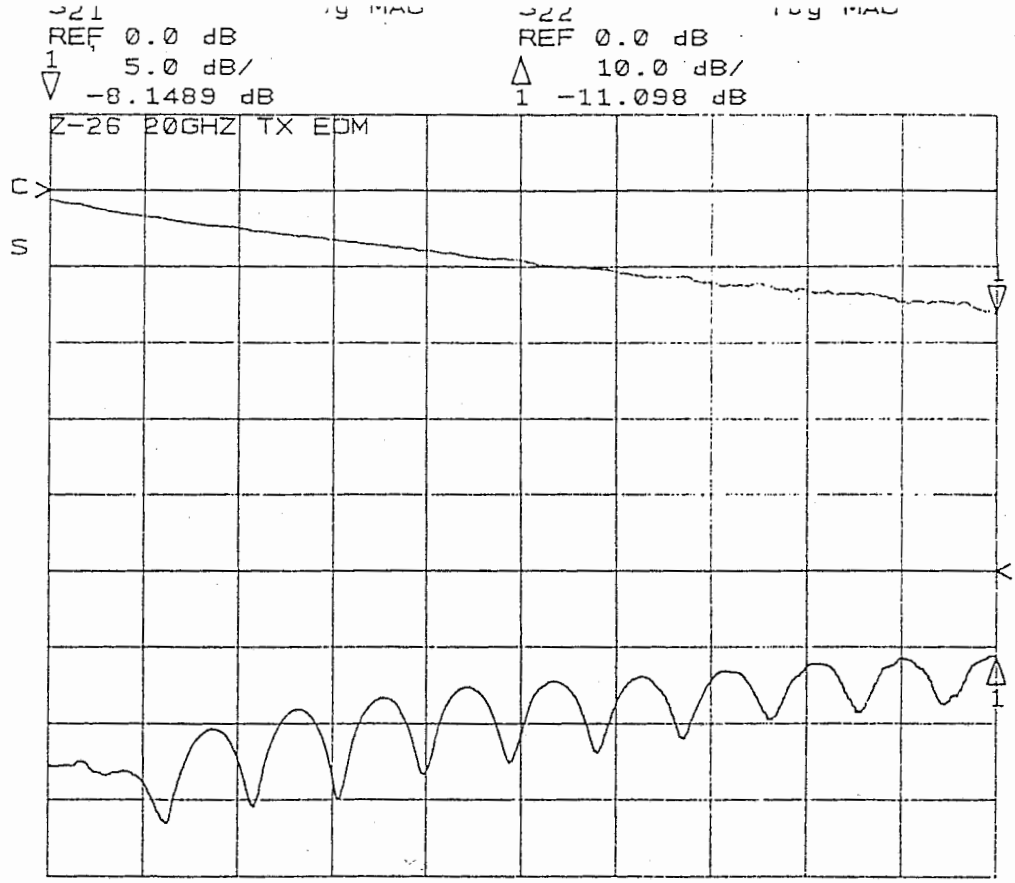
S21
REF 0.0 dB
1 5.0 dB/
-8.1489 dB
S22
REF 0.0 dB
10.0 dB/
1 -11.098 dB
Z-26 20GHZ TX EDM
C
S
1
1
CENTER 20.099502475 GHz
SPAN 39.800995000 GHz

D11

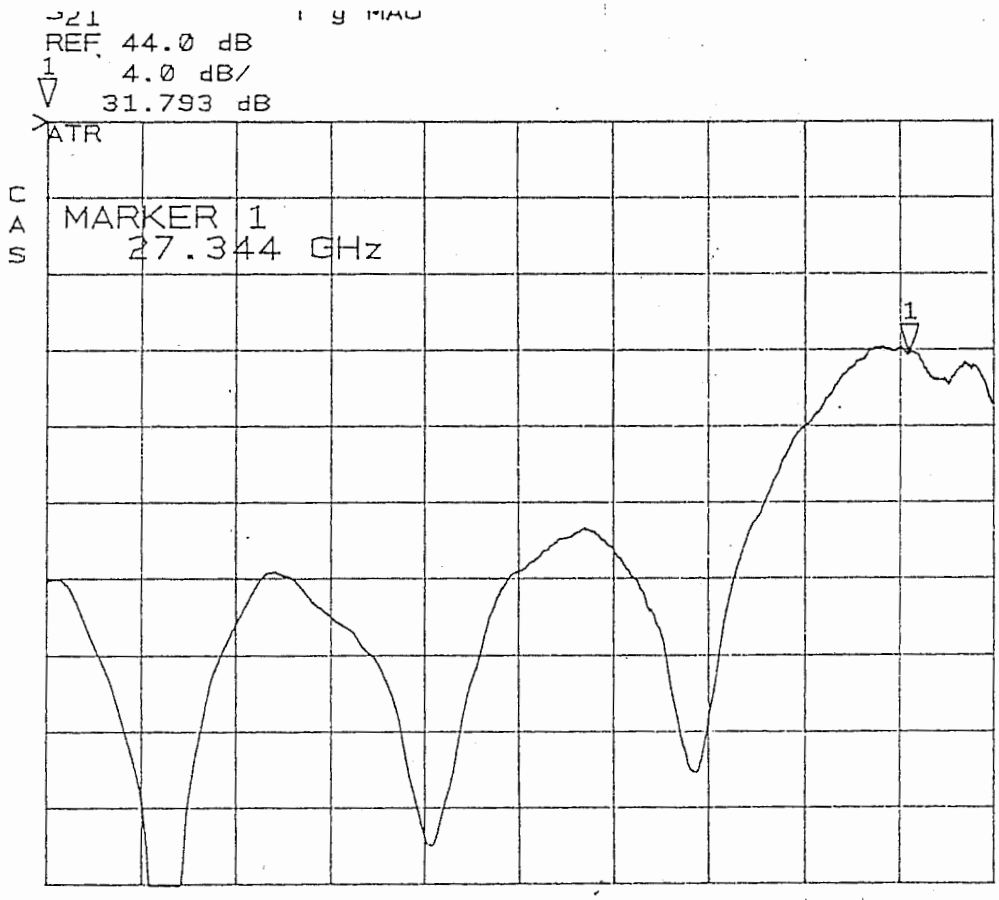
S21
REF 44.0 dB
1 4.0 dB/
31.793 dB
ATR
C
A
S
MARKER 1
27.344 GHz
1
START 0.500000000 GHz
STOP 30.000000000 GHz

D12

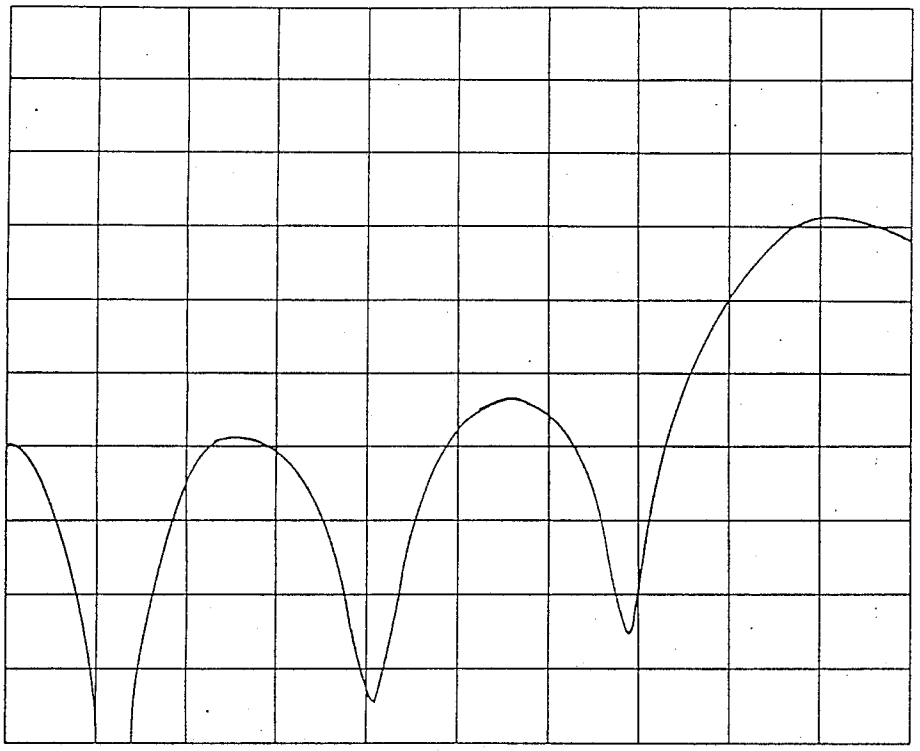

S21
REF 44.0 dB
1 4.0 dB/
33.308 dB
ATR
MARKER 1
27.9635 GHz
START 0.500000000 GHz
STOP 30.000000000 GHz

<44 4/

10/16/92
0.5-30 GHz
8-2C
3C VB.
λ-11
11SEC
32GHz

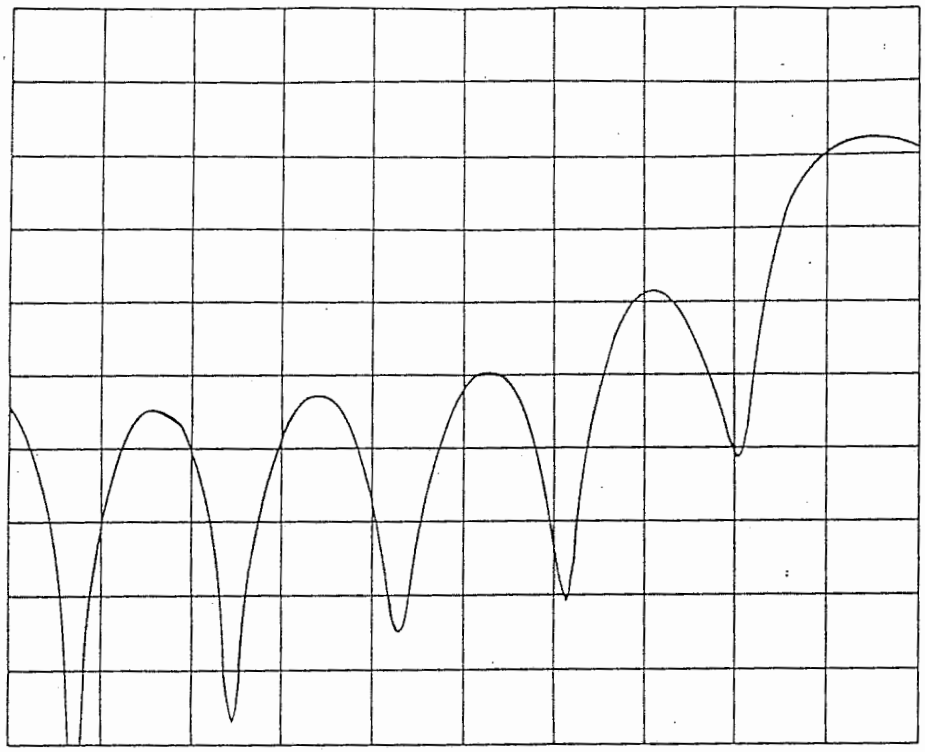

S21 Log MAG
REF 44.0 dB
1 4.0 dB/
35.141 dB
ATR
C
A
S
MARKER 1
28.4855 GHz

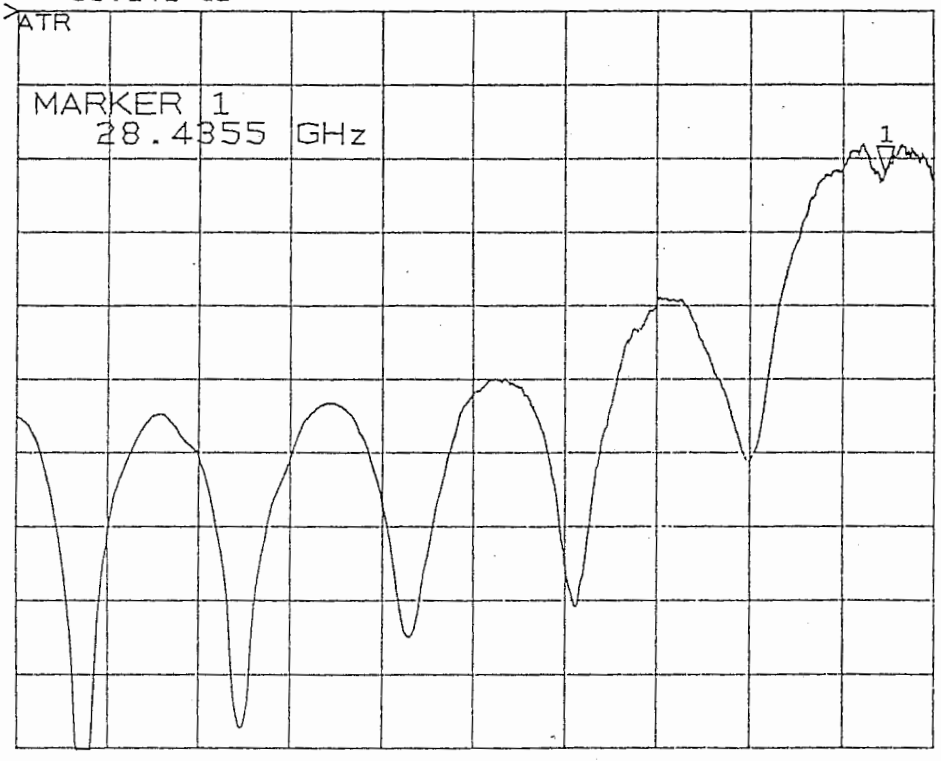

START 0.500000000 GHz
STOP 30.000000000 GHz

<44 dB 4/

10/16/97
6.5 3.6GHz
2 - 2C
λ - 11
9 SEG
3.2GHz ?
3.4V GHz

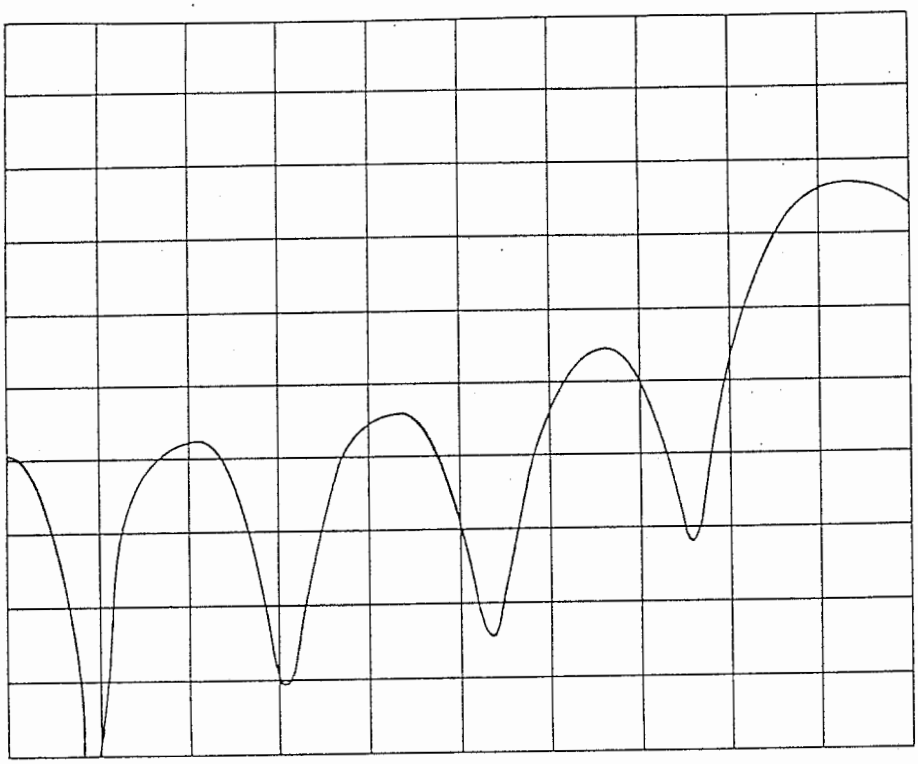

L10

3.6GHz
2 dB λ - 11
11 SEG

S21 g MAG
REF -20.0 dB
4.0 dB/

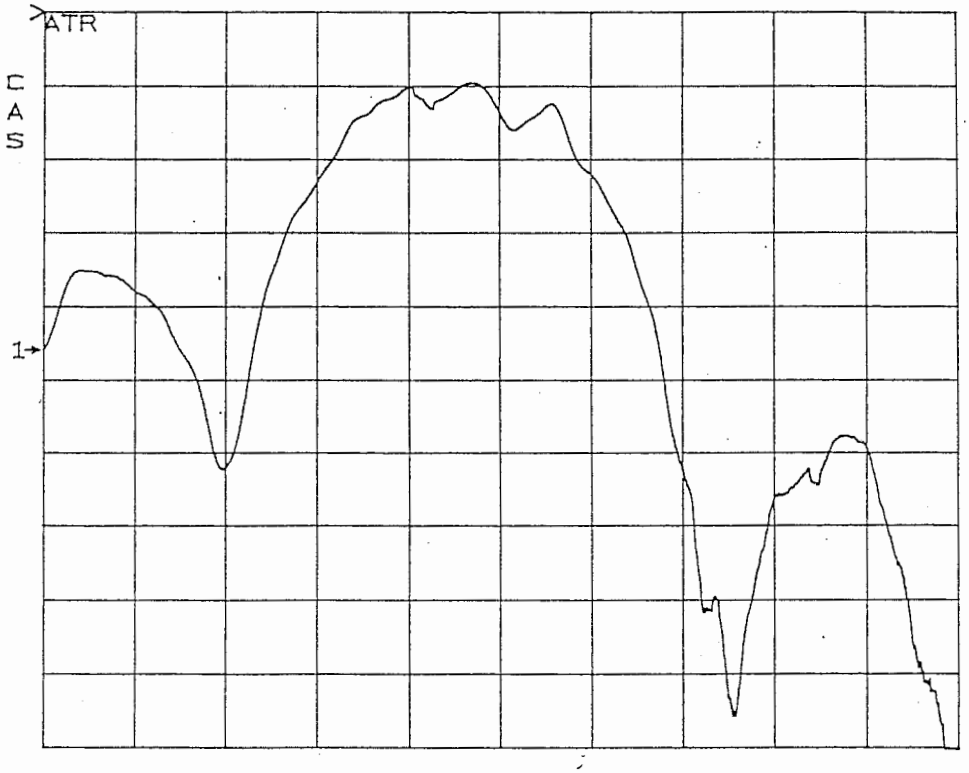

START 20.000000000 GHz
STOP 40.000000000 GHz

810

D 19

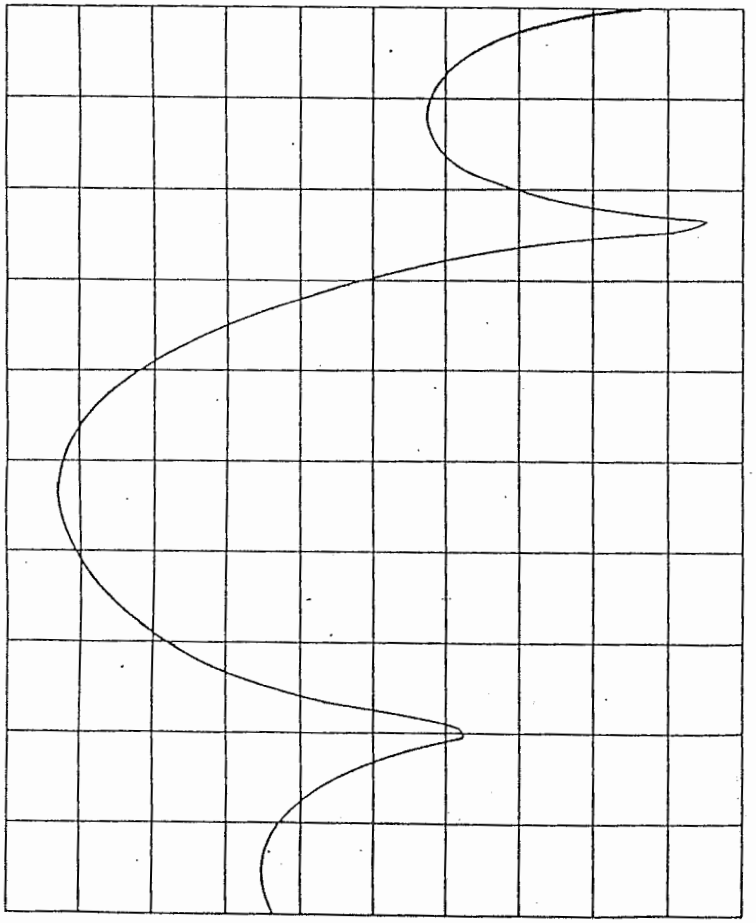

Appendix E - Sample measurements of the packaged external optical modulator (32 GHz)

The following pages (E1-E4) include the following measurements of the wafer:

SiO_2 = 0.5 um
Electrode = 8 um

Electrical Pages E1-E2

1. -Insertion loss of EOM electrode
2. -Return loss of EOM electrode with 50 Ohm broadband load attached to port two of EOM

All are taken with the HP 8510B ANA under cal. , 0.5 to 40 GHz.
Date of measurements: 10-16-1992

Optical (wafer Z-26) pages D12-D19

1. -Optical link response 11 segment, 32 GHz EOM-measurement
2. -Optical link response 11 segment, 32 GHz EOM-smoothing

Measurements 1,2 are taken with different frequency sweeps (20-40 GHz)
All are taken with the HP 8510B ANA under cal. with New Focus 0-40 GHz photodetector (included in the response curves)
Date of measurements: 11-27-1992

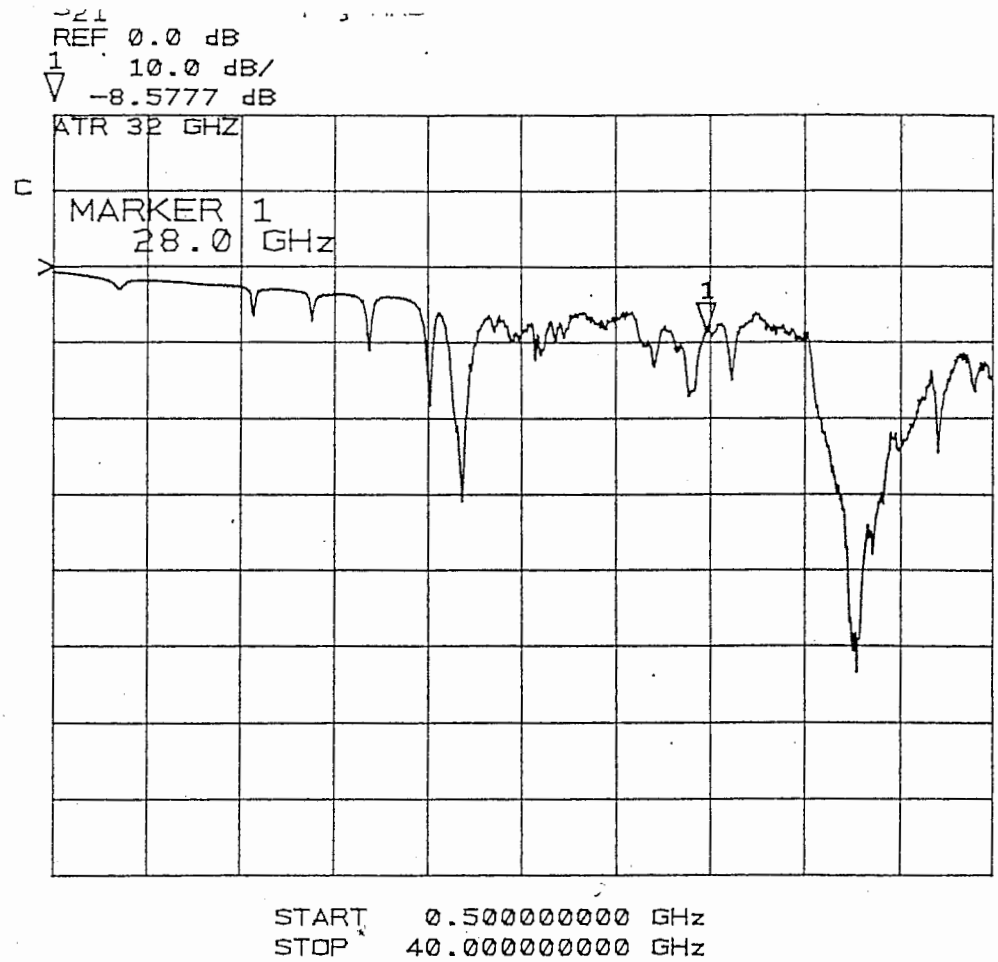
S21
REF 0.0 dB
1 10.0 dB/
-8.5777 dB
ATR 32 GHZ
C
MARKER 1
28.0 GHz
1
START 0.500000000 GHz
STOP 40.000000000 GHz

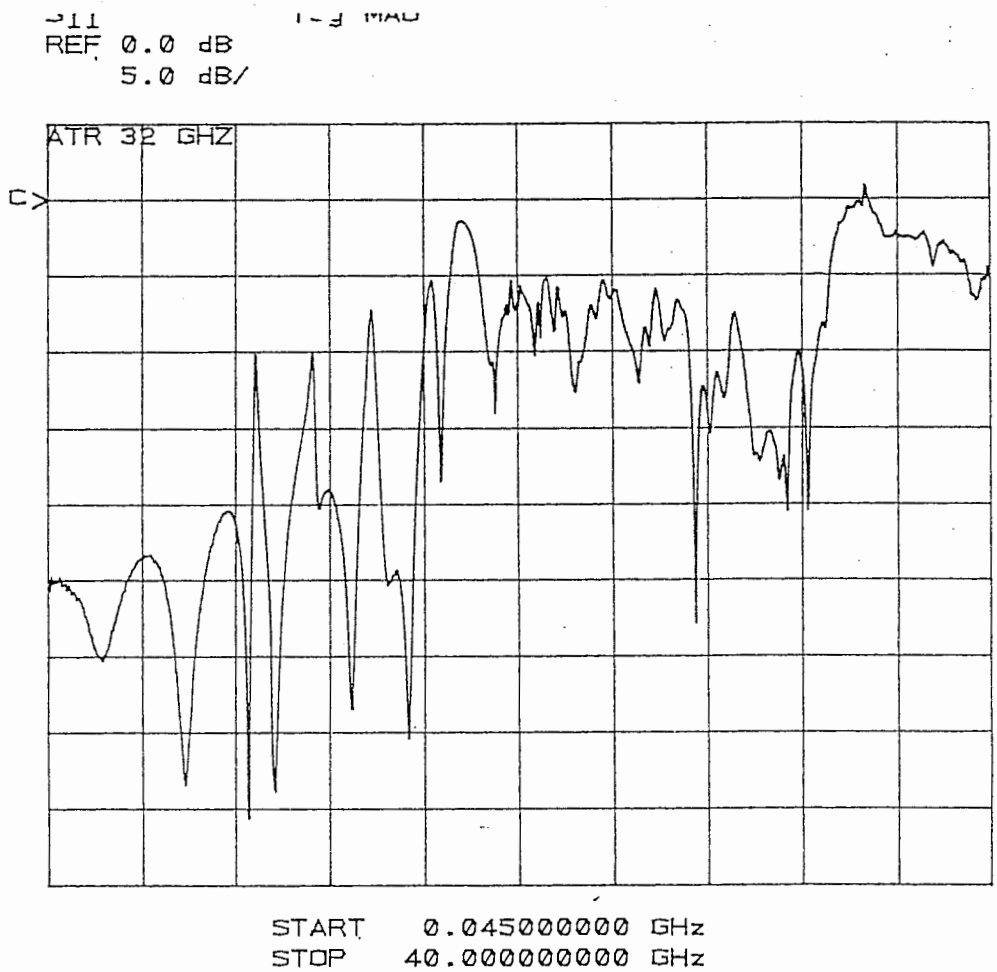
S11
REF 0.0 dB
5.0 dB/
ATR 32 GHZ
C
START 0.045000000 GHz
STOP 40.000000000 GHz

S21 log MAG
REF -42.0 dB
4.0 dB/

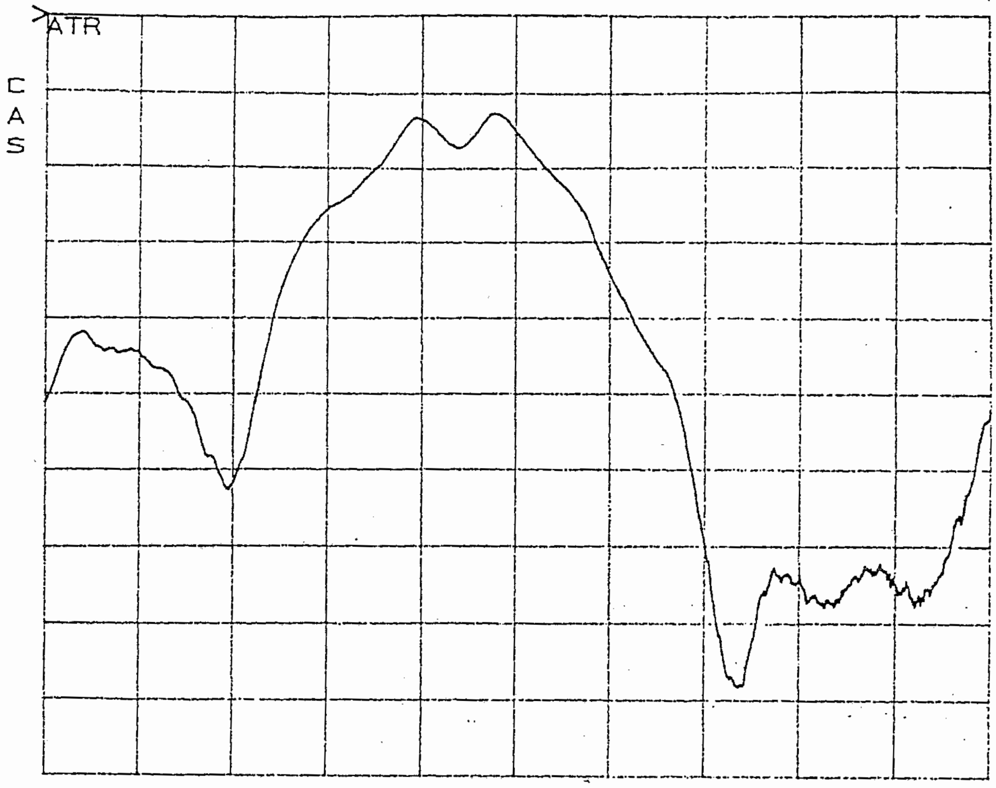

START 20.000000000 GHz
STOP 40.000000000 GHz

E3

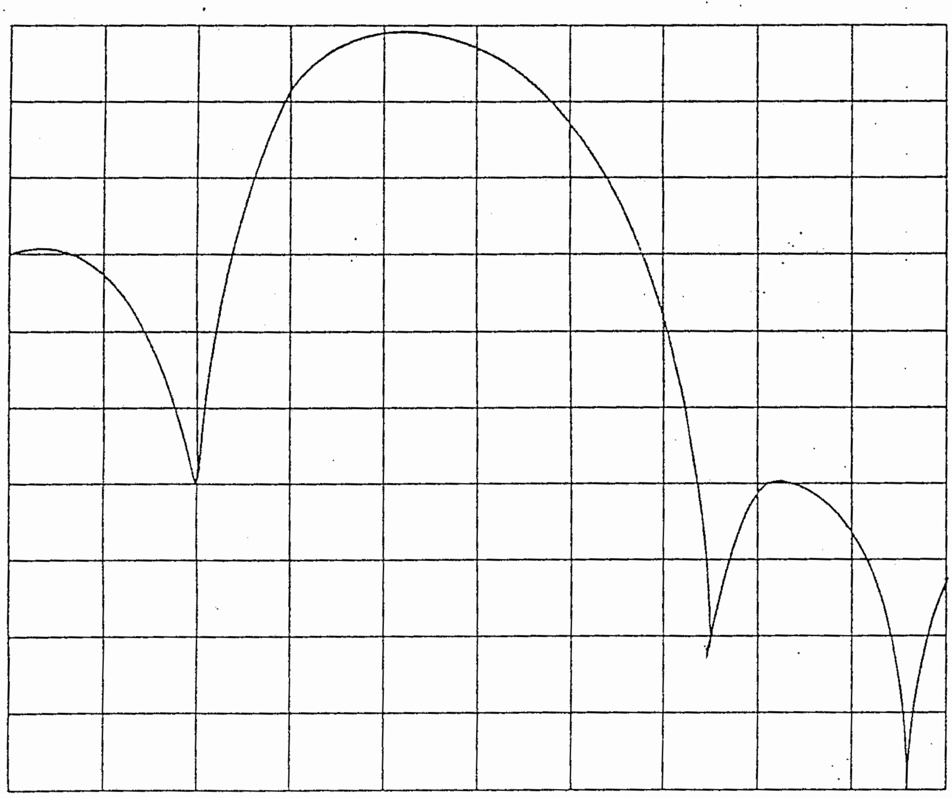

<-24 dB

Jo. Yoon

32GHz
[illegible]
Pcm
Line

E4

Appendix F - Probe station modifications for optical on-wafer probes

The following pages (F1-F12) include the design of the modified microwave probe station to accommodate the horizontal optical probes for the external optical modulator measurements:

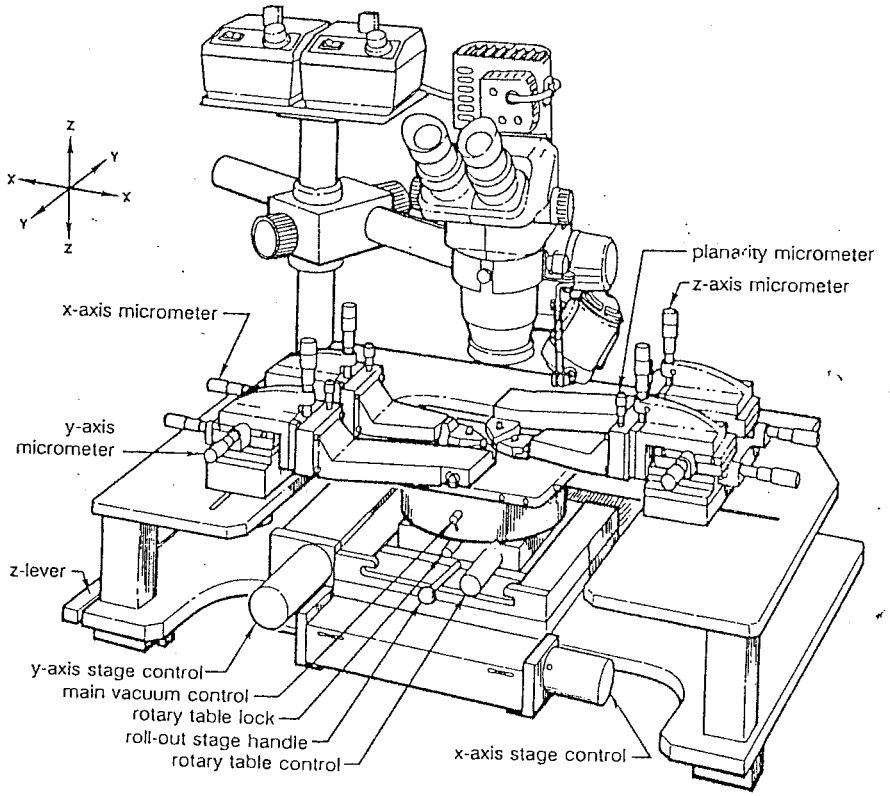

Fig. 1-1 Summit 9000™ Analytical Probe Station features

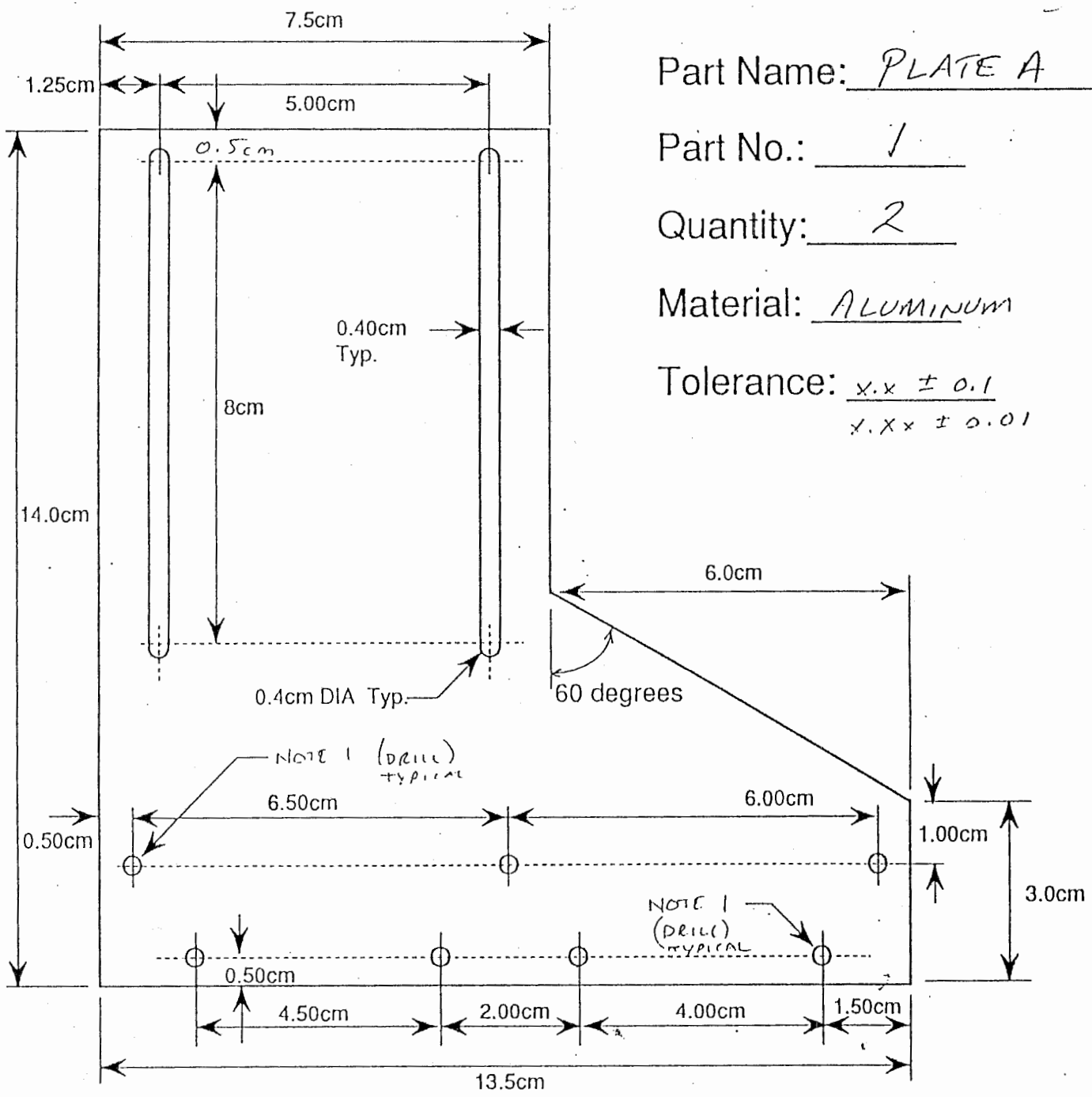

Part Name: PLATE A

Part No.: 1

Quantity: 2

Material: ALUMINUM

Tolerance: x.x ± 0.1

x.xx ± 0.01

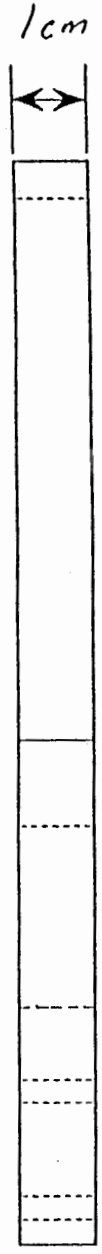

NOTE 1: 3mm screw or equivalent

Part Name: PLATE B Part No.: 2

Quantity: 2 Material: ALUMINUM Tolerance: X.X ± 0.1
X.XX ± 0.01

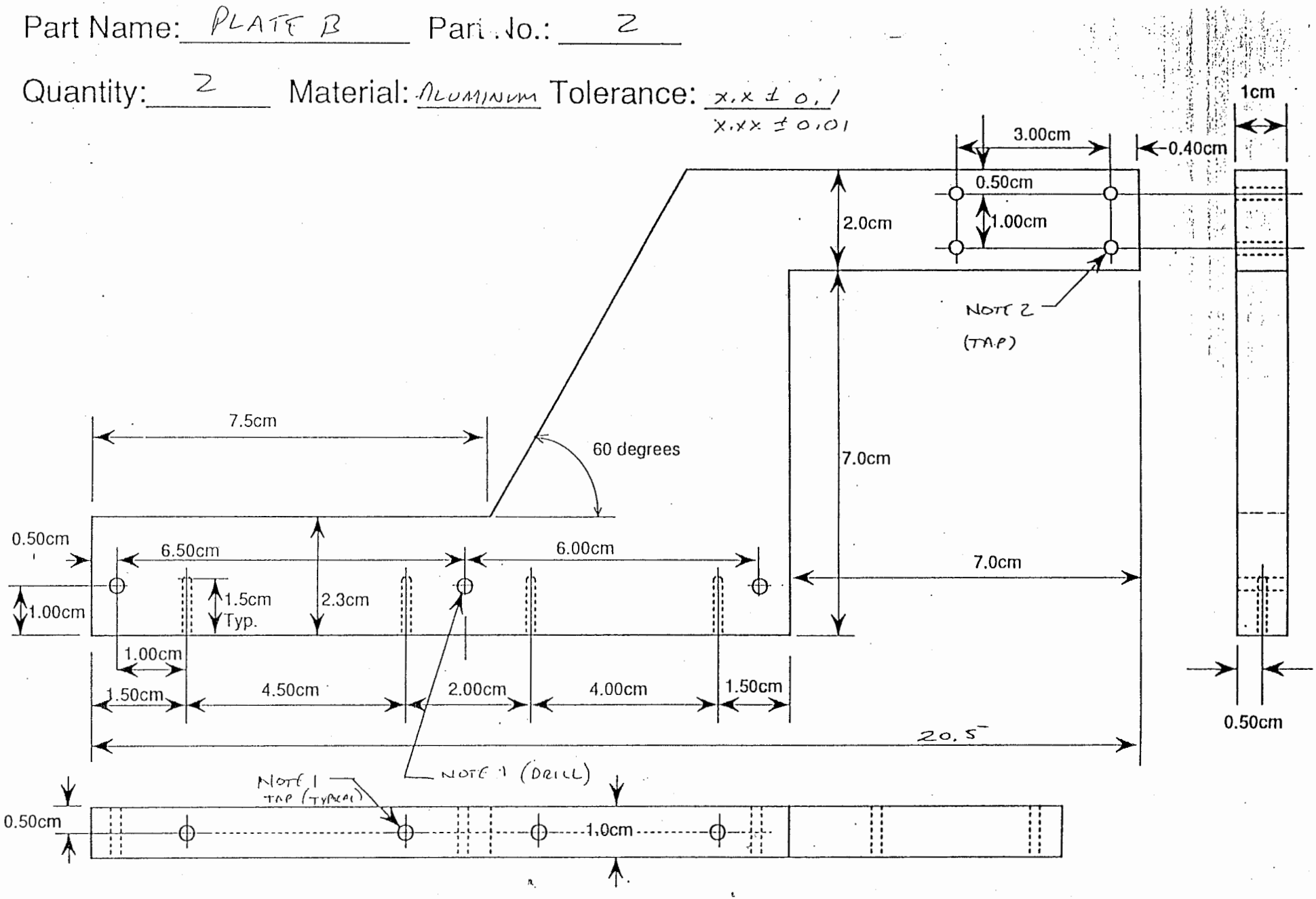

NOTE 1 : 3mm screw or equivalent

NOTE 2 : 2mm screw or equivalent

Part Name: OPTICAL BASE Part No.: 3

Quantity: 2 Material: ALUMINUM Tolerance: X.X ± 0.1

X.XX ± 0.01

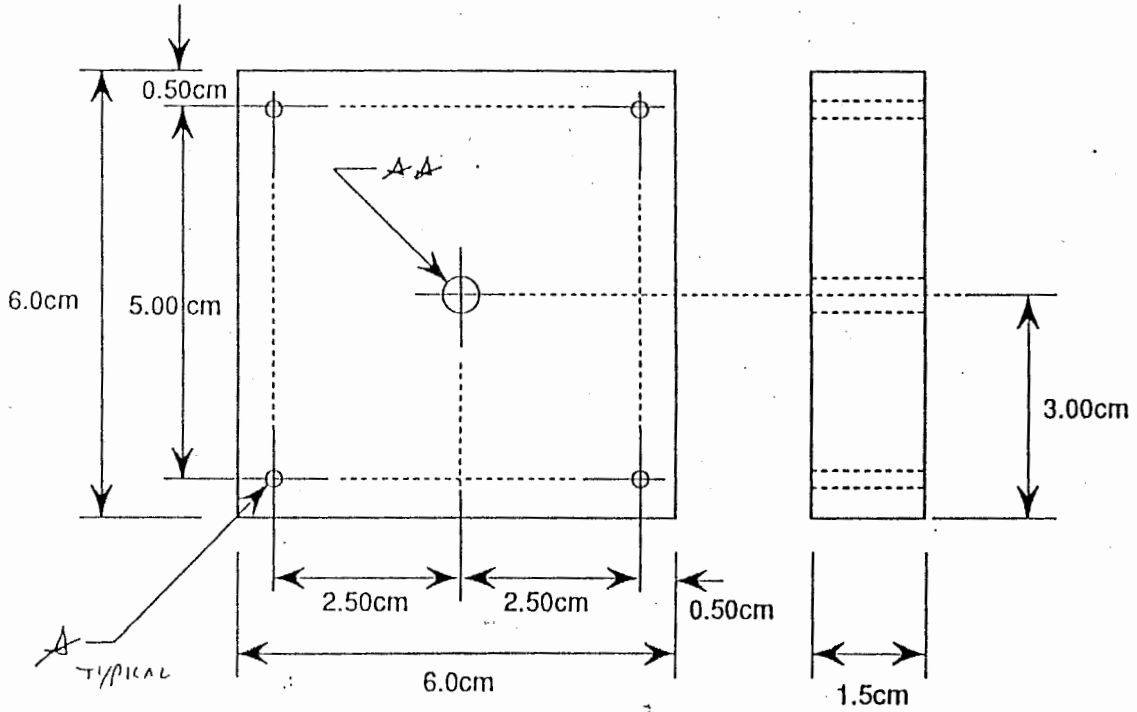

A SEE ENCLOSED PLATE (#1) FOR TAP SIZE (SCREW SIZE) AND SPACING

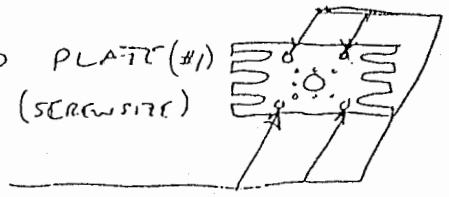

AA SEE ENCLOSED SCREW FOR DIMENSION (#2)

Part Name: BRACKET Part No.: 4

Quantity: 6 Material: ALUMINUM Tolerance: X.X ± 0.1
X.XX ± 0.01

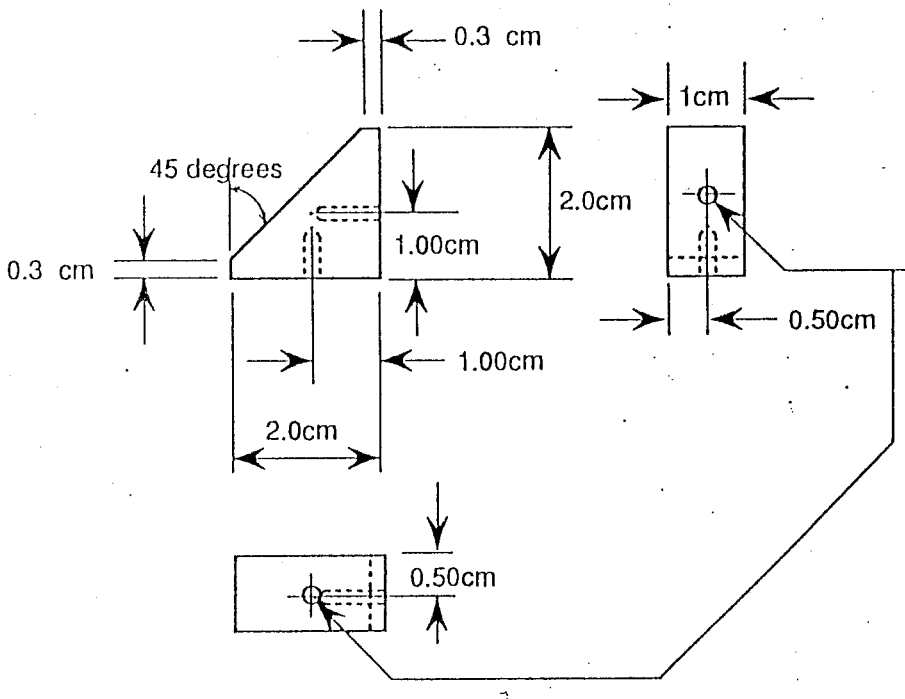

NOTE 1: .3 mm screw or equivalent

B

Part Name: FIBER HOLDER

Part No.: 5

Quantity: 2 Material: STEEL or ALUMINUM

Tolerance: X.X ± 0.01
X.XX ± 0.001

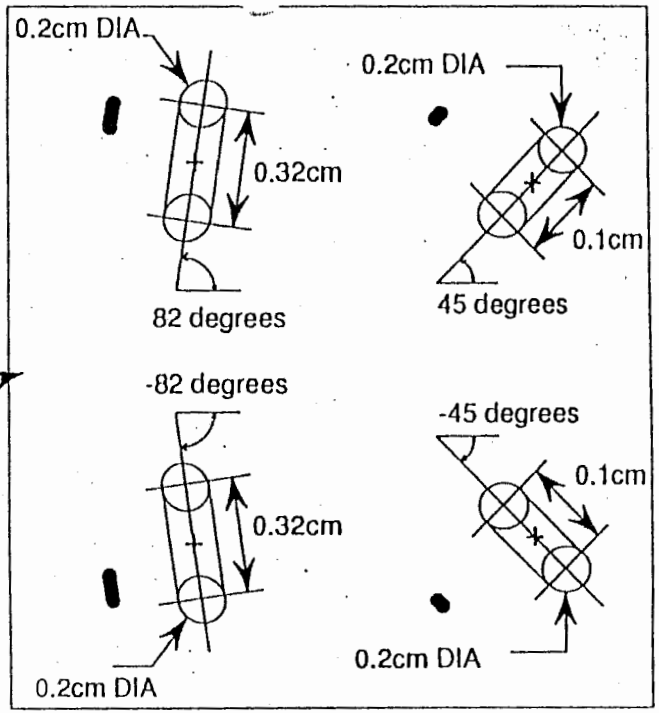

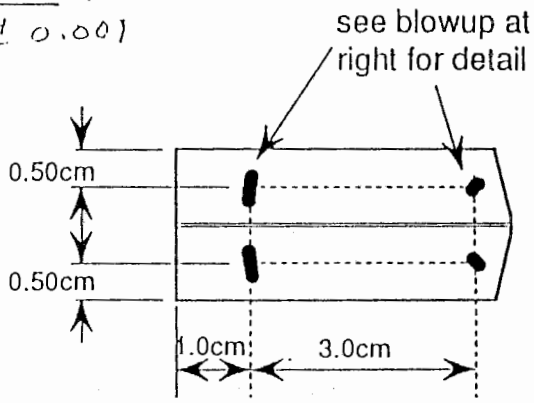

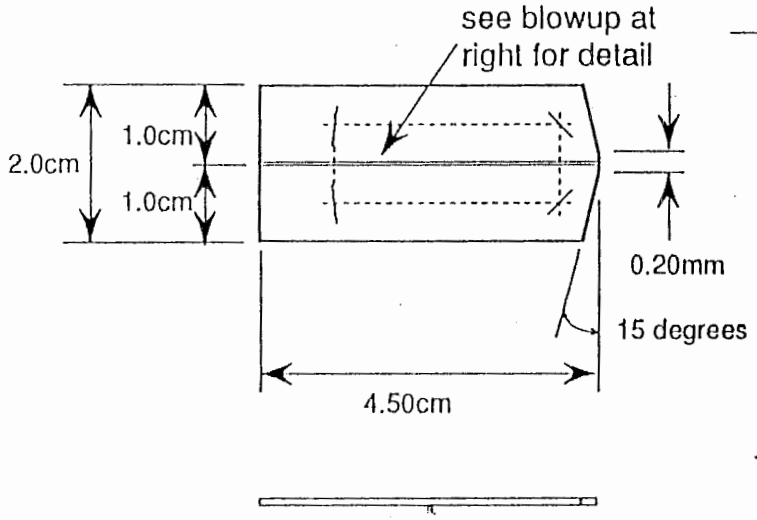

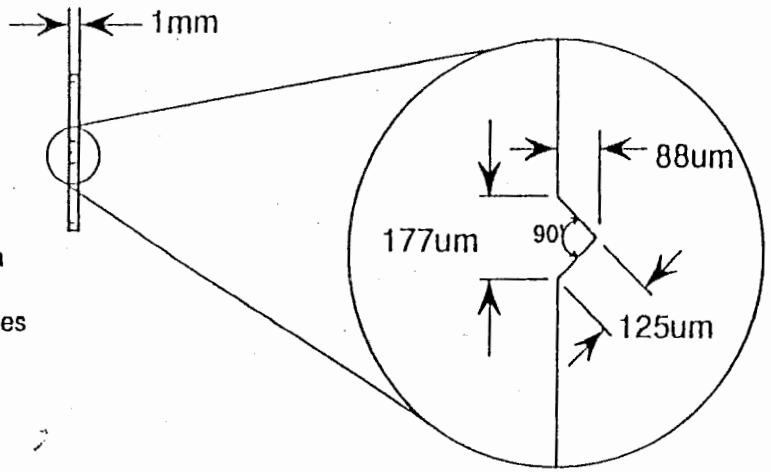

Fiber Grove Detail
Tolerance on grove ± 25um

RD

Part Name: PROBE BASE

Part No.: 6

Quantity: 2 Material: ALUMINUM

Tolerance: X.X ±0.1

X.XX ±0.01

Note the spacing between the 4 outer holes are given in inches. This is because they are going to be fitted with a non-metric piece.

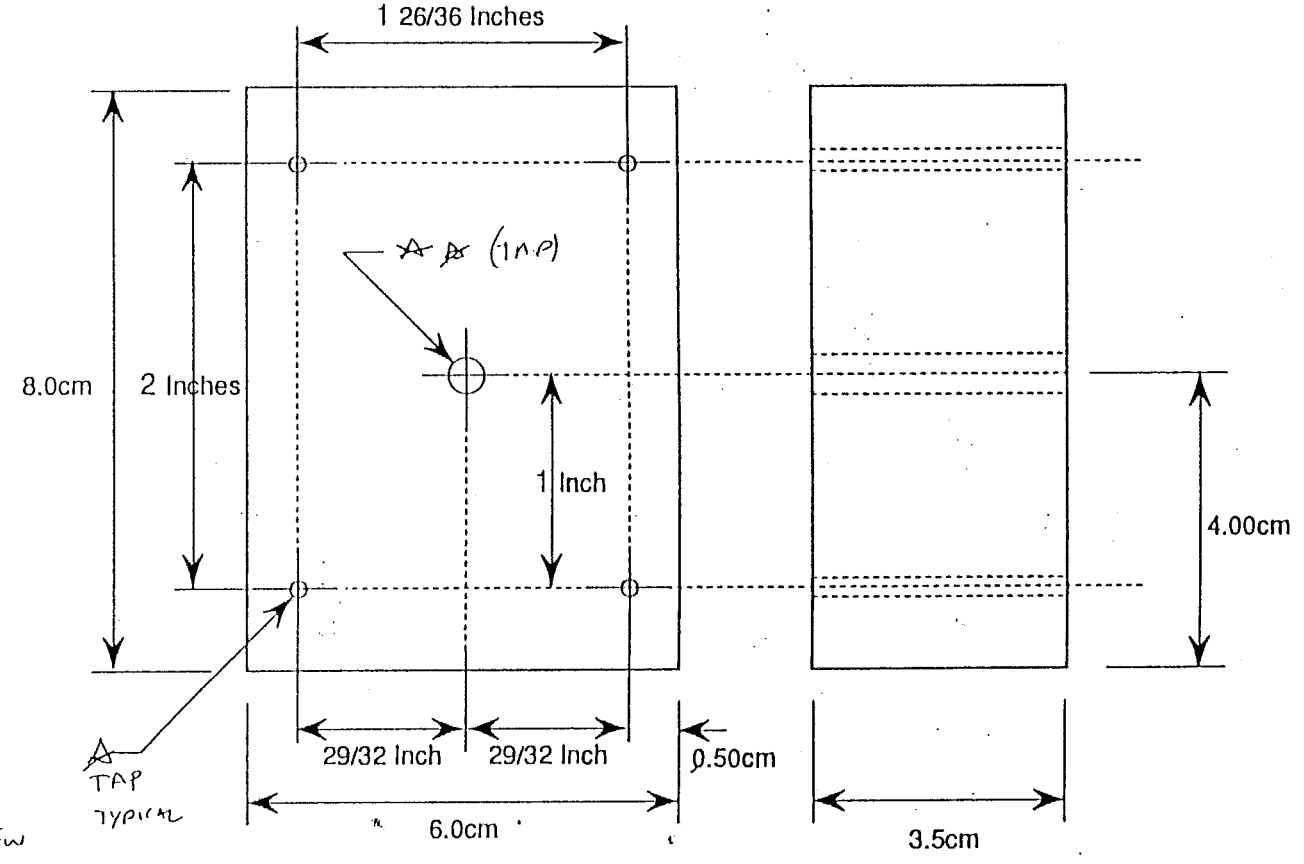

** SEE ENCLOSED SCREW (1/2) FOR DIMENSIONS

* SEE ENCLOSED SCREW # 3 FOR DIMENSIONS

5

Part Name: WAFER SUBSTRATE

Part No.: 7

Quantity: 2 - 3 Material: ALUMINUM

Tolerance: X: ± 1mm
X.X: ± 1mm

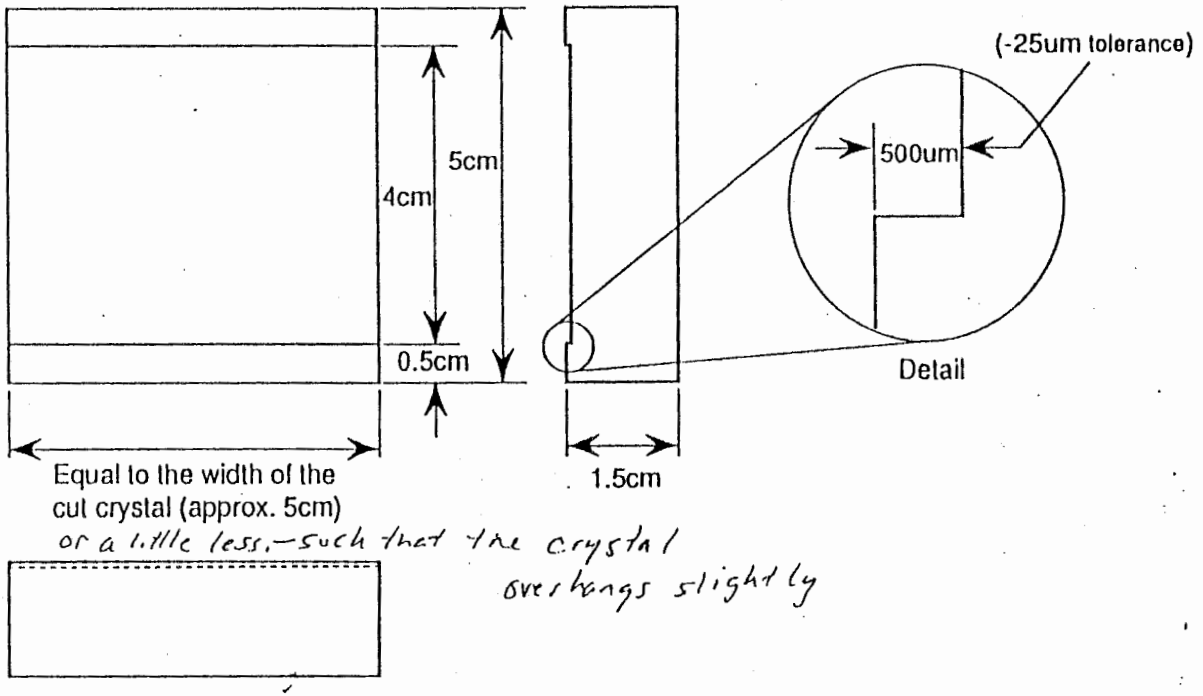

Assembly Views
No hidden detail

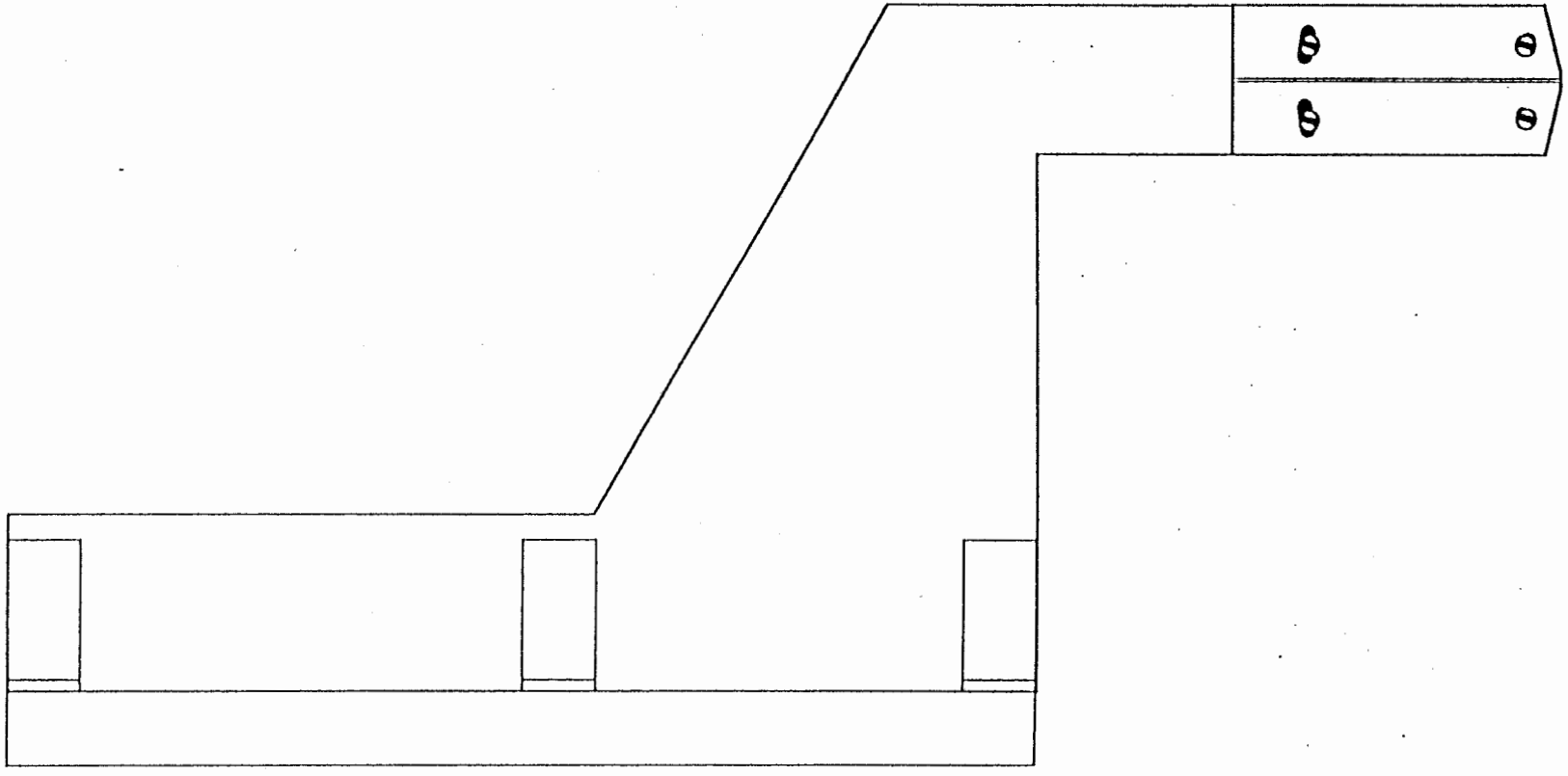

Assembly Views
No hidden detail

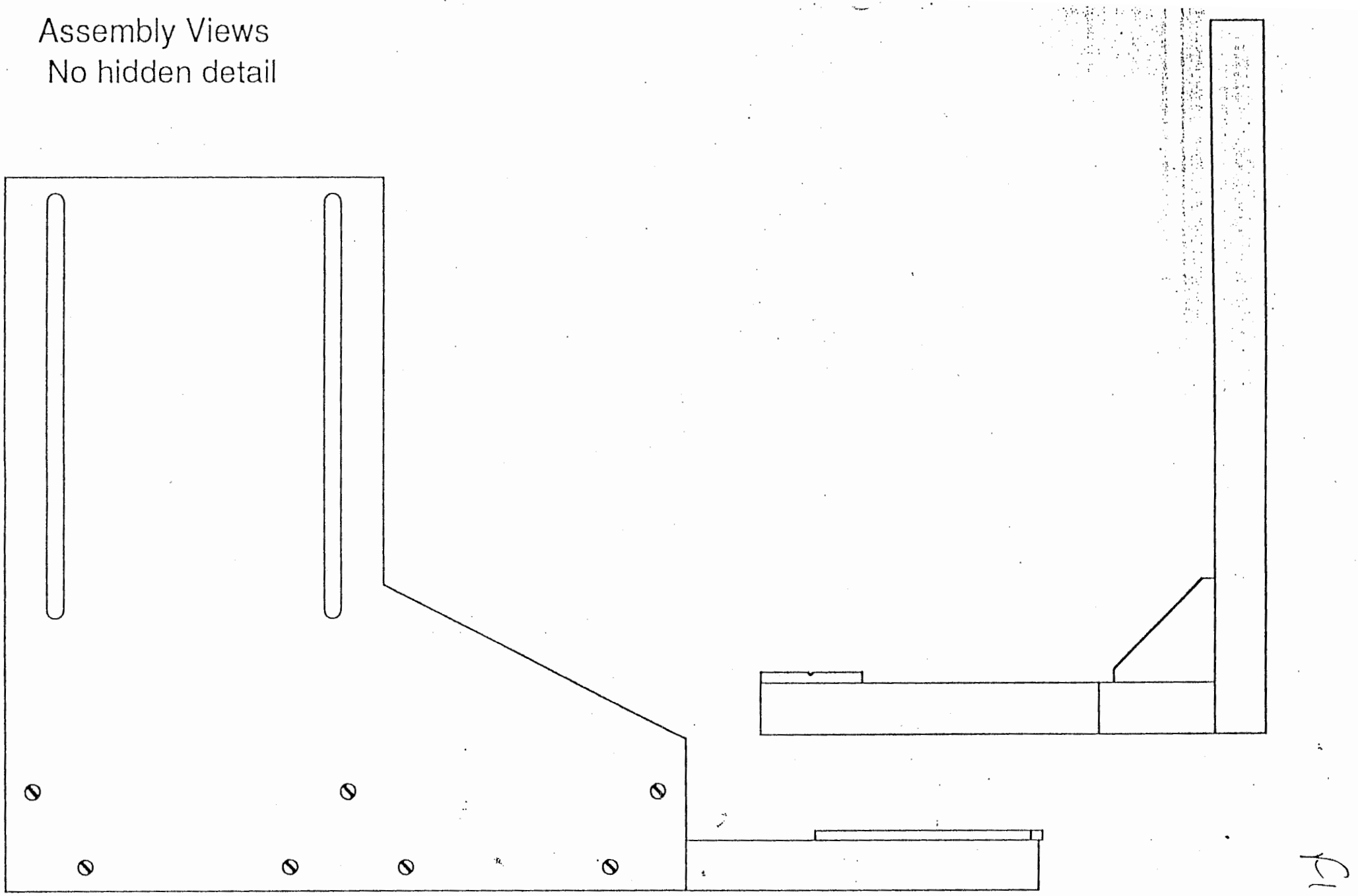

Assembly Views
With hidden details

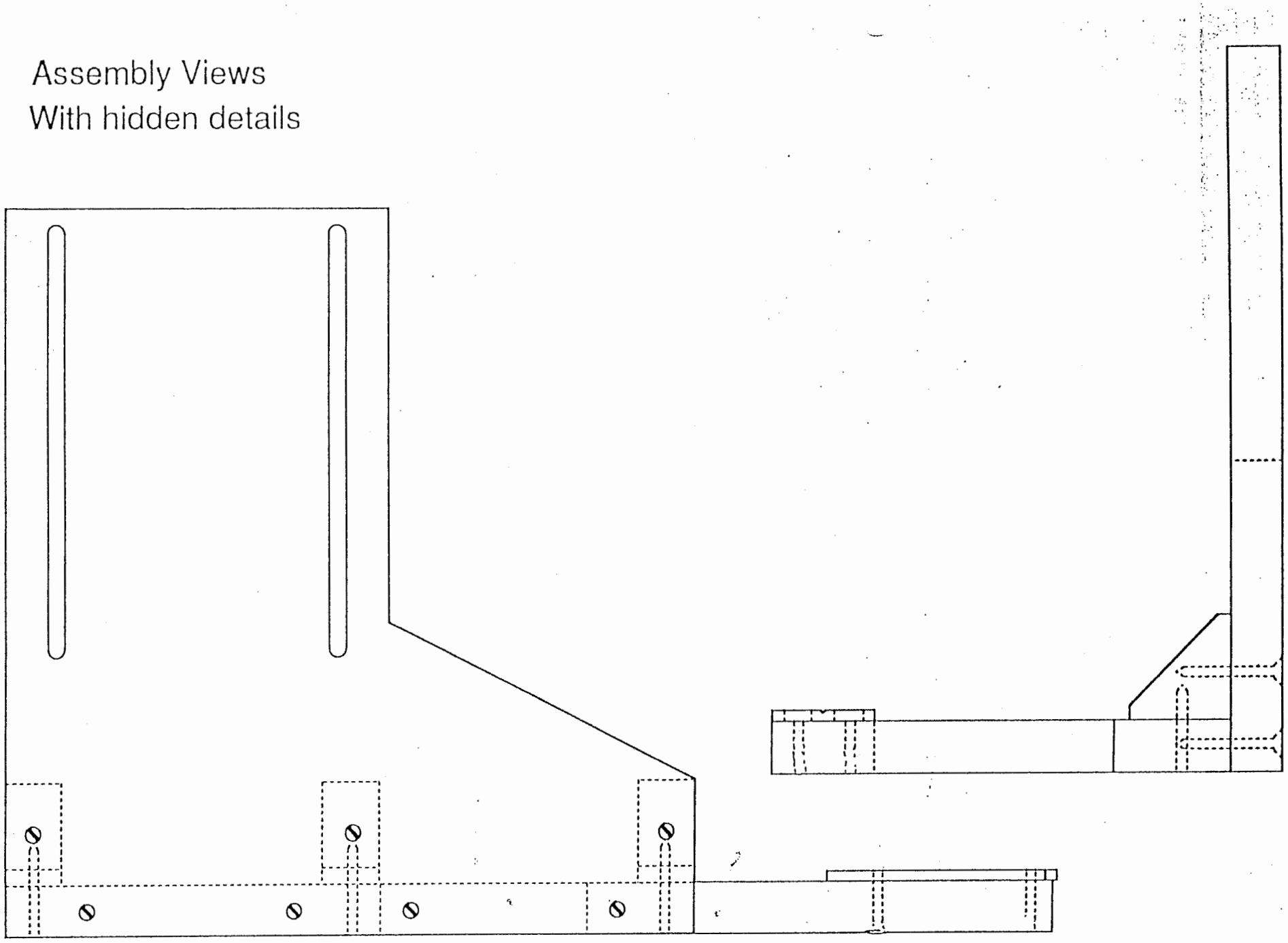

Assembly Views
With hidden details

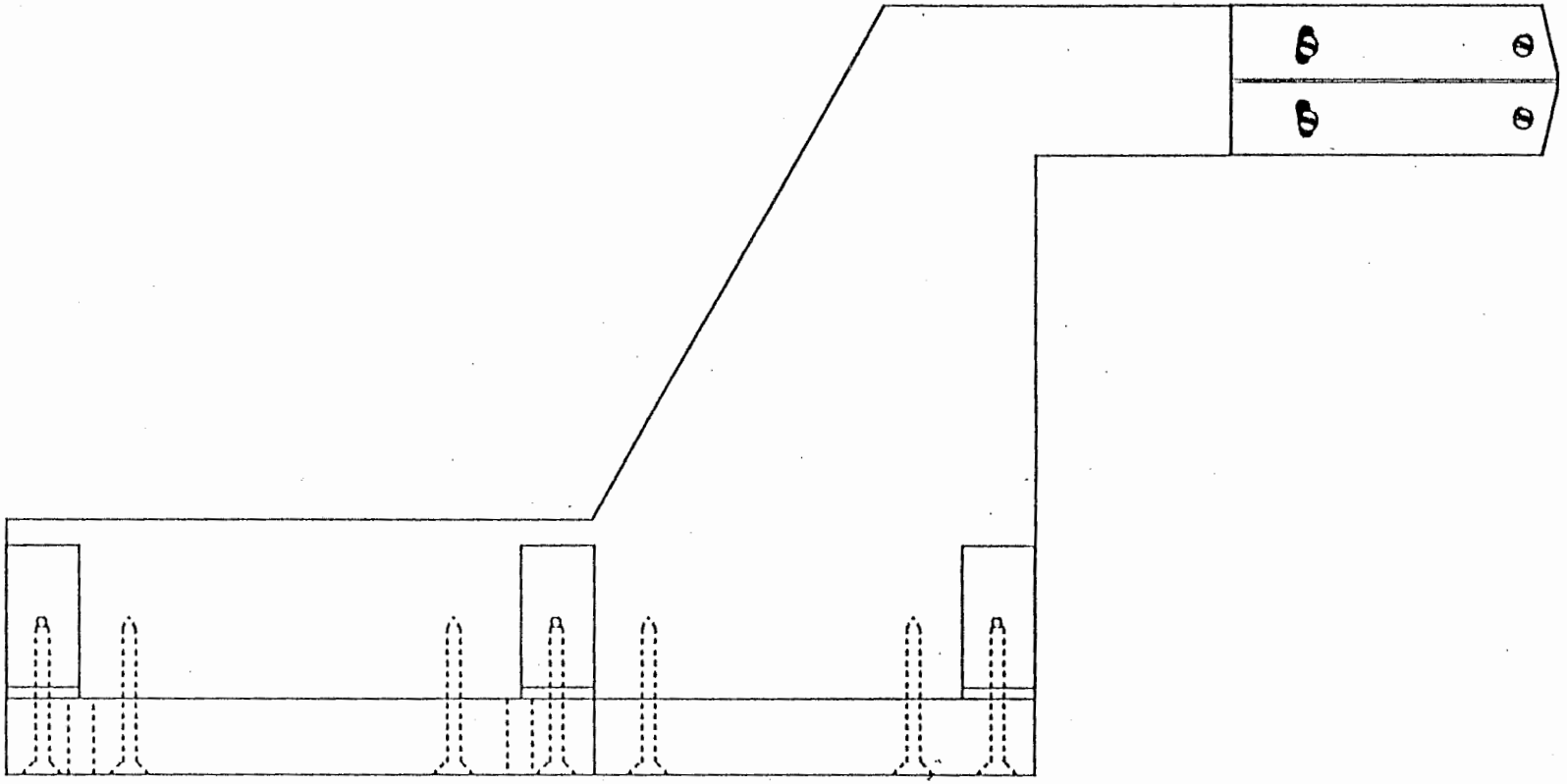

Appendix G - Theoretical responses of phase shifted coplanar EOM

The following pages (G1-G9) include the theoretical responses of the phase shifted coplanar electrodes plotted against normalized frequency as follows:

1. Composite plot of the following drawings:
2. 3- segment coplanar phase shifted electrode (log scale vertical, normalized frequency hor.)
3. 5- segment coplanar phase shifted electrode (log scale vertical, normalized frequency hor.)
4. 7- segment coplanar phase shifted electrode (log scale vertical, normalized frequency hor.)
5. 9- segment coplanar phase shifted electrode (log scale vertical, normalized frequency hor.)
6. 11- segment coplanar phase shifted electrode (log scale vertical, normalized frequency hor.)
7. 13- segment coplanar phase shifted electrode (log scale vertical, normalized frequency hor.)
8. 15- segment coplanar phase shifted electrode (log scale vertical, normalized frequency hor.)
9. 29- segment coplanar phase shifted electrode (log scale vertical, normalized frequency hor.)

All log plots are relative and do not indicate any true DC level.

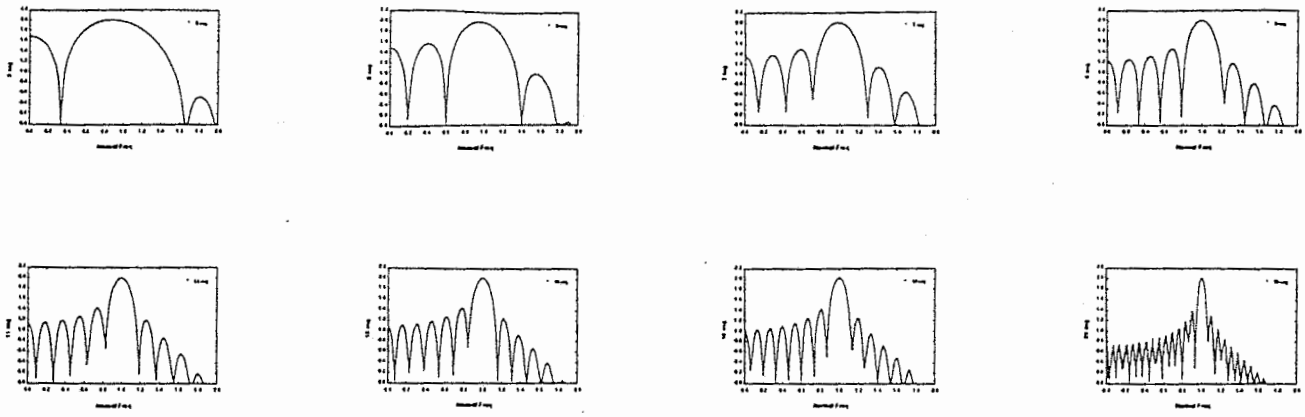

61

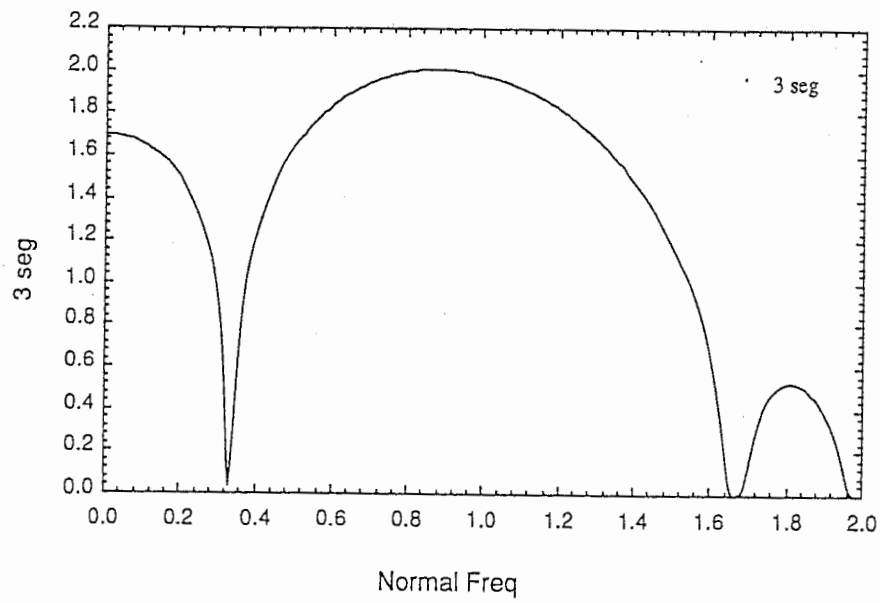
3 seg
2.2
2.0
1.8
1.6
1.4
1.2
1.0
0.8
0.6
0.4
0.2
0.0
3 seg
0.0
0.2
0.4
0.6
0.8
1.0
1.2
1.4
1.6
1.8
2.0
Normal Freq

62

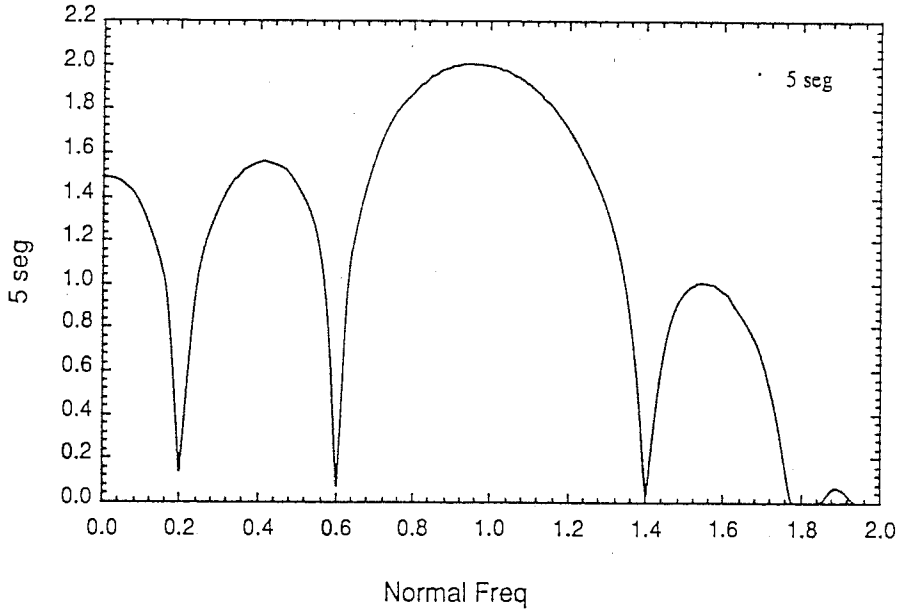
5 seg
5 seg
2.2
2.0
1.8
1.6
1.4
1.2
1.0
0.8
0.6
0.4
0.2
0.0
0.0 0.2 0.4 0.6 0.8 1.0 1.2 1.4 1.6 1.8 2.0
Normal Freq

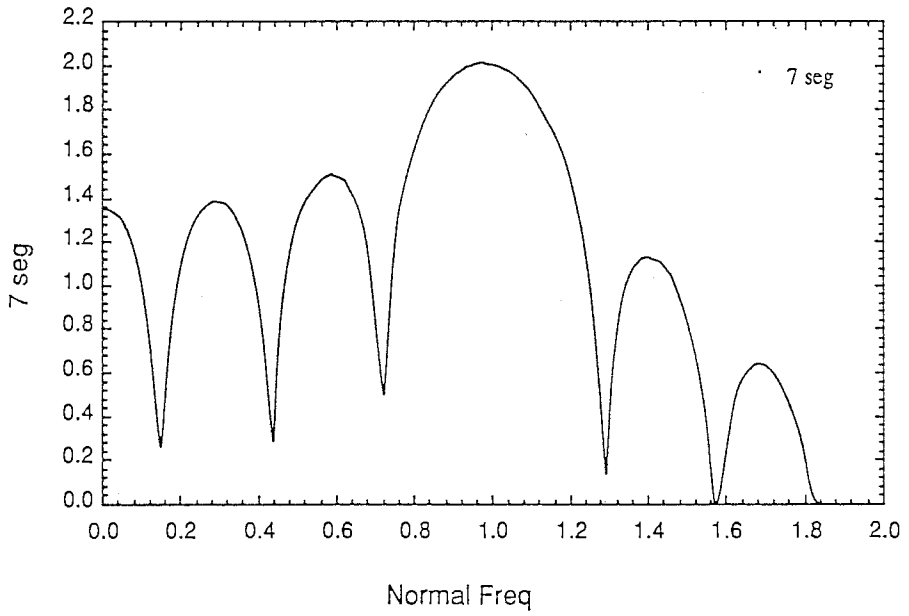
7 seg
7 seg
2.2
2.0
1.8
1.6
1.4
1.2
1.0
0.8
0.6
0.4
0.2
0.0
0.0 0.2 0.4 0.6 0.8 1.0 1.2 1.4 1.6 1.8 2.0
Normal Freq

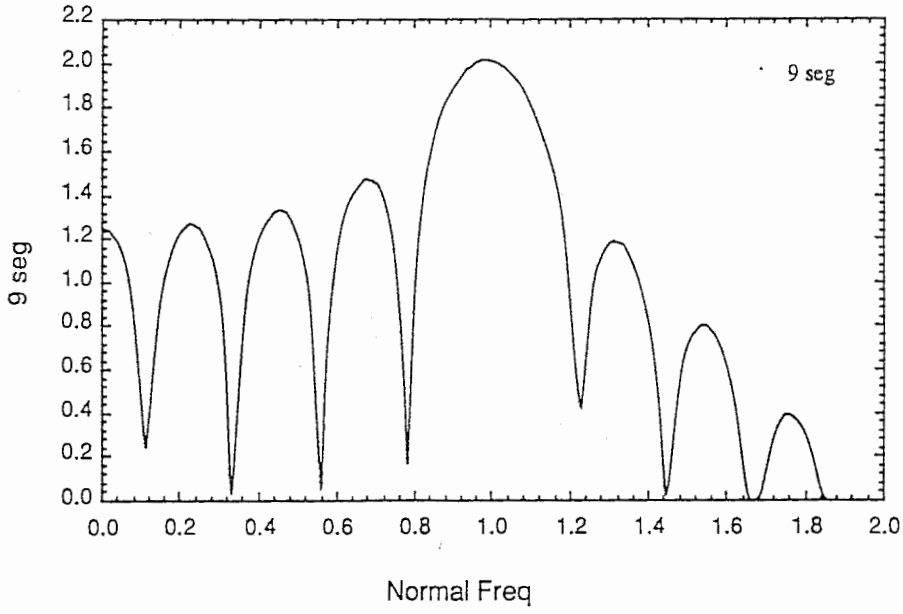
9 seg
9 seg
Normal Freq
0.0
0.2
0.4
0.6
0.8
1.0
1.2
1.4
1.6
1.8
2.0
2.2

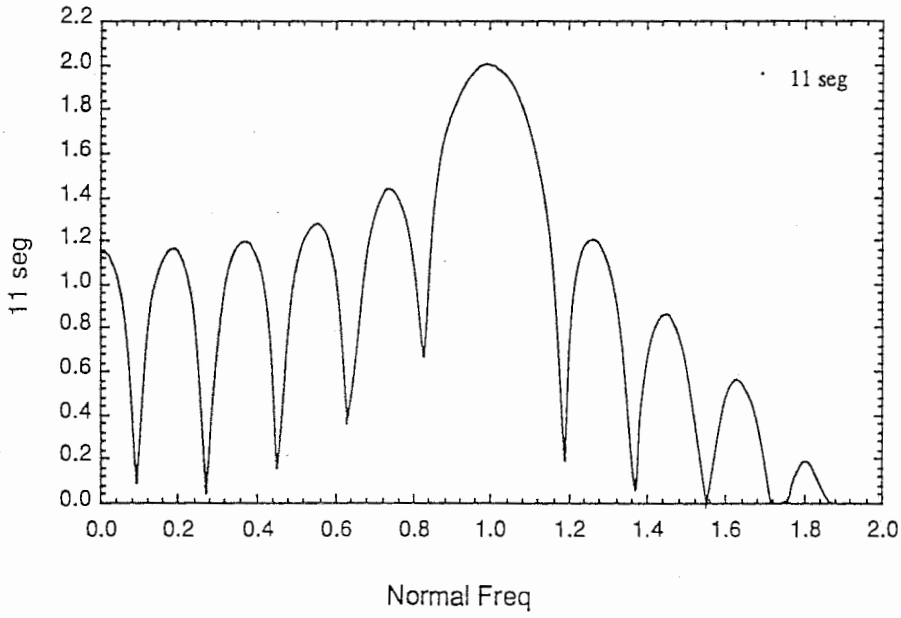
11 seg
11 seg
Normal Freq
0.0
0.2
0.4
0.6
0.8
1.0
1.2
1.4
1.6
1.8
2.0
2.2

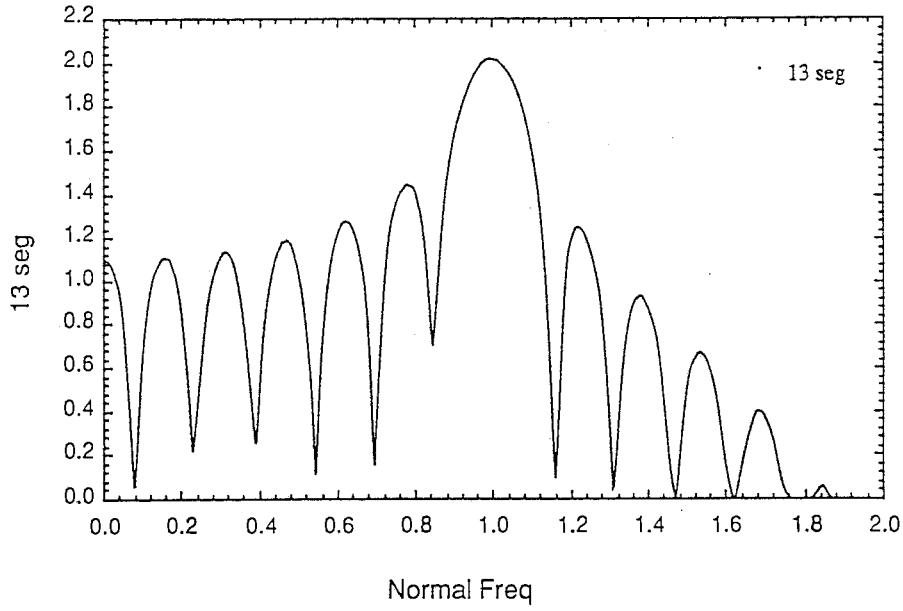
13 seg
13 seg
Normal Freq
0.0
0.2
0.4
0.6
0.8
1.0
1.2
1.4
1.6
1.8
2.0
2.2

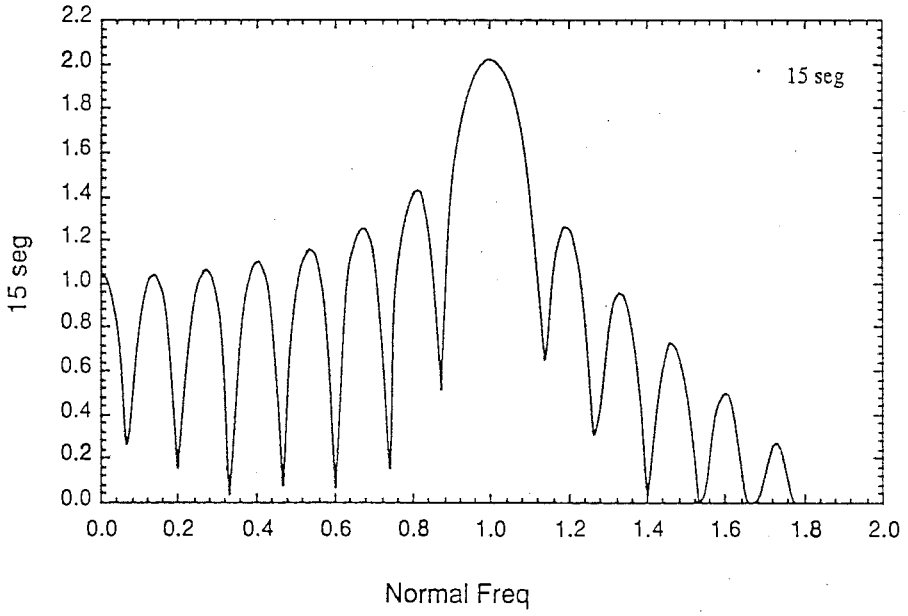
15 seg
15 seg
Normal Freq
0.0
0.2
0.4
0.6
0.8
1.0
1.2
1.4
1.6
1.8
2.0
2.2

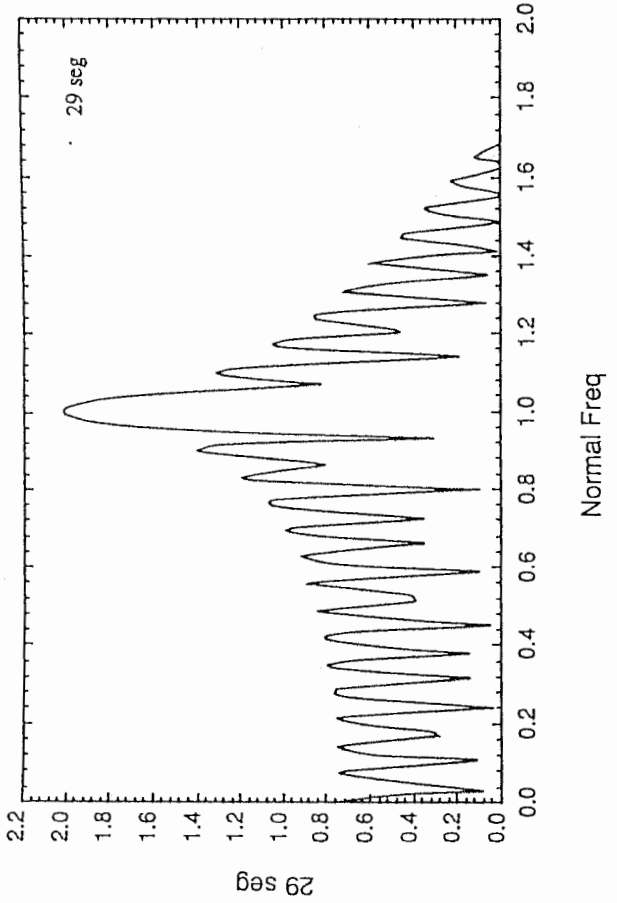

Appendix H - Basic theory of the phase shifted coplanar waveguide

The following pages give more detail to the phase shifted coplanar waveguide electrodes of the EOM design. The pages are listed as follows:

1. Center frequency response calculation
2. Percentage bandwidth data and calculation method
3. Percentage bandwidth and normalized frequency graphs vs. No. of segments
4. Location of the response nulls and associated calculation method
5. Generalized frequency response of the phase shifted coplanar electrode based EOM

H1

	A	B	C	D
1	Segmnt Length	Nm	No	F0 GHz
2	[20 GHz]			
3	0.1441	2.966	2.144	19.349379611
4	0.1441	2.966	2.150	19.326686828
5	0.1441	2.966	2.200	19.139630239
6	0.1441	3.000	2.144	19.221487133
7	0.1441	3.000	2.150	19.199093168
8	0.1441	3.000	2.200	19.014486502
9	0.1441	3.005	2.144	19.202821871
10	0.1441	3.005	2.150	19.180471351
11	0.1441	3.005	2.200	18.996220905
12	[26 GHz]			
13	0.1109	2.966	2.144	24.775050245
14	0.1109	2.966	2.150	24.745994283
15	0.1109	2.966	2.200	24.506486015
16	0.1109	3.000	2.144	24.611296025
17	0.1109	3.000	2.150	24.582622671
18	0.1109	3.000	2.200	24.346251299
19	0.1109	3.005	2.144	24.587396923
20	0.1109	3.005	2.150	24.558779196
21	0.1109	3.005	2.200	24.322863930
22	[32 GHz]			
23	0.0901	2.966	2.144	30.054978986
24	0.0901	2.966	2.150	30.019730770
25	0.0901	2.966	2.200	29.729179756
26	0.0901	3.000	2.144	29.856326326
27	0.0901	3.000	2.150	29.821542256
28	0.0901	3.000	2.200	29.534796658
29	0.0901	3.005	2.144	29.827333972
30	0.0901	3.005	2.150	29.792617385
31	0.0901	3.005	2.200	29.506425095
32	[38 GHz]			
33	0.0759	2.966	2.144	35.172253586
34	0.0759	2.966	2.150	35.131003875
35	0.0759	2.966	2.200	34.790982544
36	0.0759	3.000	2.144	34.939777571
37	0.0759	3.000	2.150	34.899071034
38	0.0759	3.000	2.200	34.563503043
39	0.0759	3.005	2.144	34.905848869
40	0.0759	3.005	2.150	34.865221305
41	0.0759	3.005	2.200	34.530300831
42	[45 GHz]			
43	0.0641	2.966	2.144	40.968798172
44	0.0641	2.966	2.150	40.920750324
45	0.0641	2.966	2.200	40.524691958
46	0.0641	3.000	2.144	40.698009070
47	0.0641	3.000	2.150	40.650593914
48	0.0641	3.000	2.200	40.259722819
49	0.0641	3.005	2.144	40.658488766
50	0.0641	3.005	2.150	40.611165598
51	0.0641	3.005	2.200	40.221048733

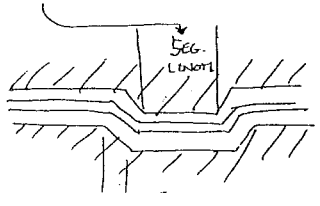

$N_o = 2.144$ (typ.)

$N_m = 2.966$ (typ.)

CENTER FREQ.

$$F_o\,(\text{in GHz}) = \frac{c}{2(N_m + N_o)L}$$

c = SPEED OF LIGHT

N_m = MICROWAVE REFRACTIVE INDEX

N_o = OPTICAL " "

L = (SEGMENT LENGTH + 75 μm)

Untitled Data #1

Thu, Nov 12, 1992 1:42 PM

H2

	segments	L3dB	R3dB	Peak dB	% BW
1	1.000	0.0000	1.2075	1.000	120.750
2	3.000	0.5250	1.2825	3.080	75.750
3	4.000	0.6525	1.2375	4.216	58.500
4	5.000	0.7275	1.2000	5.131	47.250
5	6.000	0.7750	1.1725	5.891	39.750
6	7.000	0.8120	1.1520	6.543	34.000
7	8.000	0.8380	1.1340	7.111	29.600
8	10.000	0.8720	1.1110	8.065	23.900
9	12.000	0.8935	1.0940	8.849	20.050
10	14.000	0.9095	1.0815	9.514	17.200
11	16.000	0.9215	1.0715	10.091	15.000
12	18.000	0.9305	1.0640	10.601	13.350
13	20.000	0.9375	1.0580	11.058	12.050
14	22.000	0.9435	1.0530	11.472	10.950
15	24.000	0.9485	1.0485	11.850	10.000
16	26.000	0.9525	1.0425	12.198	9.000
17	28.000	0.9559	1.0415	12.519	8.560
18	30.000	0.9589	1.0390	12.819	8.010

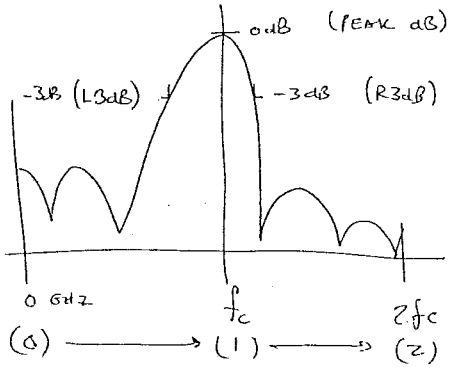

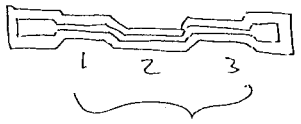

EX. 3 SEGMENTS = % BW = 58.5%

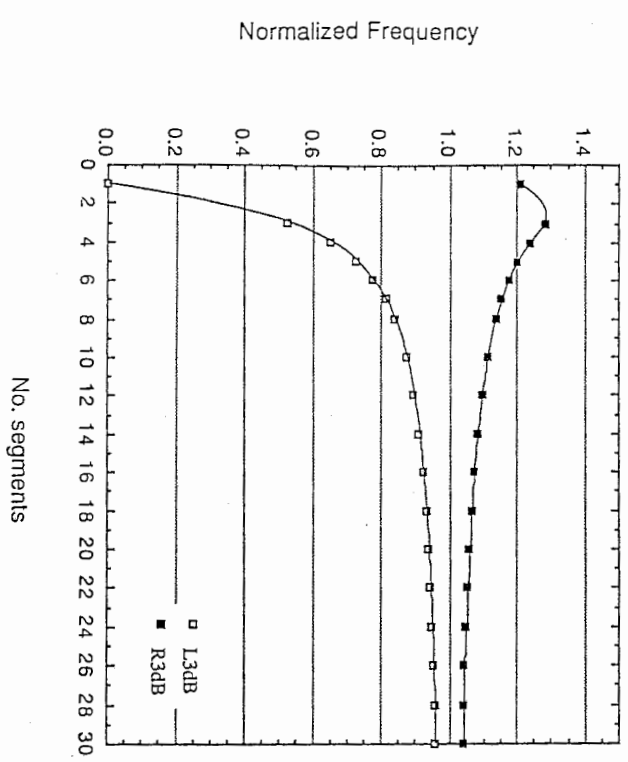

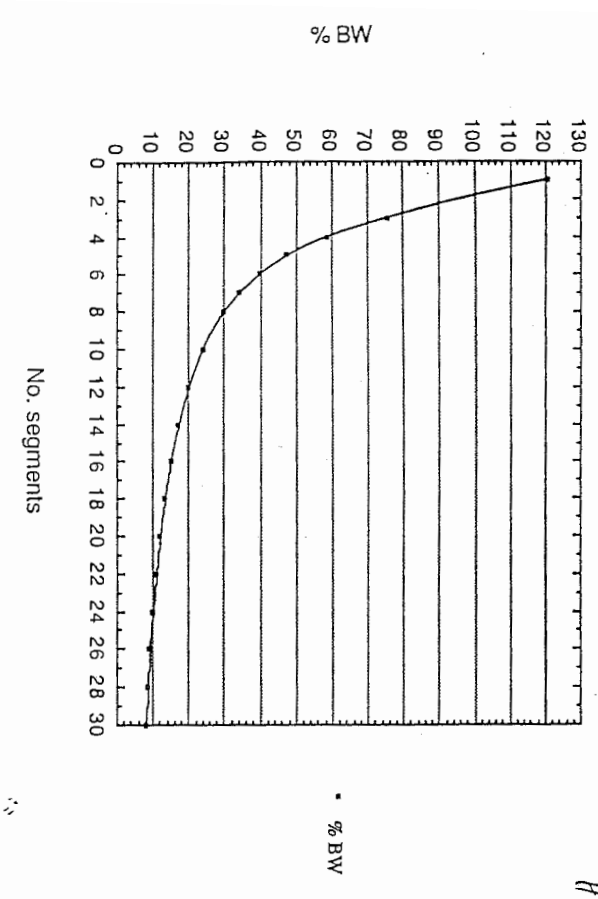

#3

GRAPH OF NULLS IN FREQUENCY RESPONSE OF SHIFTED CAN EQN

	A	B	C	D	E	K	L	M	N	O	
1	Seg:	1.00	2.00	3.00	5.00	7.00	9.00	11.00	13.00	15.00	← # SEGMENTS
2	n										
3	1.00	1.0000	0.0000								
4	2.00		1.0000	0.3333							
5	3.00		2.0000	1.0000	0.2000						
6	4.00			1.6667	0.6000	0.1429					
7	5.00				1.0000	0.4286	0.1111				
8	6.00				1.4000	0.7143	0.3333	0.0909			
9	7.00				1.8000	1.0000	0.5556	0.2727	0.0769		
10	8.00					1.2857	0.7778	0.4545	0.2308	0.0667	
11	9.00					1.5714	1.0000	0.6364	0.3846	0.2000	
12	10.00					1.8571	1.2222	0.8182	0.5385	0.3333	
13	11.00						1.4444	1.0000	0.6923	0.4667	
14	12.00						1.6667	1.1818	0.8462	0.6000	
15	13.00						1.8889	1.3636	1.0000	0.7333	
16	14.00							1.5455	1.1538	0.8667	
17	15.00							1.7273	1.3077	1.0000	← PEAK @ 1 (* f_c)
18	16.00							1.9091	1.4615	1.1333	
19	17.00								1.6154	1.2667	
20	18.00								1.7692	1.4000	
21	19.00								1.9231	1.5333	
22	20.00									1.6667	
23	21.00									1.8000	
24	22.00									1.9333	
25											

NULLS (* f_c)

NULLS (* f_c)

EXAMPLE 3 SEG

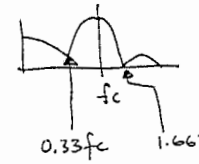

EX: 3 SEGMENTS NULL @ $f_c * 0.3333$
$f_c * 1.6667$

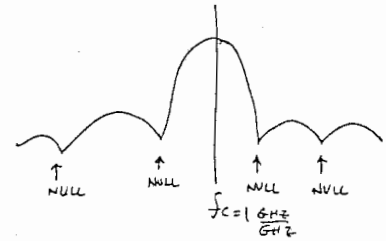

FROM: $\mathrm{ABS}\left(\frac{1}{B/2} \cdot \sin B/2 \cdot \sin\left(\frac{C}{2}(B+\pi)\right) \cdot \frac{1}{\cos(B/2)}\right)$

$B = A * \pi$, A = NORM FREQ f/f_c $\quad \sin\left(\frac{C}{2}(B+\pi)\right) \Rightarrow 0$ IF $B = \left(\frac{2n}{2} - 1\right)\pi \quad n = 0, 1, 2 \ldots$

C = # SEGMENTS

$\eta_m = 2.5660$

$S_{102} = 4.4$ $x = 2.15$ e1.3 cm.) 10cm

16-9/92

AMPLITUDE FREQUENCY RESPONSE

$$\Delta\phi_{PR} = \left(\frac{\Delta\beta_o L_i}{\theta/2}\right) \sin\left(\theta_i/2\right) \cdot \frac{\sin\left[\frac{N}{2}\left(\theta_t + \pi\right)\right]}{\cos\left(\theta_t/2\right)}$$

$$\theta_t = \theta_i = m\frac{\pi f}{f_d} \rightarrow m = 1$$

$$\Delta\beta = \frac{\pi N_o^3 r M V_o}{\lambda G}$$

$$\theta_i = \frac{2\pi N_m}{c} f L_i f$$

$$\Delta\phi_{PR} = \frac{1}{(\theta_i/2)} \sin\left(\frac{\theta_i}{2}\right) \cdot \frac{\sin\left[\frac{N}{2}\left(\theta_i + \pi\right)\right]}{\cos\left(\theta_i/2\right)}$$

EQUATION ~~WHICH~~ DESCRIBES FREQUENCY RESPONSE

$$D = ABS\left(\frac{1}{(B/2)} \cdot \sin\left(B/2\right) \cdot \sin\left(\frac{C}{2}\left(B+\pi\right)\right) \cdot \frac{1}{\cos(B/2)}\right)$$

HERE $B = A * 3.14159$ A = NORMALIZED FREQUENCY 0 - 1 - 2
0 - fd - 2fd

C = # SEGMENTS

D = RESPONSE

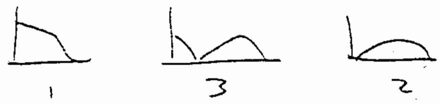

etc.

$\sin\left(\frac{B}{2}\right)$ $\sin\left(\frac{C}{2}\left(B+\pi\right)\right)$ B → 0 → π → 2π
C = 1, 2, 3 ..

$\frac{1}{(B/2)}$

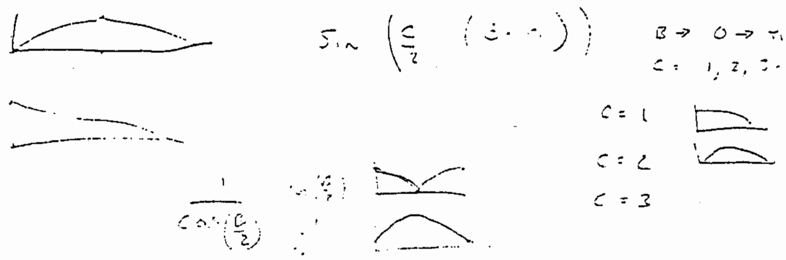

C = 1
C = 2
C = 3

$\frac{1}{\cos\left(\frac{B}{2}\right)}$

B = 0 → 2π

$CB + C\pi = 2\pi$

C = 1	$B + \pi = 2\pi$	$B = \pi$
C = 2	$2B + 2\pi = 2\pi$	$2B = 0$
C = 3	$3B + 3\pi = 2\pi$	$B = -\frac{\pi}{3}$

$$0 = \sin\left(\frac{C}{2}\left(B+\pi\right)\right)$$

$$\arcsin(0) = \frac{C}{2}\left(B+\pi\right)$$

$$= \frac{CB}{2} + C\pi$$

$$\frac{C}{2}\left(B+\pi\right) = \pi \qquad \underline{CB + C\pi} = 2\pi$$